

AD

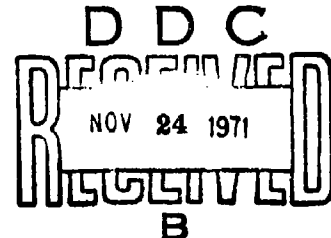
**ATMOSPHERIC AEROSOLS  
BETWEEN 700 AND 3000 m ABOVE SEA LEVEL  
PART V**

**A Study of the Effects of Atmospheric Fine Structure  
Characteristics on the Vertical Distribution of Aerosols**

**FINAL TECHNICAL REPORT**

by

Reinhold Reiter  
Rudolf Sládkovič  
and  
Walter Carnuth



July 1971

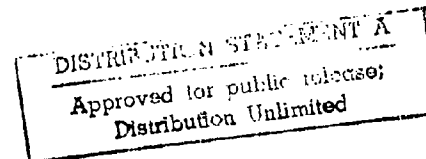
**EUROPEAN RESEARCH OFFICE  
United States Army**

**COLOR ILLUSTRATIONS REPRODUCED  
IN BLACK AND WHITE**

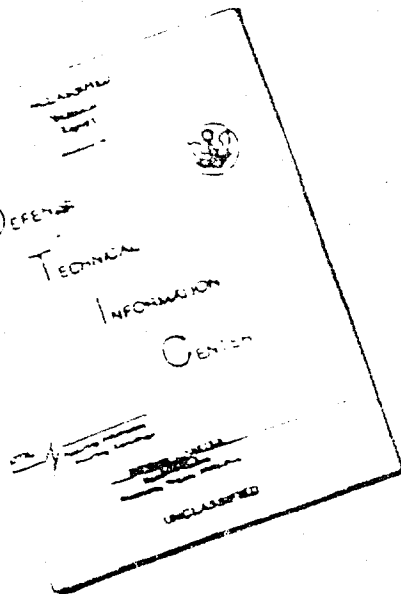
Contract Number DAJA-37-70C-2647

Reproduced by  
**NATIONAL TECHNICAL  
INFORMATION SERVICE**  
Springfield, Va. 22151

Physikalisch-Bioklimatische Forschungsstelle  
der Fraunhofer-Gesellschaft  
81 Garmisch-Partenkirchen, Germany  
Skistadion



# DISCLAIMER NOTICE



THIS DOCUMENT IS BEST  
QUALITY AVAILABLE. THE COPY  
FURNISHED TO DTIC CONTAINED  
A SIGNIFICANT NUMBER OF  
PAGES WHICH DO NOT  
REPRODUCE LEGIBLY.

AD

**ATMOSPHERIC AEROSOLS  
BETWEEN 700 AND 3000 m ABOVE SEA LEVEL  
PART V**

**A Study of the Effects of Atmospheric Fine Structure  
Characteristics on the Vertical Distribution of Aerosols**

**FINAL TECHNICAL REPORT**

by

**Reinhold Reiter**

**Rudolf Sládkovič**

and

**Walter Carnuth**

July 1971

**EUROPEAN RESEARCH OFFICE  
United States Army**

Contract Number DAJA-37-70C-2647

Physikalisch-Bioklimatische Forschungsstelle  
der Fraunhofer-Gesellschaft  
81 Garmisch-Partenkirchen, Germany  
Skistadion

Table of contents

	page
<u>ABSTRACT</u>	
<u>I. OBJECTIVES AND BACKGROUND</u>	2
<u>II. OBTAINING OF DATA</u>	5
<u>1. Technical Facilities</u>	
a) <u>Cable Car Telemetry Systems</u>	
b) <u>Recordings of Natural Radioactivity in             the Air (Concentration of RaB and RaC)</u>	6
c) <u>Recording of Aitken Nuclei Concentration             at the Stations</u>	6
d) <u>Recording of Polar Conductivities and             Space Charge Densities at the Stations</u>	7
e) <u>Numerical Processing of Recorded Data</u>	7
<u>2. Volume of Processed Data</u>	7
<u>III. DATA PROCESSING</u>	8
<u>1. The Physical-Mathematical Fundamentals for         Data Processing</u>	8

<u>2. Brief description of the Overall procedure of Technical Data Processing</u>	8
<u>3. The Computer Program as Such</u>	9
<u>4. Description of Final Data Tables</u>	9
 <u>IV. STATISTICAL RESULTS</u>	 11
<u>1. Preliminary Remarks; Kind of Relations Studied; Principles of Selection</u>	11
<u>2. Relation <math>A_i = f(G-T)</math>, Inversions</u>	13
<u>3. Relation <math>A_i = f(G-PT)</math>, Inversions</u>	14
<u>4. Relation <math>A_i = f(G-E)</math>, Inversions and Other Barring Layers</u>	15
<u>5. Relation <math>A_i = f(G-PT)</math>, General Cases Other than Inversions</u>	16
 <u>V. DETAILED CASE STUDIES</u>	 17
<u>1. Preliminary Remarks</u>	17
<u>2. Example A, 5 Oct 1970, Figs 11 through 14 Spontaneous formation in the medium altitude zone of a most sharply defined inversion, which from noon on descends. Equilibrium of diffusion set from the be- ginning.</u>	19

3. Example B, 18 Nov 1970, Figs 15 through 19.

Well-defined, spontaneously formed inversion,  
with height of barring layer and intensity of  
barring effect varying, Equilibrium of diffu-  
sion retained.

22

4. Example C, 14 October 1970, Figs. 20 through  
23.

Sharply defined inversion with predominantly  
insignificant vertical variations but consi-  
derably fluctuating barring effect. Vertical  
aerosol gradient in stationary equilibrium  
on basis of aerological structure.

24

5. Example D, 11 December 1970, Figs. 24 through  
26.

Inversion at constant height. Vertical aero-  
sol gradient not in equilibrium on basis of  
aerological structure.

27

6. Example E, 17 October 1970, Figs. 27 through  
30.

Case of two simultaneously existing inversions  
one of which is suddenly formed newly and the  
other disintegrated. State of equilibrium is  
not attained.

27

7. Example F, 30 September 1970, Figs. 31 through  
34.

Clearly defined inversion descents slightly,  
remains at constant level for some time, fi-  
nally ascents steeply with simultaneous dis-  
integration. Largely set equilibrium of diffu-  
sion.

29

<u>8. Example G, 26 September 1970, Figs. 22 through 38.</u>	
<u>Considerable vertical and structural variations of an inversion. Equilibrium of diffusion is not attained.</u>	31
<u>9. Example H, 26 September 1970, Figs. 39 through 43.</u>	
<u>Analysis of (a) the upper boundary of the exchange layer, and (b) an ascending inversion located below.</u>	34
<u>10. Example I, 17 September 1970, Figs. 44 through 48.</u>	
<u>Upper boundary of an exchange layer. Slight vertical movement.</u>	36
<u>VI. THEORETICAL SUPPLEMENT FOR COMPUTATION OF EDDY DIFFUSION COEFFICIENTS</u>	38
<u>VII. CONCLUSIONS</u>	40
<u>VIII. OUTLOOK ON ADVANCED STUDIES IN THE NEAR FUTURE</u>	42
<u>1. General</u>	42
<u>2. Procedures to be applied</u>	43
<u>a) Lower Troposphere</u>	43
<u>b) 3 km a.s.l. up to lower stratosphere</u>	43

IX. REFERENCES

44

X. APPENDIX

45

1. Figures 1 - 482. Legends to the Figures 1 - 483. Individual Runs and Data TablesExamples A - J4. Tables I - XII5. The Computer Program

ABSTRACT

Our research work for the purpose of studying vertical aerosol exchange up to 3000 m a.s.l., which was explained in our previous reports, has consistently been carried on. It comprises the obtaining, to the extent possible, of uninterrupted recording data, on the one hand, and, on the other, the development of appropriate methods of electronic data processing and their application toward the derivation, for practical utilization, of relations between aerological parameters and the incremental exchange coefficient. Following are details on the investigations conducted:

Obtaining of Data: Continuous recording of RaB and RaC at 700 m, 1800 m, and 3000 m a.s.l.; computation of the main vertical exchange coefficients for the strata between these levels, and computation of the ionization rate profile. Recording of air conductivities and of the concentration as well as the particle size spectrum of Aitken nuclei at the same levels. Application of these data for computing the vertical profiles of the Aitken nucleus profiles, from the soundings of air conductivities between the said levels. Performance of more than 400 soundings between 700 m and 1800 m a.s.l., and more than 1000 soundings between 1000 m and 3000 m a.s.l., by means of the cable car telemetry systems, for obtaining the profiles of the following parameters: wind velocity, temperature, humidity, polar air conductivities, and potential gradient. Application of the profiles of aerosol particle concentration as computed from the air conductivity profiles, for computing the profile of the incremental exchange coefficients.

Data Handling: Development of computer programs for automatic computation, from the said recordings, of all essential parameters and their altitude dependence; automatic transfer of the data to parameter data tables.

Scientific Processing of Data: Derivation of significant statistical relations between aerological data such as gradients of temperature, of potential and equivalent potential temperatures, of vapor pressure, on the one hand, and the incremental exchange coefficients, on the other. Detailed analyses to investigate the interrelations between all essential parameters, and to deduce appropriate principles of classification as a basis for future improved statistical data processing.

In the appendix, numerous graphs, copies of original recordings, and parameter data tables illustrate the relations found, up to now, and afford a glimpse into our analysing workshop. The most important computer program is printed out in full.

The narrative portion is concluded by a preview of advanced studies intended for the near future.

#### I. OBJECTIVES AND BACKGROUND

Our investigations carried out during the period from 1 July 1970 until 30 June 1971 are based upon the preparatory work of the preceding years of operation. The fundamental problem of the current investigations which have been greatly expanded, instrumentation-wise, by the telemetry system aboard the Zugspitze cable car, has been expounded in detail in the preceding report (1) and in a publication (2). It is assumed, therefore, that a reiteration of the final objective of our research may here be dispensed with. Earlier and more recent literature references to be considered have been thoroughly discussed in (1,2), also. New publications by other scientists of any importance have not since been added.

The subject to be presented, however, in this chapter is how does the work performed during the reporting period differ significantly from that of the preceding period up to the middle

of 1970. During the latter it was our objective (a) to shield the cable car telemetry systems against all effects of the weather and to obtain by them homogeneous series of recordings; (b) to develop and apply the physical and mathematical bases for the complete numeric evaluation of the recording runs, up to and including computation of the incremental exchange coefficients; (c) to continually record at the three stations the Aitken nuclei concentrations, natural radioactivity (RaB, RaC), and polar conductivities, and to utilize them in the evaluations; and (d) to derive initial deductions from the results.

The performance of evaluating operations was predominantly based on manual processes. However, certain phases of the computations, e.g. those of Aitken nucleus concentration from the total electric conductivity of the air, and of the incremental exchange coefficients from the vertical gradients of the conductivity data, were already performed electronically with the Hewlett Packard desk computer.

Now, during the reporting period of 1 July 1970 through 30 June 1971, the entire evaluation technique was completely changed. A new computer (Intertechnique Multi 8) with 12 k words (1 word = 9 bit) affords us the possibility to perform the entirety of all computation processes in one single operation, and to print them out in tables. A considerable portion of the time, however, had to be used to develop computer programs, to test them and adopt them to the computation problem in all details. The newly acquired accessory equipment such as fast reader and fast tape perforator afforded new possibilities to optimize the computation work, however, initially required time consuming conversions of the computer programs. Furthermore, it was necessary to transfer our stock of primary data, i.e. the crude data read from the recordings, on punch tapes by means of teletype, and do this both retroactively to the greatest extent possible, and continually up until they were caught up actu-

ally with the daily soundings.

Hence, there was only a relatively short period left for a thorough statistical processing of the data material as the same can only be based upon the final tables from the computer. Nevertheless, it is possible in this report to convey some interesting - tentative - results. These as well as the detailed analyses described below are in this case based upon Zugspitze cable car soundings only. Analog processing of the Wank cable car soundings will be done later. Also the vertical wind profiles recorded by both systems shall be considered at a later date.

It is by no means gratifying to merely process the data obtained statistically, "blindly", as it were. Such a "blind statistics" is even bound - if solely relied on - to lead on to wrong tracks and into incomplete knowledge. It is rather an indispensable necessity to analyse in detail and "individually", such series of soundings as belong together. Only from such practice, i.e. from an undeniably time consuming detailed analysis, grows the foundation of experience upon which a meaningful and successful statistical evaluation may be based. Part of this report will, therefore, deal with the initial results of such detail analyses.

Our long-range objective is - beside the continuation of the soundings, computer work, and detailed analysis - (1) a complete synopsis of the existing interrelations, and (2) solution of the problem to render the disclosed interrelations applicable for practical use.

## II. OBTAINING OF DATA

### 1. Technical Facilities

#### a) Cable Car Telemetry Systems

During the reporting period the telemetry system in the Wank cable car was working without any troubles. In order to obtain data by it which are comparable in every respect to those obtained by the Zugspitze cable car system, the arrangement of the instruments in the bottom of the Wank cable car was changed. The inlet tube for the measuring air flow was assimilated to that of Zugspitze cable car in length, diameter and position relative to the body of the car.

To begin with, the telemetry system of the Zugspitze cable car required some further improvements.

Due to the large altitudinal difference traversed, condensation would occur occasionally on some of the sensitive electronic parts such as resistors of extremely high ohmic value. We therefore had to resort to installing those parts into sealed cartridges which are kept dry inside through anhydrous CaO. This solved the problem, and even the most severe weather conditions during the run or during waiting period at Zugspitze peak no longer affected the functioning of the unit.

Furthermore, it was possible to completely eliminate a disturbing sensitivity of the cable car equipment as well as the relay station at St. Martin's, to nearby lightning strokes; so, interesting recordings are now available from inside the thunderclouds.

Both systems have repeatedly been tested, calibrated and compared with one another in the laboratory.

b) Recordings of Natural Radioactivity in the Air  
(Concentration of RaB and RaC).

Recordings of RaB and RaC concentrations at the 3 stations were made without interruption, evaluated and utilized within the scientific program. This was done, on the one hand, by computing the mean vertical exchange coefficients between 700/1800 m and 1800/3000 m a.s.l., and on the other hand by using the data in computation of the ionization rate. The results of the recordings for the reporting period are compiled in X. Appendix, Section 4.

c) Recording of Aitken Nuclei Concentration at the Stations.

Aitken nuclei concentration and particle size distribution within the Aitken nuclei range were recorded at the two stations of Wank peak and Garmisch-Partenkirchen without any interruptions or disturbances. All data have been continually analyzed. These (and many other) data are picked up and processed at the latter station by our electronic computer system. Apart from basic research studies on Aitken nuclei and their behavior, these data are primarily used as a basis at 700 m and 1800 m a.s.l., for the conversion of total conductivities into nuclei concentrations.

A new Aitken nuclei counter of the make Environment/one, USA, was installed and put into operation at the Zugspitze station. This unit is smaller and lighter than the GE units, which is essential for operation at Zugspitze peak with the limited space available. But despite considerable expenditure of repair and reequipment efforts, it unfortunately was not yet possible to obtain homogenous recording series over more than a few weeks.

d) Recording of Polar Conductivities and Space Charge Densities at the Stations:

During the reporting period, instruments were put into operation for the recording of polar conductivities and space charge densities at 1800 m a.s.l. (Wank peak) and 700 m (valley floor). From the terminals of our cable car recording range, they furnish data, continuous in time, for direct comparison and link-up. The instruments are functioning satisfactorily, even under bad weather condition. The equipment that had been previously installed at Zugspitze peak has, without interruption, been yielding recorded data which have been evaluated.

e) Numerical Processing of Recorded Data

The methods of numerical processing of recorded data are outlined in (1,2).

2. Volume of Processed Data

From 1 July 1970 through 31 May 1971, we made

413 recording runs by Wank cable car telemetry system and 1,015 recording runs by Zugspitze cable car telemetry system.

The manual evaluation operations that were still necessary have all been completed.

During the same period 380 Wank cable car and 900 Zugspitze cable car runs were transferred to punch tapes and mathematically analyzed by computer. The final results are printed out in tabulated form. Based on the fact that each run yields roughly 500 individual data, our file presently comprises 650,000 data.

### III. DATA PROCESSING

#### 1. The Physical-Mathematical Fundamentals for Data Processing

The physical-mathematical computation operations are described in every detail in (1), Chapter IV (also cf (2)). They were retained in every detail, hence there is no need for reiteration here.

#### 2. Brief Description of the Overall Procedure of Technical Data Processing

Processing of the data, starting with transfer from the moving cable car up to the print-out of the completed tables is shown in Fig.1.

The sensors and the transmitter on the running cable car transmit the measured values to the receiver in codified form and in the known manner. Thereupon follows the electronic decoding of the data and their analog recording on three xy-recorders. The y-channel of each of the three recorders is fed with the analog pressure signal as parameter of altitude. The x-channels are occupied by the analog data for polar air conductivities, wet and dry temperatures and potential gradient + wind speed. The three record sheets obtained per sounding are then subject to intermediate manual processing: the relative values are read off at the main levels (vertical intervals of 100 or 200 m) and at the secondary levels in between. These secondary levels are determined by the processing scientist, based upon the given aerological fine structures of the soundings. These relative values are then compiled in a work chart (intermediate table) per sounding. Thereupon, they are punched (per sounding) on an 8-channel punch tape by means of a teletypewriter. These tapes are then checked for errors (omissions, wrong signs, logical errors) with the aid of a test program; defective tapes are corrected (rate of errors not in excess of 5%). This test pro-

cess is not reflected in the diagram. After the test, the punched tapes are read via the fast reader, into the core store of the computer. The reading time per sounding is approx. 2 seconds. With the aid of the computer program meanwhile developed, which likewise has to be read into the core store of the computer, the result data are computed. The computation process takes 120 seconds. Thereupon, the result data are punched by means of a fast perforator on a punch tape (approx. 80 seconds per sounding). It is advisable to punch the data of several soundings, one after the other, on a continuous tape of 250 m length. The latter is then fed into another teletype-writer which will print out the result data in the form of clearly arranged tables. They are then furnished to the scientist who will study the mutual correlations of the data, taking into consideration any characteristic atmospheric conditions.

### 3. The Computer Program as Such

The computer program is described in full in Chapter X, Appendix, 5.

### 4. Description of Final Data Tables

In Chapter X, Appendix, 3, a number of Final Data Tables are printed, true to original, as supplements to individual runs. They are arranged as follows:

Headings: Z = Zugspitze system ( W = Wank system)  
Number of run; Date; Hour of start of run.

#### a. Main levels (Haupt-Niveaus")

Vertical intervals 100 m for Wank system;  
Vertical intervals 200 m for Zugspitze system.

b. Special levels, selected by temperature structure ("MP-Temperatur")

Vertical intervals are roughly 30 m as a minimum.

c. Special levels selected by humidity structure -- to the extent applicable -- ("MP-Feuchtigkeit")

Vertical intervals see b.

d. Special levels, selected by air conductivity structure -- to the extent applicable -- ("MP-Leitfähigkeit")

Vertical intervals see b,

Meaning of letters designating vertical columns of Tables:

Z	: Number of level
H	: Altitude (m.a.s.l.)
P	: Pressure (mb)
T	: Air temperature ( $^{\circ}$ C)
TF	: Wet temperature ( $^{\circ}$ C)
PT	: Potential temperature ( $1/10$ $^{\circ}$ K)
EPT	: Equivalent potential temperature ( $1/10$ $^{\circ}$ K)
E	: Water vapor pressure (mb)
S	: Specific humidity ( g/kg )
RF	: Relative humidity (mm%)
+L	: Positive polar conductivity ( $10^{-14}$ 1/Ohm.m)
-L	: Negative polar conductivity ( $10^{14}$ 1/Ohm.m)
+/-	: Ratio of both conductivities
L	: Total conductivity (see above)
DH	: Height difference (m)
TV	: Virtual temperature ( $^{\circ}$ C)
G-T	: Gradient of T
G-E	: Gradient of E
G-S	: Gradient of S

G-RF : Gradient of RF  
 G-PT : Gradient of PT  
 I : Ionization rate ( $\text{ions/cm}^3 \text{ sec}$ )  
 N : Number of Aitken nuclei ( $\text{cm}^{-3}$ )  
 A : Incremental exchange coefficient ( $\text{g cm}^{-1} \text{ sec}^{-1}$ )  
 D : Diffusion coefficient ( $\text{cm}^2 \text{ sec}^{-1}$ )

Definition of sign of gradients:

The gradients are positive when:

T : decreases with height  
PT : increases with height  
E : increases with height  
S : increases with height  
RF : increases with height

The meanings of the letters and gradients should be born in mind when later the Tables and graphs are discussed.

#### IV. STATISTICAL RESULTS

##### 1. Preliminary Remarks; Kind of Relations Studied; Principles of Selection

Our basic idea in the statistical analyses was to find significant relations between the fine structure characteristics of the meteorological parameters, on the one hand, and the respective value of the incremental vertical exchange coefficient  $A_i$  on the same vertical interval, on the other hand. There are numerous possibilities of doing so. After preliminary tests, the following relations appeared sufficiently promising to be numerically investigated (for legend see above).

- a)  $A_i = f(G-T)$  Inversion
- b)  $A_i = f(G-PT)$

- c)  $A_1 = f(G-E)$  Inversions and other barring layers
- d)  $A_1 = f(G-IT)$  General relation,

There was no question, from the outset, that all values from the computer tables were not suitable to be "blindly" used for differentiation of the structure of these relations. The definition of the principles of selection, however, is a tentative one and may be varied or supplemented by other, additional ones in subsequent, more exhaustive investigations. In regard to the above defined relations, the following principles of selection were applied in the following:

- a) Data of such vertical intervals only were used (no matter whether bounded by main or special levels) containing distinct temperature inversions ( $G-T$  negative). These inversion layers were required to have settled both in time and position; cases with a marked vertical movement of the inversion level were excluded, likewise such with a sudden formation or disintegration of the inversion structure. That pair of values was used at that vertical interval where the steepest negative gradient of  $T$  was reached.
- b) Same definition as a).
- c) Again, data of only one vertical interval were used per run, with the following conditions applied: if there was no negative  $G-T$  value anywhere that vertical interval having the lowest positive value was selected; if there was a vertical interval with  $-G-T$ , the latter was used; if there were several such the highest negative  $G-T$  value was used as criterion of selection. At the same time,  $G-E$  was required to show a maximum.
- d) Almost all existing pairs of values were used, except such, derived from periods or layers where the structure was subject to rapid changes in time, a transformation of the local meteorological conditions was in progress, or where fog or

precipitations were traversed during a run. Likewise, values from layers with distinct inversions have not been included; they belong under b).

In the following part of this we show the distribution of the individual pairs of values as dots in the graphs, on the one hand, and each time a respective statistical evaluation, on the other. The latter was made with our Hewlett Packard computer which, in the meantime, has been equipped with an extended memory. The pairs of values were keyed into the computer. The latter then separated them according to A-values. To this end, each A-decade was subdivided into 10 equal intervals. The computer automatically determined the 40 mean values between  $A_1 = 0.1$  and  $A_1 = 1000$ , plus the pertinent criteria of significance

$$\sigma_M = \pm \sqrt{\frac{\sum_{i=1}^n (x_i - \bar{x})^2}{(n-1)2n}}$$

The results of these statistical investigations are presented in the form of "stepped graphs". In the discussion of the graphs below the above listed criteria of selection should be born in mind, as appropriate.

## 2. Relation $A_1 = f(G-T)$ , Inversions

Fig. 2 shows the scattering of the individual pairs of values for the relation  $A_1 = f(G-T)$  in the case of a typical inversion (see Section IV.1.a). The study covers the period of 28 July 1970 through 17 February 1971 with a total of 388 pairs of values. The graph is analogous to Fig. 23 in (1). A comparison of the result depicted in said graph with that in Fig. 2 reveals this: In principle the earlier result agrees quite well with the more recent one except that the relation  $A_1 = f(G-T)$  is now much more pronounced, the scattering of the values is narrower.

Fig. 3 shows the analogous result of a statistical analysis with statement of scatter  $\sigma_M$ . This graph clearly shows: There is

a strict, significant relation between an incremental exchange coefficient in the range of  $A_i = 0.1$  through 300, and the temperature gradient in the range of - 0.1 through  $-10^{\circ}\text{C}/100\text{ m}$ , provided that the inversion in the vertical interval under consideration is a genuine, stable and largely motionless one to which the  $A_i$  and G-T values apply. The relation is independent of season or time of day.

Hence, the function presented in Fig. 3 is already ripe for practical application.

### 3. Relation $A_i = f(G-PT)$ , Inversions

Fig. 4 shows the scattering of the individual pairs of values for the relation  $A_i = f(G-PT)$ . It, again, applies to cases of typical inversions. The principle of selection is defined in Section IV.1. a) and b). The period of the study, again, stretches from 28 July 1970 through 17 February 1971 and covers a total of 289 pairs of values.

With the scattering of values not too wide a surprisingly clearly defined logarithmic relation is found between incremental exchange coefficient  $A_i$  and potential temperature gradient G-PT:

If in a defined vertical interval with an inversion the potential temperature gradient increases, the intensity of exchange in the same layer is decreased. The following rule may be stated: Per  $1^{\circ}\text{C}/100\text{ m}$  increase of G-T,  $A_i$  is decreased by one decimal power.

Fig. 5 shows the analogous result of a statistical analysis with statement of scatter  $\sigma_M$ . True it is greater than in Fig. 3, nevertheless between  $A_i = 100$  and  $A_i = 0.8$  the relation may be considered well established. The volume of data material is to be further increased in order to make the relation come out even more clearly. This particularly applies to the value range of  $> A_i = 150$  and  $< A_i = 1$ .

Aside from these statements we feel justified in claiming that this function  $A_i = f(G-PT)$ , too, may already be practically applied.

We consider the statement important that now we have two criteria, independent from each other, to quantitatively state the barring effect of an inversion, viz. the function in Fig. 5 and that in Fig. 3. From now on, the layer having the strongest barring effect may immediately be determined from the aerological data: negative temperature gradient and positive potential temperature gradient must be at maximum values.

#### 4. Relation $A_i = f(G-E)$ , Inversions and Other Barring Layers

In studying the relation between the incremental exchange coefficient  $A_i$  and the gradient of water vapor pressure ( $G-E$ ) we have dropped the demand that a genuine, stable and stationary inversion must exist. With the aid of the gradients of temperature and potential temperature we have merely searched for a barring layer in general (for definition of principle of selection see Section IV.1.c). For the layers thus defined we then studied the above described relation, using data from the period of 28 July 1970 through 17 February 1971. The graph containing the individual pairs of values is shown in Fig. 6; the results of the statistical analysis is presented in Fig. 7. Between  $A_i = 100$  and  $A_i = 1$  we find a significant logarithmic function having a relatively narrow scatter with only 263 pairs of values. It appears desirable to increase the data, particularly in the limiting zones. The rule has been established that  $A_i$  will be increased by one decimal power when the negative value of  $G-E$  is increased by 1 mb/100 m - and vice versa. This is comprehensible in principle since the vertical exchange of water vapor, too, is controlled by the amount of the  $A_i$  value. Nevertheless, it is probable that the graphs 6 and 7, for the first time, convey a tangible picture of the function as such as it is actually applicable in the atmosphere.

With this function, now, we have an independent third criterion by which to locate layers having a barring effect, and to determine the degree of their barring effect.

#### 5. Relation $A_i = f(G-PT)$ , General Cases Other than Inversions

Within the scope of the previous studies we had limited ourselves to either typical inversions (Sections 2 and 3) or, at least, layers of such aerologic structure as to permit the inference of a barring effect, including inversions (Section 4). To the extent that criteria of selection were applicable at all, the values of one layer, at maximum two layers, per run were, in this manner, to be taken into consideration. The study now being discussed, however, covers all layers (any number per run) except such containing an inversion. As explained in Section IV.1.d), the following have also been left outside of consideration: cases with a rapid transformation of the weather condition, with precipitations, or runs entirely or partly through clouds.

Preliminary studies have revealed that above all the potential temperature gradient is very well suited for this kind of a general statistics.

In order to determine whether seasonal differences might play a part in this we have subdivided the entire period from which values are available, into 28 July 1970 through 12 November 1970, and 13 November 1970 through 17 February 1971. We shall here dispense with a presentation of the distribution of individual pairs of values, even more so as, in view of the large volume of data, this kind of evaluation would have been too expensive.

The results of the statistical investigations are shown in Figs. 8 and 9, with statements as to the respective scatters. From both figures a clear and strict relation becomes apparent ( $A_i = f(G-PT)$ ), scattering only insignificantly in the range between  $A_i = 1000$  through  $A_i = 1$ . At  $A_i < 1$  the relation becomes

uncertain. As demonstrated by Fig. 10 the results from both periods of time are in good agreement with one another, hence there is no seasonal impact.

The relation depicted in Figs. 8 through 10 applying to those atmospheric layers which are not of the nature of an actual inversion, clearly deviates from that deduced for typical inversions (Fig. 5). The reason for this deviation is yet to be clarified.

The function  $A_1 = f(G-PT)$  resulting from Figs. 8 through 10 is suited for deducing, in practical work, from G-PT values the strength of vertical exchange, unless typical inversions are being dealt with in which case the function pursuant to Fig. 5 is to be applied.

## V. DETAILED CASE STUDIES

### 1. Preliminary Remarks

The following case studies are partly based upon the original recordings by cable car telemetry system and pertinent parameter data tables supplied by the computer. The wind profiles are not yet taken into consideration. The graphs and tables are compiled in SECTION X, APPENDIX, 3. They, at the same time, afford a glimpse into our "Analysis Workshop". The numbers of the levels in the recordings correspond to the numbers of levels in the tables. On the other hand, the case studies are based upon a study of changes in time of certain structural elements at the inversion level and pertinent numeric values of functions:  $A_1 = f(G-T)$ ,  $A_1 = f(G-E)$  and  $A_1 = f(G-PT)$ . Separate graphs which are given consecutive figure numbers serve this purpose (SECTION X, APPENDIX, 1). In the graphs on which the values of the aforesaid 3 functions are entered, we have also plotted the "normal progress" of each respective function, in the form of dotted areas, which also, based upon Figs. 3, 5, 7,

indicate the mean scatter. The examples to be discussed hereinafter, are marked with identification letters in alphabetical order. These letters have been transferred to all graphs, recordings and tables (also those in SECTION X, APPENDIX, 3,) so no doubts may arise as to their correlation.

The runs of one and the same day bear encircled numbers in chronological sequence. These, too, are also found on all recordings, graphs and tables, hence the variations of all data in the course of time are readily recognized.

Following are some necessary remarks on the problem of equilibrium. An aerological structure, e.g. the variation of temperature across an inversion layer, and the vertical aerosol profile across the same vertical interval can be in lawful correlation to one another (as shown, e.g. in Figs. 3, 5, 7) only if there had been enough time for the setting of some stationary condition. There are two possibilities:

- a) A temperature inversion is created, very rapidly, say in less than 1 or 2 hours, through some processes which are known in principle. At the moment of its formation, the aerosol profile cannot, as yet, have been accommodated by this inversion to the instantaneous barring effect. The adaptation process requires a few hours; for instance, by evacuation or coagulation of aerosol particles above the inversion and concentration below, until equilibrium has been set based upon the mere eddy diffusion process. Not until then can a lawful correlation exist, and parameters be within the normal ranges of the functions per Figs. 3, 5, 7.
- b) With the barring effect of an already existing inversion being constant in time, the source strength of the aerosol in the layer below the inversion may change, or aerosol may be brought in or drawn off, through advective processes. In this case, again, the equilibrium of diffusion

is temporarily disturbed and time is required for readjustment.

- c) It may happen that aerosol fluxes from some source into the lower atmospheric layers, where it will spread for the time being. At the upper boundary of the thus developed haze layer, an exradiation of heat begins. This causes continuous cooling and formation of vertical temperature structures which react back upon the vertical aerosol distribution. In this instance, again, the result may be a disturbance of the eddy diffusion equilibrium of long duration.

Other processes are possible which shall not be discussed in this context. The following studies are to show the meteorological conditions under which an equilibrium of diffusion is, as a rule, encountered, or not encountered, and what numeric relations will be found in each respective case.

2. Example A, 5 Oct 1970, Figs 11 through 14

Spontaneous formation in the medium altitude zone of a most sharply defined inversion, which from noon on descends.

Equilibrium of diffusion set from the beginning.

Looking, to begin with, at the original soundings (APPENDIX) we find that at around 1100 CET (run 0) neither T nor TF show any distinctive structure, and this is true of the entire vertical interval. The temperature gradient, however, is weak, and humidity is decreasing with height. The polar conductivities  $+L$  and  $-L$  are steadily increasing from level 11 to level 5. The causes of their variations above level 5 do not concern us in this report. At 1157 CET (run 1) already, a sharply defined inversion exists immediately below level 6, with humidity decreasing with increasing height, which is clearly reflected in the behavior of  $+L/-L$ . In the course of the day the picture of a typical temperature inversion with humidity break

becomes more and more distinct. At the same time the abruptness of the break of  $+L$  and  $-L$  keeps increasing, and the aerosol concentration below the layer of the break is continually growing (the values of  $+L$  and  $-L$  are decreasing). Thus the gradient of the aerosol concentration across the layer of the break is getting steeper and steeper. From noon until night the level of the inversion is continuously descending.

Let us now take a look at the detailed analyses in Figs. 11 through 14. Fig. 11 shows changes in regard to altitude and time for:

- a) the layer where the inversion is located ( $-G-T_{\max}$ );
- b) the level with a minimum value; and
- c) a maximum value of the equivalent potential temperature EPT.

With regard to b) and c) the following must be added: in case of well defined, stable inversions scarcely variable in time or space, or other barring layers, a minimum of EPT is encountered above the barring layer, with a maximum within or below its level. In the absence of barring layers EPT, as a rule, decreases evenly with decreasing height. Thus barring layers normally also identify themselves by an "inversion" in the course of EPT, which, however, proceeds inversely to T. The fact that this EPT inversion (signs: - and = in Fig. 11) is convected together with the temperature inversions proper (sign:  $\sqcup$ ) is clearly apparent from Fig. 11. This figure also reflects the time slope of  $A_i$ . During the descent, to begin with,  $A_i$  increases. In the evening, when the inversion has settled,  $A_i$  drops to a minimum value of only 0.3.

In Fig. 12 we study the variations with time in the range of the function  $A_i = f(G-T)$  within the inversion layer of runs 1 through 4. The variation of the pairs of values occurs exclusively inside the (dotted) normal range. Thus,  $A$  during

the descent (run 1 after 2 to 3) increases, it is true, but G-T, too, changes by a corresponding amount as the function shows. Hence, structure of inversion, and control of the vertical aerosol distribution by it are in a true-to-function relation to each other. We arrive at an analogous result if we study Fig. 13 ( $A_i = f(G-PT)$ ). Except for run 1 the pairs of values are within the normal range of the function. Hence, the behaviour of G-PT and the pattern of the vertical aerosol structure correspond to each other. From these finding we may deduce that equilibrium of diffusion has practically existed from the beginning. No analogous conclusion may be drawn in regard to the relation  $A_i = f(G-E)$ , as illustrated by Fig. 14. In this instance all pairs of values are exclusively outside of the normal range. The E-gradients are much greater than would be permissible with regard to the  $A_i$  values. Hence, a change must have occurred in absolute humidity (e.g. caused by advection) above or below the barring layer, which was not related, across the barring layer, to the eddy diffusion process, whereas by contrast the aerosol distribution did obviously correspond to the barring effect of the layer.

Conclusions drawn from this example:

Even in case of spontaneous formation of a very sharply defined inversion, and during a slow and constant descent of the same, the discovered "normal relations" between  $A_i$  and G-T or G-PT, respectively, are being retained. Thus they adequately describe the vertical distribution of aerosol; the state of equilibrium prevailed. A deviation of the values outside of the normal range of  $A_i = (G-E)$  reveals an advective change of humidity. This emphasizes the high value of such detailed analyses. The rule that there has to be a minimum of EPT above the barring layer, and a maximum within its level, is met at all times. It may additionally serve as an indicator of the barring layer.

We are here dealing with a case where rapid formation of an inversion and the transformation of the vertical aerosol structure

went hand in hand together in such a manner, that the condition of equilibrium for the eddy diffusion was met at all times. Conditions for the occurrence of this situation remain yet to be defined.

3. Example B, 18 Nov 1970, Figs. 15 through 19.

Well-defined, spontaneously formed inversion, with height of barring layer and intensity of barring effect varying,  
Equilibrium of diffusion retained.

The soundings (for a selection pertaining to Example B see X., APPENDIX 3) already show that we are here dealing with a (spontaneously formed) inversion and barring layer which is subject to considerable fluctuations in time as to its structure and height. As demonstrated by Fig. 3 the maxima of -G-T and -G-E are located at the same respective altitude, which level, however, fluctuates considerably. A maximum of EPT above the inversion level and a minimum within the same cannot be found.  $A_1$ , too, fluctuates considerably from run to run, and the rule is confirmed: If the inversion level descends the barring effect of the inversion is temporarily reduced ( $A_1$  is increased), as is demonstrated by runs 3 and 6.

As is recognized from Figs. 16 and 17 the values are fluctuating precisely within the normal range of the function  $A_1 = f(G-T)$  and  $A_1 = f(G-PT)$ . So, with the exception of runs 2 through 4, diffusion equilibrium prevails as in Example A. The change from run 2 via 3 to 4 is indeed striking. Whereas  $A_1$  is changed considerably, G-T and G-PT remain practically constant, the full "normal" scatter of the function is traversed. This means that during the vertical movement of the inversion from 2 via 3 to 4 the aerological structure of T and PT is retained whereas the permeability of the barring layer is reduced temporarily. A local perforation of the layer by turbulences in the early afternoon with relatively extensive insolation, is likely to be the main cause thereof. This example indicates how, by means of such a detailed analysis interfering factors may be isolated.

Considering Fig. 16 we observe that the normal range is considerably exceeded in both directions. The values are not, however, all shifted in one direction as in Example A. This rules out progressive changes of absolute humidity due to advection. Turbulence caused, forced vertical transportation of water vapor is, much rather, to be considered as a cause (transitions from 4 to 5, from 5 to 6). It is, however, a striking observation that the transition 2-3-4 again appears to be out of place: While the water vapor gradient remains constant,  $A_1$  varies considerably. This means again that here a variation of the inversion had temporarily been forced, pointing toward interference with the system from the outside (e.g. heat irradiation). It is interesting that in this case a variation of the vertical aerosol structure was triggered (as a consequence whereof a higher  $A$ -value resulted for run 3), not however one of the aerological structure and of the vertical distribution of water vapor.

For the present example we have plotted the vertical profile of the incremental exchange coefficients  $A_1$  and of the water vapor from run to run as a special representation in Fig. 19. This representation does not only show very impressively the variation in the fine structure of the  $A_1$  profiles but also the vertical displacement of the layers having maximum barring effect ( $A_1$  minima). What we want to demonstrate, however, is that just these sometimes very thin layers of highest resistance to eddy diffusion are indicated in the E profile by a peak-like dip of water vapor concentration. This is true even in the case of a splitting into two barring layers with a small difference in height (run 6). At the same time we recognize a problem in the E profile for run 3: Here it is not so much a dip but much rather a sharply confined increase of E with height that is characteristic. Such findings with the aid of detailed analyses are conductive to understanding deviations from normal behavior observed from time to time.

The gathering of such exceptions and the investigation of the conditions under which they occur is important for the following reason: In order to reduce, on a pertinent basis, the scatter in the statistical investigations it is necessary to introduce a more detailed subdivision. Most of all, the complex causal nexus of the various parameters may gradually be cleared up in this manner.

Conclusions drawn from the example:

In the case of spontaneous formation of an inversion and intensive vertical movement of the same, the discovered "normal relations" between  $A_1$  and G-T or G-PT, respectively, are retained and depict the vertical aerosol distribution which corresponds to a stationary setting of equilibrium. A "breaking out" of the values from their normal distribution, insignificant for G-T and G-PT, and quite considerable for G-E, points to a convectively forced variation in the vertical aerosol distribution, which can no longer be lawfully related to the aerological structure. The vertical water vapor gradient, in this case, behaves differently from the vertical aerosol gradient. With the barring layer sharply descending,  $A_1$  is temporarily increased. Barring layers are always indicated by conspicuous deviations of the E profile across very small vertical intervals.

4. Example C, 14 October 1970, Figs. 20 through 23

Sharply defined inversion with predominantly insignificant vertical variations but considerably fluctuating barring effect. Vertical aerosol gradient in stationary equilibrium on basis of aerological structure.

Example C concludes, for the time being, those cases of inversions which are distinguished by the vertical aerosol gradient being in equilibrium on the basis of the given aerological structure, in other words, where the normal relations of our function are fully or largely met.

As is shown by the original recordings in APPENDIX, 3 we are, from run 1, dealing with a sharply defined inversion the strong barring effect of which is clearly expressed by the profile of the air conductivities. Only early in the morning (run 0) an inversion is just slightly indicated, with only a very weak barring effect. The vertical movements can be clearly recognized on the original recordings, e.g. by comparison of run 6 with run 8.

To begin with, the variation as a function of time and altitude is shown in Fig. 20. In the forenoon we find that the ascent of the inversion layer from run 1 through run 3 results in a weakening of its barring effect (increase  $A_1$ ; in Examples A and B we had found a weakening with a descent of the inversion), whereas later in the afternoon the opposite relation is found. Hence, vertical movement, no matter in which direction, may lead to either a weakening or a strengthening of the barring effect. We are thus compelled to restrict our statement to the more generalized form: Vertical movement of a barring layer results in a change to its barring effect. The nature of the individual relation is certainly depending upon the causative reasons for the movement of the inversion (advection processes, anticyclonic descent). In order to determine these, further detailed analyses will be needed. In the context of this discussion of the examples the implications of microscale and mesoscale meteorological conditions and processes are not to be discussed in any detail. A deepening of the detailed analyses in this direction is in process.

In the instant case we again find a minimum of EPT above the barring layer, but no marked maximum below.

Figure 21 shows the variations with time of our values relative to function  $A_1 = f(G-T)$ . We notice that the fluctuations of the values largely remain inside the normal range. An insignificant breaking out (deviation from equilibrium) occurs from 5 through 6 to 7. This means that in Fig. 20, too, we must

consider the temporary descent of the inversion level (run 6) as the expression of an interfering process. At any rate, the fact is again conspicuous that  $A_i$  changes considerably, e.g. from run 5 to 6, although the aerological structure of T has been retained (G-T constant). The attenuation of the aerosol gradient encountered at the same time therefore must be due to an exterior cause, e.g. perforation of inversion by local turbulence. It is striking, however, that, as Fig. 22 indicates, the variation of the values is largely within the normal range of the function  $A_i = f(G-E)$ , at least the transition 5-6-7 is within. Again, aerosol and water vapor behave differently in the case on a disturbance of equilibrium. It is surprising, however, that (see Fig. 23) the values for  $A_i = f(G-PT)$  are almost exclusively outside of the normal range of this function. What conclusions have to be drawn therefrom is yet to be investigated, using all available meteorological data.

Conclusions drawn from this example:

Vertical movements of the barring layer result in variations of their barring effect and a disturbance of the diffusion equilibrium. What direction such a variation may take cannot necessarily be predicted, until such time that the causative reasons for the interfering process are known. It appears certain that detailed analyses of the demonstrated kind will lead to recognition if the causes of interference of microscale and mesoscale meteorological conditions are included in future investigations. For because three basic function are available, based on G-T, G-E, and G-TE, it is, as a rule, possible from the agreement of the individual values with two of these to isolate the one which is most of all affected by the disturbance of equilibrium. This may later lead to isolation of the interfering cause.

5. Example D, 11 December 1970, Figs. 24 through 26.

Inversion at constant height. Vertical aerosol gradient not in equilibrium on basis of aerological structure.

In Figs. 24 through 26 we are studying the case of cyclic variations (runs 1 through 4) of the value obtained, in the range of functions  $A_1 = f(G-T)$ ,  $A_1 = f(G-E)$ , and  $A_1 = f(G-PT)$ . All data obtained from these runs are far outside the normal ranges of the three functions. Vertical movements of the barring layer did not occur. Convective interference, also, must be excluded. To what extent persistent advective processes were determining in this case in the formation of this exception remains to be investigated. For it is striking that this low-lying inversion has been formed through the inflow of near-ground polluted cold air. But although this near-ground cold air layer was soon settled a state of equilibrium did not come about.

To begin with, our example shows that even with inversions at rest and seeming freedom from interferences we must be prepared for extraordinary results. If it were not possible to recognize and isolate these (e.g. on the basis of detailed analysis) such values would result in a considerable scattering within the data material. However, the investigation of the causative relations must not be neglected, particularly in such unclear cases. Exactly these may supply valuable insights.

6. Example E, 17 October 1970, Figs. 27 through 30.

Case of two simultaneously existing inversions one of which is suddenly formed newly and the other disintegrated. State of equilibrium is not attained.

Here we are dealing with a relatively complex case. It is remarkable for the only one initially existing inversion and barring layer descending and disintegrating. Prior to its disappearance, however, a second inversion and barring layer

was forming about 400 m above which also descends and goes on existing to the end - if with a weak barring effect. From the picture of the original recordings (X., APPENDIX, 3), layer I owes its formation to a layer of haze actively conveyed to the spot at little short of 1500 m a.s.l. ( minima of +L and - L during run 1). In the following we consider the original recordings along with Fig. 27. This initially striking aerosol structure is reduced to a mere trace during run 2, but during run 3 it is suddenly sharply defined again at 1200 m a.s.l. During runs 3 through 6 layer I is disintegrating or hazily merging with layer II which has meanwhile descended and whose existence was first hinted at during runs 3 and 4. Presumably the transition was as indicated with dots in Fig. 27. As is apparent considerable instability prevails in the present case, impeding the setting of a stationary equilibrium of diffusion, as will also be seen from Figs. 28 through 30. First we cast a glance at the variation with time of  $A_i$  in Fig. 27. We note that with a rapid descent of both I and II the barring effect is reduced ( $A_i$  is steeply increased, runs 2 and 3 for layer I; runs 3 through 5 for layer II). A regeneration of the barring effect for both layers occurs when the descent has come to rest (runs 4 through 6 for layer I; runs 7 and 8 for layer II).

We now consider the position of the data relative to the normal ranges of our three basic functions. In doing so we go from the following sequence of values:

Runs 1 through 6 at level of layer I; runs 7 and 8 at level of II, pursuant to the merger of both layers as indicated (dotted) in Fig. 27.

The poorest agreement is found relative to function  $A_i = f(G-PT)$  in Fig. 28. With regard to the G-PT values the exchange coefficients are too low. i.e. the barring effect appears "too strong". This above all applies to runs 5-6-7. But this is the very vague transition phase from I to II with disintegration of II. It is not surprising, then, if during this time interval

an equilibrium situation does not prevail. The positioning of the individual values relative to the normal distribution is already notably better in Fig. 29 ( $A_1 = f(G-E)$ ). Surprisingly, the above mentioned transition phase of runs 5-6-7, of all things, is not out of line here: water vapor gradient and aerosol gradient are here apparently triggered by the same atmospheric process. By contrast, the values of runs 1 through 3, i.e. during the descent of layer I, are outside of normal distribution: The barring effect of the layer appears to be stronger, during this time interval, for the aerosol than for the water vapor. With regard to function  $A_1 = f(G-T)$ , however, - see Fig. 30 - all values of our example (excepting run 5) are within its normal range. From this it would be concluded that with regard to vertical aerosol distribution, approximate diffusion equilibrium must have temporarily prevailed, after all.

Conclusions drawn from this example:

Descent movements of barring layers are coupled with a temporary reduction of their barring effect. The latter is regenerated when the vertical movement has come to rest. In case of a double inversion with disintegration of the lower layer and the suggestion of merger with the descending upper one, the diffusion equilibrium is temporarily disturbed. A discrepancy develops between vertical water vapor and aerosol distribution. A minimum of the equivalent potential temperature above the barring layers, and a maximum near the barring layers were not found which also points toward disturbed equilibrium conditions.

7. Example F, 30 September 1970, Figs. 31 through 34

Clearly defined inversion descents slightly, remains at constant level for some time, finally ascents steeply with simultaneous disintegration. Largely set equilibrium of diffusion.

Interest is particularly held by the phases of ascent and disintegration of the inversion or barring layer. For this reason,

we have represented only runs 4 through 7 by their originals and tables in X. APPENDIX,3. As with the previous runs (from which a descending movement of the inversion is recognized), an increase of temperature and decrease of humidity with height within the inversion zone is also very distinct with run 4. Just one hour later (run 5), however, the T-inversion has temporarily disappeared whereas the humidity decrease was retained, although this structural detail has risen somewhat. During run 6, a T inversion with humidity decrease is again recognized, if at a considerably higher level than before. Hardly any structures are left for recognition during run 7, traces are derived from the tables.

In Fig. 31 we consider the variations with altitude and time. In the morning the well defined inversion descends by about 100 m. During this descending movement the  $A_i$  values are relatively high. With the barring layer becoming stationary, however,  $A_i$  reaches minimum values between no more than 0.6 and 1.5. At 1300 hours an ascent commences, immediately triggering a steep increase in the  $A_i$  values which persists until disintegration of the layer. It is remarkable that in instant case, again, a minimum of the equivalent potential temperature is found above the barring layer (100 m - 200 m vertical interval), with a maximum approximately at the level of the barring layer as such. Only in the case of vertical movements of the barring layer, the EPT maximum, too, is above the barring layer (runs 2 and 7).

Fig. 32 shows that the individual values (2 through 4) are in just barely satisfactory relation to the normal range of function  $A_i = f(G-T)$  only during the time that barring layer has nearly or fully settled. But during the vertical movement they are far outside thereof (1 to 2; 4 to 6).

The two pairs of values for a very low-lying near-ground inversion in the morning ("low"), which rapidly disintegrates thereafter, are within the normal range. The values of our example

are quite satisfactory with regard to the normal distribution of  $A_1 = f(G-E)$ , according to Fig. 33. However, we notice a contrast to Fig. 32: While the inversion has become stationary the values fall insignificantly outside of the normal distribution. The vertical aerosol gradient turns steeper, temporarily, than would correspond to the vapor pressure gradient, whereas agreement prevails during the vertical movements. The values in Fig. 34 are completely outside of the normal distribution of  $A_1 = f(G-PT)$ . We find a cyclic sequence with extreme deviation during the stationary phase of the barring layer. No explanation can be offered therefor, as yet.

Conclusions drawn from this example:

It was confirmed again: Vertical movement (no matter whether up or down) of the barring layer results in an increase of its permeability, its becoming stationary results in a strengthening of the barring effect. The  $A_1$  values of the example are in satisfactory agreement with functions  $A_1 = f(G-T)$  and  $A_1 = f(G-E)$ , slight deviations from the former are found during the vertical movement, from the latter during the stationary phase. The superimposed minima or maxima, respectively, of EPT are found to exist throughout, even during the vertical movements.

8. Example G, 28 September 1970, Figs. 35 through 38.

Considerable vertical and structural variations of an inversion. Equilibrium of diffusion is not attained.

This example concludes our discussion of cases with vigorous vertical movements of barring layers. The original runs in APPENDIX, 3 already show that not only does a distinctive vertical unrest prevail but also the pattern of the structures is changing rapidly. We immediately pass on to Fig. 35. The variations with time of  $A_1$  are particularly remarkable. Steep increases of  $A_1$  are invariably found when - in accordance with our earlier experience - the level of the barring layer

is rapidly changed. This is very drastically demonstrated by the transition from run 2 to 3:  $A_1$  is increased by two orders of magnitude and remains persistently high during the subsequent ascent movement (3 to 4). Not until the stationary condition of the barring layer exists during runs 6 and 7, does  $A_1$  arrive at a minimum. Renewed disquiet from runs 7 through 10 causes  $A_1$  to increase again.

The vertical displacements of the various structural elements, according to Fig. 35, present an almost confusing picture: True, minimum and maximum of EPT are still always found and in not too great vertical distance from the inversion level (as a maximum a few 100 m, as an average 200 m), but the maximum is sometimes above, sometimes below the barring layer. Even the respective strongest gradients of T and E are not - as usual - close to each other. Vertical differences up to 150 m are encountered. Besides, maximum G-T is sometimes above, sometimes below maximum G-E.

Due to the sometimes extremely poorly developed temperature gradients Fig. 36 contains only very few individual values. As was to be expected, they are far from the normal distribution of function  $A_1 = f(G-T)$ .

It is all the more surprising that, in Fig. 37, the individual values fit very well into the normal distribution of  $A_1 = f(G-E)$ . Although most certainly the setting of an eddy diffusion equilibrium was not possible in our instance the variations with time of the aerosol gradient (expressed in terms of the behavior of  $A_1$ ) and of the water vapor gradient (G-E) are in good agreement with each other. The interferences, apparent from the continuous structural changes of the aerological pattern and from the vertical variations, thus took effect, in Example G, upon aerosol and water vapor distribution analogous to and on the basis of, the normal relation of  $A_1 = f(G-E)$ . In Fig. 38, the individual values of our example are far from the normal distribution of  $A_1 = f(G-PT)$ : We find a cyclic sequence for runs

2 through 7 and another one from 7 through 10. We find it interesting that the first cycle, if defined only from 2 through 6, comprises exactly the first ascent, the second cycle from 7 through 10 the second ascent. It appears to be possible to describe, with the aid of these cyclic "movement graphs", the structural variations connected with processes of ascent or general vertical displacement, and later to improve our understanding of them functionally. At any rate, in retrospect we may say that the cycles in the following earlier figures were connected with vertical movements of the barring layer: Fig. 34 (runs 2 through 6, initial lingering, then rapid ascent with disintegration of the inversion); Fig. 30 (runs 4 through 8, initial descent, then merger with lower disintegrating inversion). An exception relative to all three normal functions is formed by Example D with its cycles. True, there is no vertical movement here, but a clearly cyclic loosening up of the inversion structure (runs 1 through 5) by turbulences in the course of the day. So it will be necessary to pay still more attention to such graphs with a cyclic pattern, in the future, along with further meteorological parameters.

Conclusions drawn from this example:

In the case of violent structural and vertical changes of the barring layer eddy diffusion equilibrium cannot come about. It is, however, possible that variations of the vertical aerosol profiles and water vapor profiles are running in conformity with each other and are jointly controlled by the interferences determining the complex pattern. Again it is shown that vertical movements of the barring layer are connected with a reduction of its barring effect. During vertical movements a cyclic sequence of the values is found relative to the normal distribution of the function  $A_1 = f(G-PT)$ .

9. Example H, 26 September 1970, Figs. 39 through 43.

Analysis of (a) the upper boundary of the exchange layer,  
and (b) an ascending inversion located below.

With this example we leave the analysis exclusively of inversions or similar structures analogously belonging thereto. We consider parameters from the zone of the upper boundary of the exchange layer. However, in the present case there is also an inversion which we shall include in our considerations. The inverse temperature gradient is only rather poorly defined, however.

To begin with we go back to the original recordings in X. APPENDIX, 3. The position of the upper boundary of the exchange layer there has been marked with E, that of the inversion with I. In the profile of +L (partly also in that of -L) the increase by increments with height is recognized at the two levels so marked. Until evening (run 6), however, the structures disintegrate to a large extent. What clearly remains is the +L increment in the zone of the loosened-up structure of E.

In Fig. 39 we consider the variations in time and space of the two formations. From the value tables to Example H it is seen that the exchange layer is marked by a minimum and a subjacent maximum of the equivalent potential temperature EPT similar to what we had found with stationary inversions as a rule. The altitudes, of these structural details are entered in Fig. 39. Whereas in the course of the day the upper boundary of the exchange layer perpetually descends, the - weakly defined - inversion ascends in increments, above all from run 5 to 6. The rule found confirmed for stationary inversions, according to which EPT shows a minimum above the inversion, and a maximum below it, applies in the present case, too. These EPT structure details follow suit with the vertical movement of the barring layer proper.

Now a few words on the variation with time of the  $A_i$  values, considering Fig. 39: The barring effect of the inversion is

the greatest in the morning, and steadily decreases in the course of the slow ascent of the layer ( $A_i$  is growing). Another deterioration of the barring effect occurs in the evening as the layer ascends again. By contrast, the diffusion resistance through the upper boundary of the exchange layer increases by increments ( $A_i$  decreases) as the latter descends. In conjunction with the commencing disintegration of both layers in the evening, consistently the  $A_i$  values increase.

Due to the very scantily developed inverse temperature gradient a study with respect to function  $A_i = f(G-T)$  is foregone. Fig. 40 merely reflects the travelling times for the runs, and the symbols for the exchange layer (E) and inversion (I).

On Fig. 41 we note that the individual values for I are within the normal range of function  $A_i = f(G-E)$ , even so when G-E is positive (viz. when water vapor pressure is increased with height). The values of E, too, just barely meet these requirements, however, no dependence upon the water vapor gradient is apparent. The values for  $A_i = f(G-PT)$  in Fig. 42 are entirely outside of the normal distribution for this function. This is independent of whether they pertain to the exchange layer or to the inversion.

In Fig. 43 we have plotted the vertical profiles of  $A_i$  for runs 3 and 6. These once more very clearly illustrate the following processes:

- a) descent and increase of barring effect of the upper boundary of the exchange layer;
- b) ascent and decrease of barring effect of the inversion. finally approximate mutual touching of the two layers.

Conclusions drawn from this example:

The upper boundary of the exchange layer, too, is characterized by a minimum of EPT plus a subjacent maximum of EPT. During descent of the upper boundary of the exchange layer its barring effect toward eddy diffusion is increased.

10. Example I, 17 September 1970, Figs. 44 through 45.Upper boundary of an exchange layer. Slight vertical movement.

In conclusion, we shall discuss the case of an upper boundary of the exchange layer which was sharply defined throughout the day. The original runs in APPENDIX, 3 very convincingly demonstrate the following within the zone of this layer: (a) an increase in temperature; (b) a decrease in humidity; and (c) a sharp increase in conductivity, i.e. a decrease of the aerosol concentration. These vertical variations are very distinct during runs 1,3,4; during run 2 the structure are loosened up, and the level of the layer has descended somewhat. In the following figures we have plotted, for comparison, the values of the main levels separately from the values of the special levels.

In Fig. 44 we first consider the variations with time and with altitude. To begin with it is to be pointed out that this level, too, is distinct for sharply defined minima of EPT above it, and corresponding maxima within its level. These EPT structural details follow suit in the slight vertical movement of the upper boundary of the exchange layer. During the temporary descent of the layer (run 2)  $A_i$  arrives at a maximum, i.e. movement reduces barring effect as with a true inversion.

Fig. 45 shows that all individual values are outside of the normal range of function  $A_i = f(G-T)$ . If we concentrate on the main levels only, G-T changes in the course of the day, it is true, but this has little impact on  $A_i$  (maximum during 2, see above). If we consider the special levels we obtain a cyclic progress which is surely coming close to the true conditions and corresponds to our experience gathered so far on the occurrence of cyclic interrelations.

In Fig. 46, using the values from the special levels we find a time slope which, it is true, keeps to the border line of the normal range of our function  $A_i = f(G-E)$  but in agreement with

the latter's direction. If we lean on the values from the main levels only,  $A_1$  remains unaffected by the variations of G-E.

An analogous conclusion is drawn from Fig. 47. If, however, we start from the values of the special levels we are again met with a cyclic pattern, although all the values are far from the normal distribution of function  $A_1 = f(G-PT)$ .

In Fig. 48 we have plotted the vertical profiles of  $A_1$  for runs 2,3,4. The stepped curves are based upon the values from the main levels. The  $A_1$  values from the special levels within the barring layer level are indicated (solid) and identified by numerals in circles. It is seen how across 1000 m from the barring layer downwards, consistently high  $A_1$  values are encountered which is appropriate for an exchange layer. The loosening-up of the structure of the barring layer is clearly recognizable.

Conclusions drawn from this example:

Values derived from the special levels afford a much deeper insight into the true interrelations. The upper boundary of the exchange layer is again marked by EPT minima and maxima, one above the other with intervals of 150 m up to 300 m (EPT maximum within the levels of the layer). These structural details join in any vertical movements of the barring layer. Vertical movements lead to a weakening of the barring effect of the layer. The vertical movement is expressed in cyclic pattern or part of the values relative to the normal ranges of our main functions.

## VI. THEORETICAL SUPPLEMENT FOR COMPUTATION OF EDDY DIFFUSION

COEFFICIENTS

In (1.2) only the asymptote solution to the stationary combined diffusion ( $D$ ) and coagulation ( $K$ ) equation

$$D \frac{\partial^2 N(z)}{\partial z^2} - K N(z)^2 = 0 \quad (1)$$

was used for the calculation of the eddy diffusion coefficient  $D$  (pages 25 et sequ. of (1)), i.e. that solution which extends to infinity. This presupposition without which the equation (1) is not analytically solvable applies strictly speaking only in that case where  $D$  does not vary with height. Where diffusion coefficient  $D_i$  differ from layer to layer, the partial solutions  $N_i(z)$  to (1) must, for reasons of continuity, be so joined together that the diffusion current  $J = - D \partial N / \partial z$  is a steady one. If  $N_i(z)$  and  $D_i$  designate the nuclei concentration and diffusion coefficient in the vertical interval from  $z_i$  through  $z_{i+1}$ , the following must then apply:

$$D_i \frac{\partial N_i}{\partial z}(z=z_i) = D_{i-1} \frac{\partial N_{i-1}}{\partial z}(z=z_i) \quad (2)$$

to all  $i$ 's.

Under these premises the equation (1) is no longer analytically solvable. The general solution or its inverse function, respectively, has the following form:

$$Z - Z_0 = \pm \int_{N_0}^N \frac{dx}{\sqrt{(N_0')^2 + \frac{2K}{3D} (x^3 - N_0^3)}} \quad (3)$$

wherein  $N_0$  and  $N'_0$  designate the nuclei concentration and its derivative at position  $z_0$ . In the source-free stationary case,  $N$  must decrease with height, and the minus sign on the right side of (3) applies.

Solution (3) represents an elliptic integral which is solvable only through methods of approximation. In addition, this is a variation problem. Therein,  $D$  in the integrand must be selected so that both members of the equation (3) are in agreement with each other. The derivative  $N'(z)$  needed for the joining condition (2) are easily obtained from the inverse function  $z(N)$ :

$$N' = \sqrt{(N'_0)^2 + \frac{2K}{3D} (N - N_0)^3} \quad (4)$$

The equations (2) through (4) must be solved by layers wherein it would be best to use, for the top layer, the asymptote solution, compute therefrom the diffusion current at the lower border, and use the latter to solve the equation (3) for the next lower interval. This operation is to be repeated as often as necessary.

It is true that in principle this problem is solvable with the aid of our Hewlett-Packard desk computer with extended memory. However, this procedure requires such a high expenditure of computation effort that it would hardly appear applicable to the routine analyses. At present, a computer program is being developed for this purpose, with the aid of which it is being studied on a few selected examples what size deviations are permissible from the results of the procedure now applied in a routine manner. It is noted that due to the wide range of variation of  $D$  it will not be necessary to strive for a maximum of exactitude.

The procedure can always be used on any cases of particular interest in order to obtain more exact results.

The results of such comparisons will be reported and discussed in the next report.

#### VII. CONCLUSIONS

So much is certain that it would not have been possible to carry out either the statistical investigations or the detailed analyses on individual examples, without the preceding change-over of the routine evaluations and data processing to a largely electronic basis. It was only this measure that resulted in a sufficiently comprehensive mass of homogenous data from all available soundings for statistical purposes, on the one hand, and in a complete stock of all necessary parameters of the most varied kind per sounding for the detailed analyses, on the other. In practical processing of the electronically obtained data it was revealed that the most recently developed procedure of electronic data processing fully meets requirements.

The statistical analyses in logical continuation of the earlier research work revealed that there is a significant relation between the highest inverse temperature gradient and the incremental exchange coefficient, providing that there are stationary inversions with a set eddy diffusion equilibrium. The scatter of this relation is unimportant. The relation applies to an  $A_i$  range from 0.1 to 300. Under the same conditions (stationary situations, barring layers) a significant relation may be derived, too, between the highest positive gradient of potential temperature and the incremental exchange coefficient. It applies to the  $A_i$  range from 0.8 to 100. The scatter is not great, more data must be added.

The third of the three derived main functions for describing the behavior of  $A_i$  in structural zones (inversions, barring layers, upper exchange boundary), is based upon the vertical gradient of water vapor pressure. Again, a significant relation

was found with relatively insignificant scatter of values. It is valid for the  $A_1$  range from 1 through 100.

Finally it was attempted to discover more general interrelations which would apply quite generally, independently of structural details (inversions, barring layers). In doing so, another relation was found to stand the test:  $A_1 = f(G-PT)$  whose scatter is surprisingly small and whose range of applicability is between  $A_1 = 1$  and 1000.

Such main functions which are to have more general validity can be derived only if certain criteria of selection are applied. Such criteria, however, can grow only from sufficient experience. With increasing experience, however, the criteria must be improved, supplemented or, if need be, essentially changed, each of which means a reprocessing of the data material. This work, this is understood, can be performed only in a step-by-step manner.

In developing criteria of classification and selection, the detailed analyses proved to be especially helpful. Systematic work according to this method has only just begun. It already resulted in a series of valuable results. Some of these are: A minimum of the equivalent potential temperature is found 100 m or not more than 300 m above an inversion or barring layer resting in eddy diffusion equilibrium, and a maximum is found within the level of the layer proper. Within the zone of the barring layer proper the gradient of potential temperature reaches a maximum, likewise the negative gradient of the vapor pressure. If the temperature gradient is positive, it assumes a minimum, if it is negative, a maximum. As a rule, a minimum of the vapor pressure, narrowly limited in space, is also found within the level of a barring layer. If barring layers get into vertical movement their barring effect is reduced for the duration of such movement. After the barring layer becoming stationary its barring effect may be regenerated. Temporary interferences leading e.g. to a vertical movement of the barring layer or

triggering a loosening-up of its structure due to locally limited convection are usually expressed in cyclic patterns of the time slope of the essential parameters in the level of the barring layer.

The above discussed detailed analyses which, in the form presented, represent only an initial step, are calling, in order to be fecundated, for the use of all available microscale and mesoscale meteorological parameters (radiation, wind profiles, cloudiness) and their variations with time.

Although it is absolutely necessary to further increase the data material, to further develop and improve the scientific procedures of analysis, still some results are available even today which are possible of practical application by the meteorologist. This applies most of all where it is necessary, from the profiles of aerological data as supplied by radiosondes, to draw conclusions, quickly and directly, upon the conditions of vertical propagation of suspended matter.

#### VIII. OUTLOOK ON ADVANCED STUDIES IN THE NEAR FUTURE

##### 1. General

Since the methodism for recording the exchange conditions up to 3000 m a.s.l. is now completely commanded and fully developed, it would be the obvious next step to expand the investigations at least up to and including the tropopause level. This expansion is further encouraged by another fact:

A program is being carried under contract with US AEC at our institute, for the investigation of stratospheric-tropospheric exchange using the tracers Be7, P32, S35 plus fall-out heavy-metals, the concentration of which is recorded at Zugspitze station for 24 hours at a time (see (3)). The tropopause structures are analyzed with the aid of radio-sonde data from the

Atlantic Ocean and Europe, and attempts are made to calculate the trajectories.

So the following situation exists:

- a) With the aid of cable-car telemetry systems we gain a precise insight into the exchange conditions obtaining between 0.7 and 3 km a.s.l.
- b) With the aid of the above-mentioned tracers we can survey transportation processes from the stratosphere down to the upper troposphere.

If it were possible, now, by means of appropriate additional methods to also cover the exchange conditions between upper troposphere or, even better, between lower stratosphere and 3 km a.s.l., we would have the chance to completely investigate the overall exchange from the stratospheric deposits at 10 or 20 km down to the surface of the earth at 0.7 km a.s.l. Such an expansion of our research program would increase our yield of findings by a multiple in regard to the vital problem of the atmospheric aerosol exchange.

## 2. Procedures to be applied

### a) Lower Troposphere

The procedures per 1) - 5) will be applied without restriction during the continuation period.

### b) 3 km a.s.l. up to lower stratosphere

The only one but the most effective and useful method to present itself is a combination of Rawinsonde with Lidar. Under good weather conditions and with a powerful Lidar, aerosol structures as far as the Junge layer at approx. 15 km may be covered and observed in time. The aerological data necessary for the scientific analysis of the aerosol movements are supplied by a special Rawinsonde of our own. The technical requirements for

such an essential and methodic expansion are presently being reviewed. Already now, some preparations are being made, such as the construction of a balloon filling hall adjacent to the new institute building (for radiosonde balloons), the construction of which has just begun, and the erection of a lidar observation and set-up room on the roof platform of the institute. Negotiations with suppliers have been conducted and technical details agreed on.

#### IX. REFERENCES

- 1) Reiter, R., R. Sládkovič and W. Carnuth:  
Atmospheric Aerosols between 700 and 3000 m a.s.l.,  
Part IV., Contract DAJA-37-690-1357, July 1970.
- 2) Reiter, R., R. Sládkovič and W. Carnuth:  
On Fine Structures and Control of Vertical Aerosol Exchange between 700 and 3000 m a.s.l.  
Arch. Met. Geophys. Bioklim. Ser. A (in print).
- 3) Reiter, R., R. Sládkovič; K. Pötzl, W. Carnuth and  
H.-J. Kanter:  
Measurement of Airborne Radioactivity and its Meteorological Application.  
Contract AT (30-1)-4061, Oct. 1970,  
Arch. Met. Geophys. Bioklim. Ser. A (in print).

X. APPENDIX

1. Figures 1 - 48

2. Legends to the Figures 1 - 48

3. Individual Runs and Data Tables

Examples A - J

4. Tables I - XII

RaB concentration measured on the Zugspitze (Z), the Wank (W) and in Garmisch-Partenkirchen from July 1970 to June 1971

5. The Computer Program

for computation of all necessary values from the original runs. Tables of results as examples, see 3.

1. Figures 1 - 48

Fig. 1

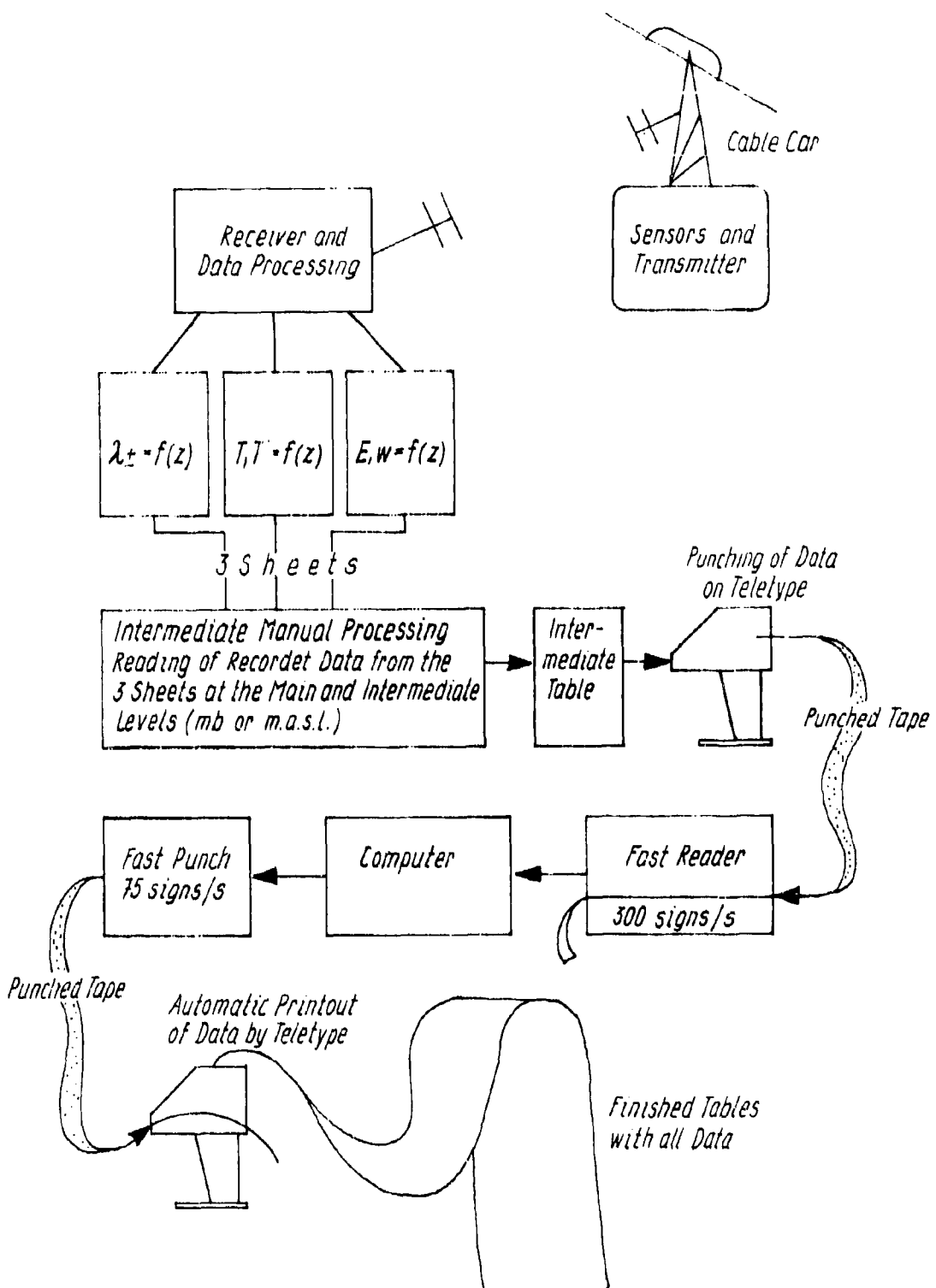


Fig. 2

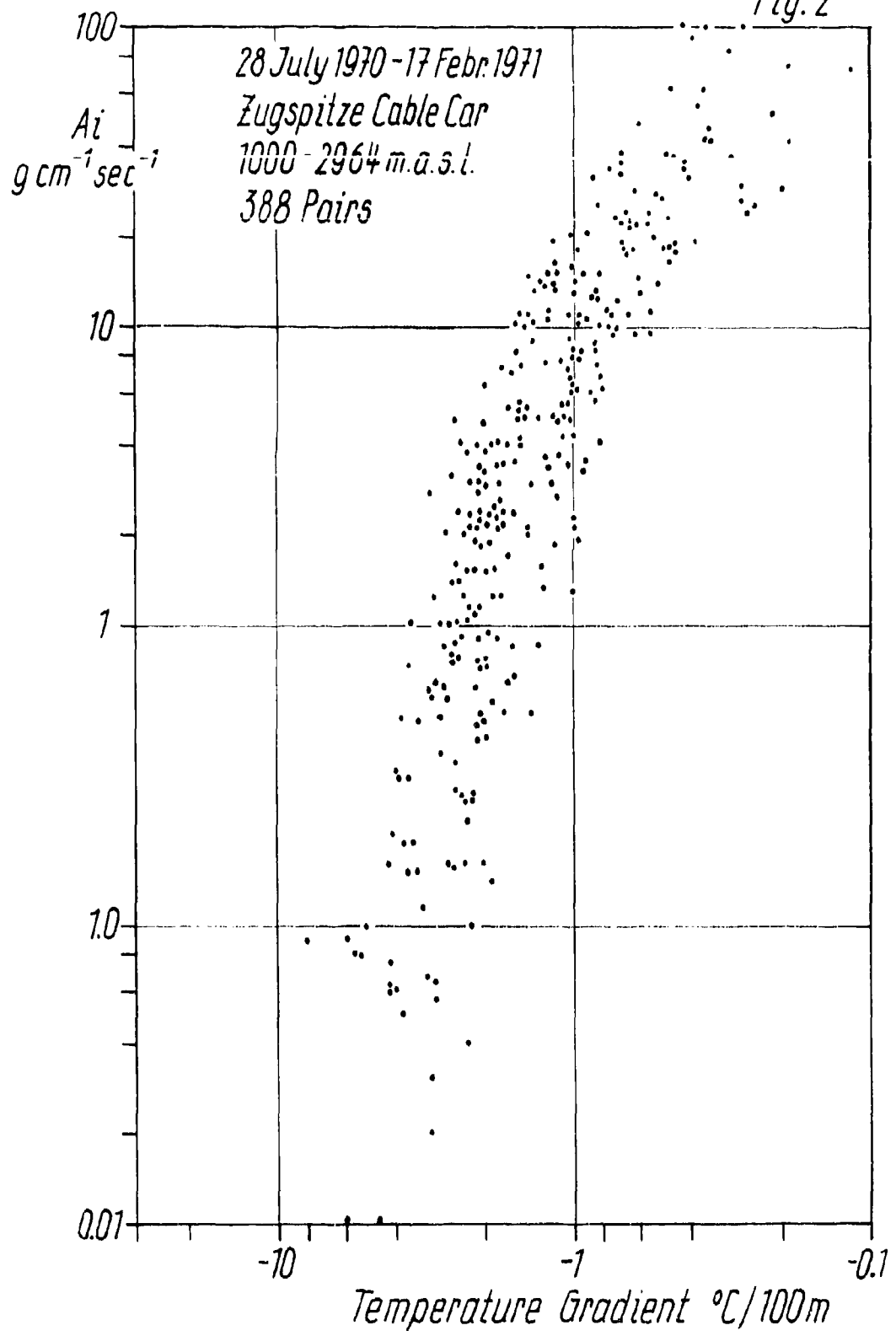


Fig.3

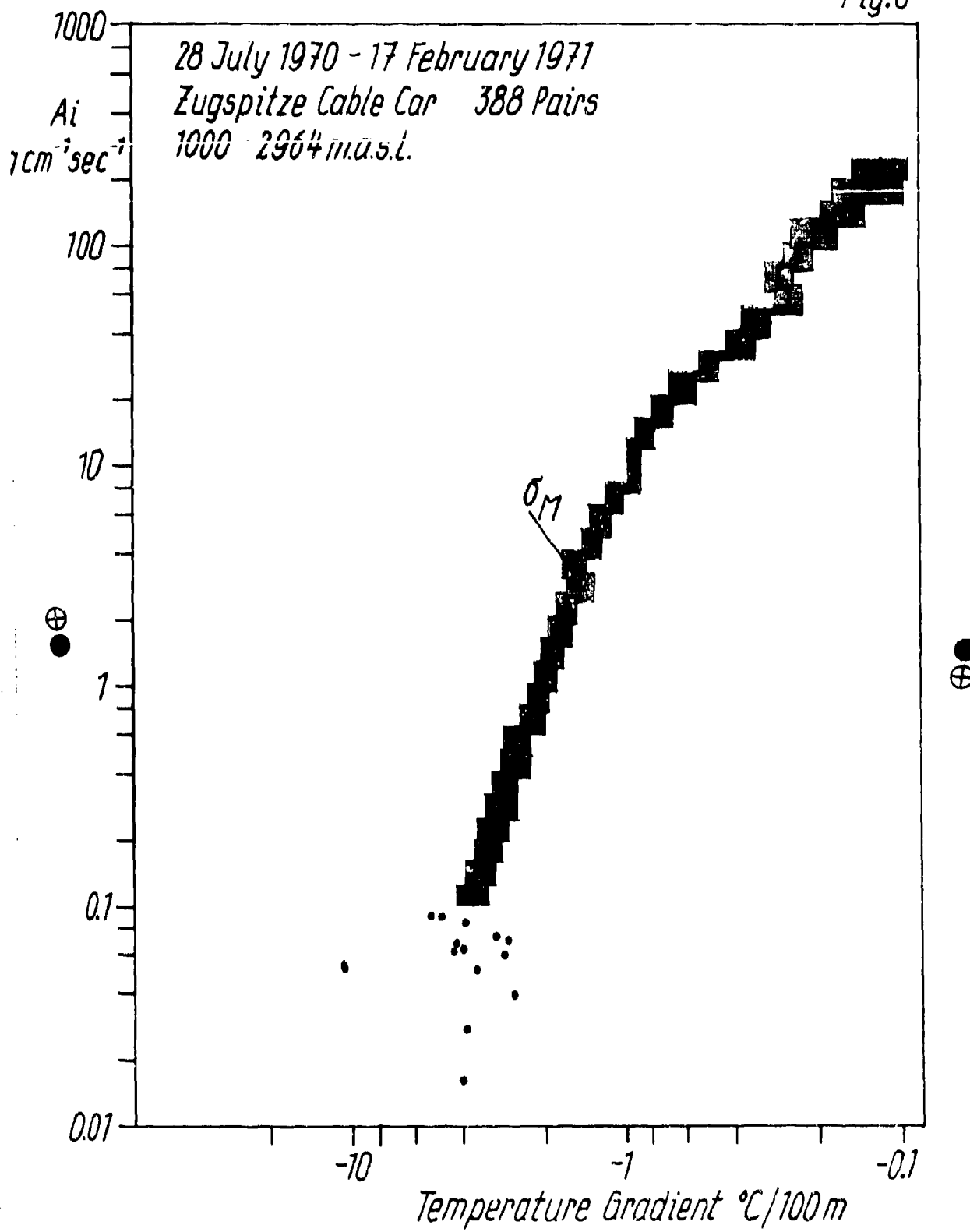


Fig 4

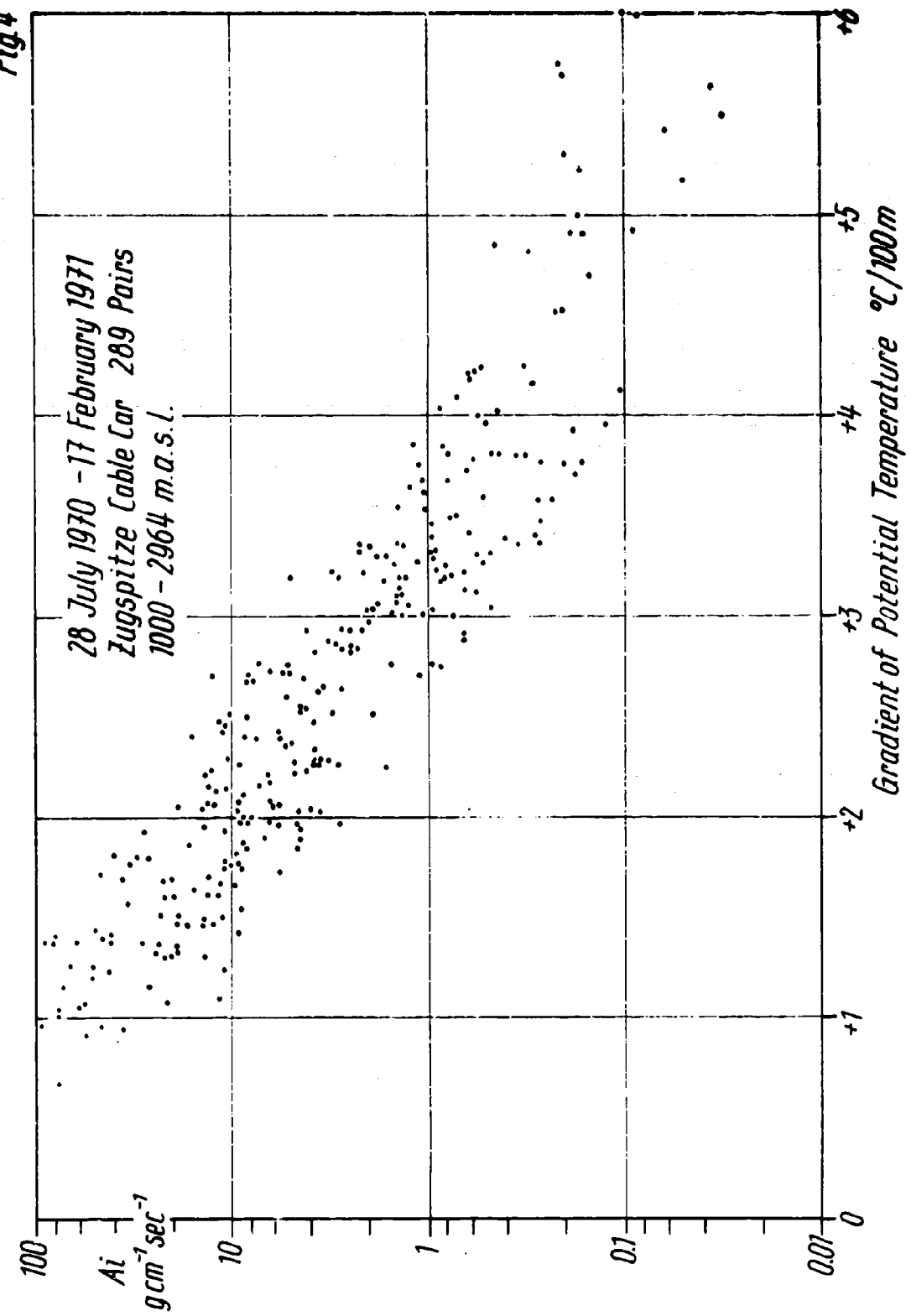
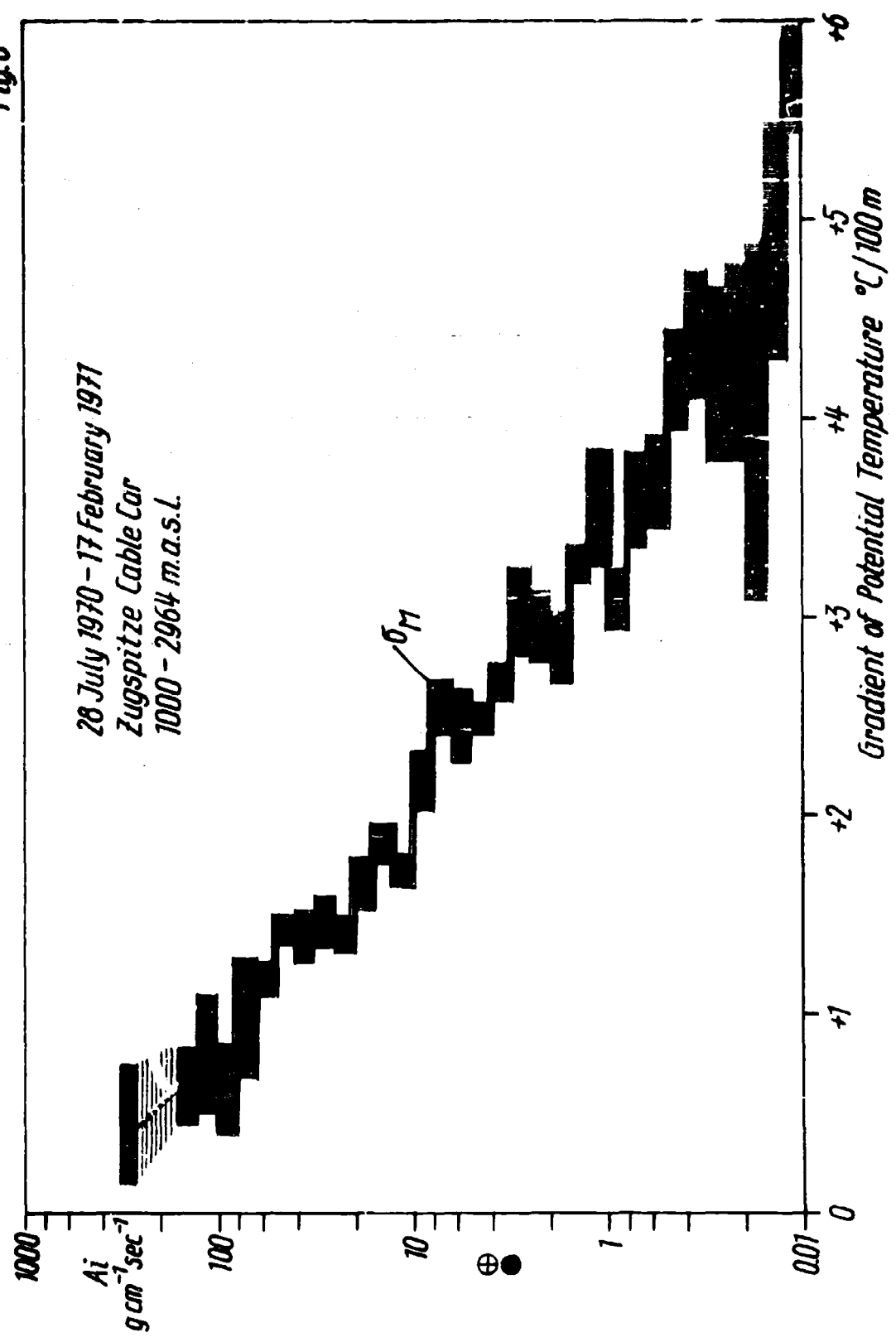


Fig. 5



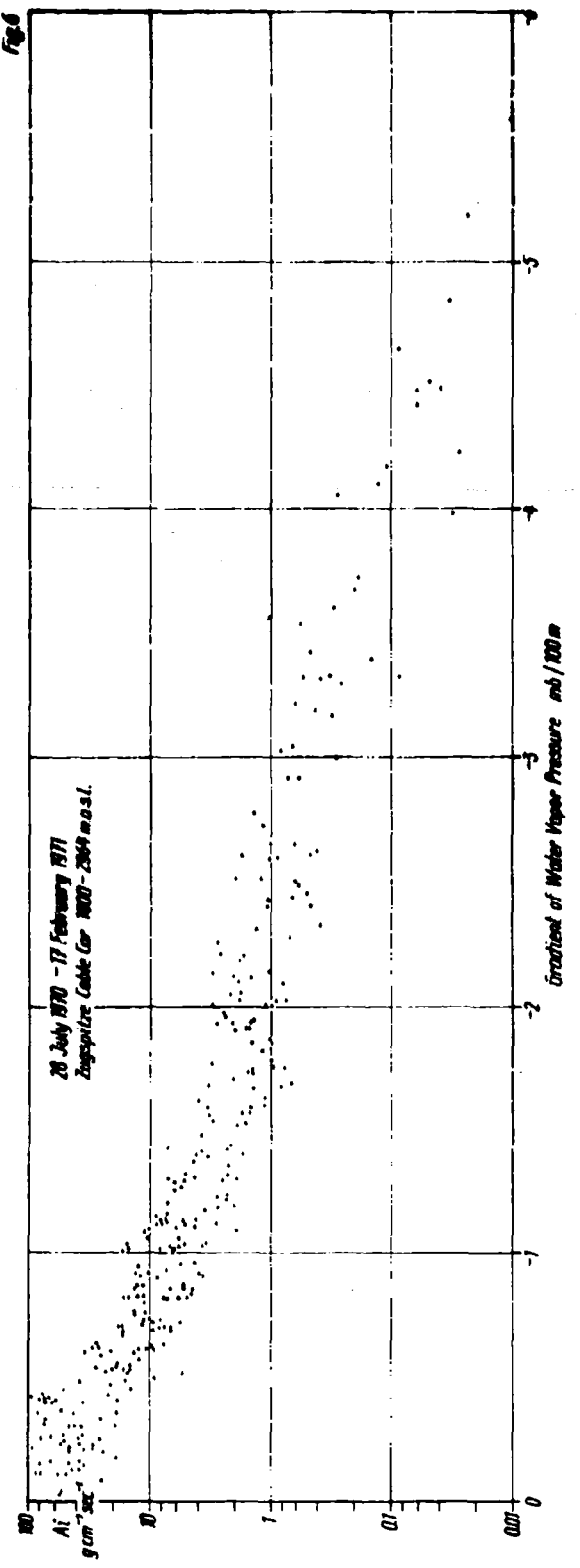
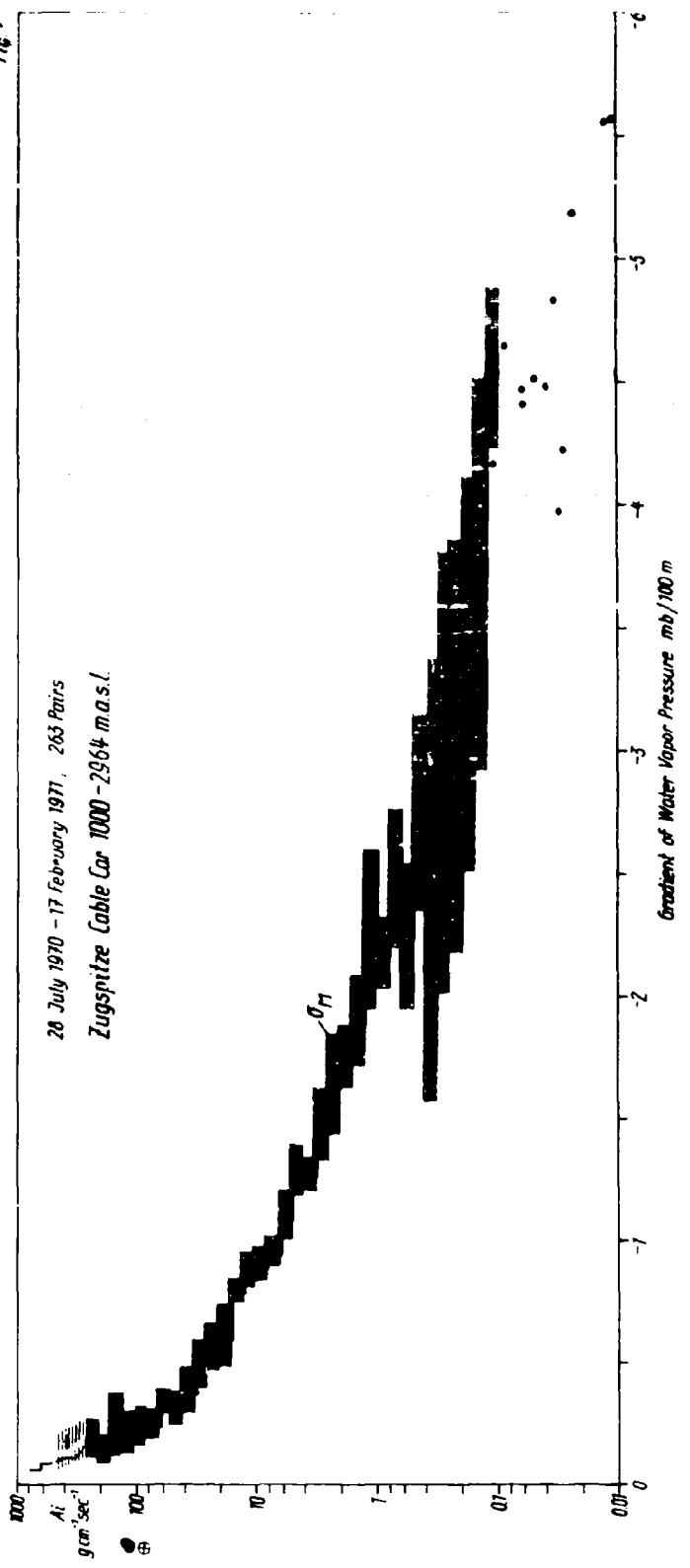
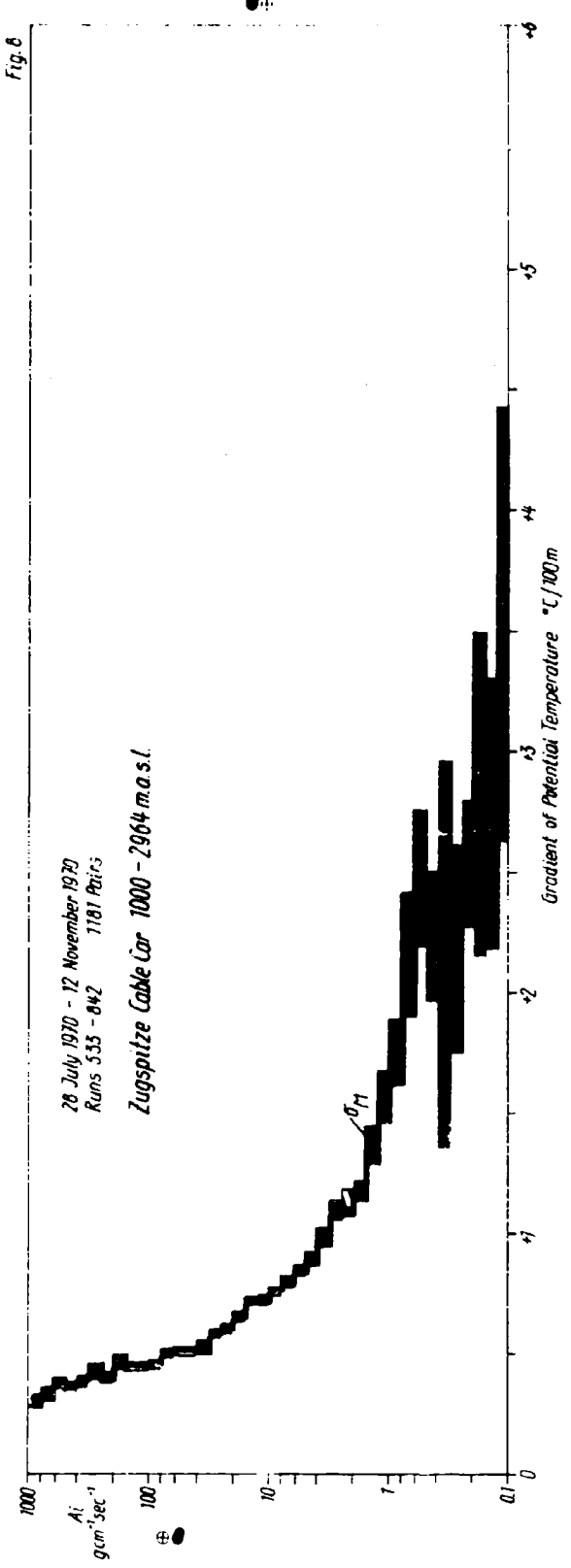


Fig. 1





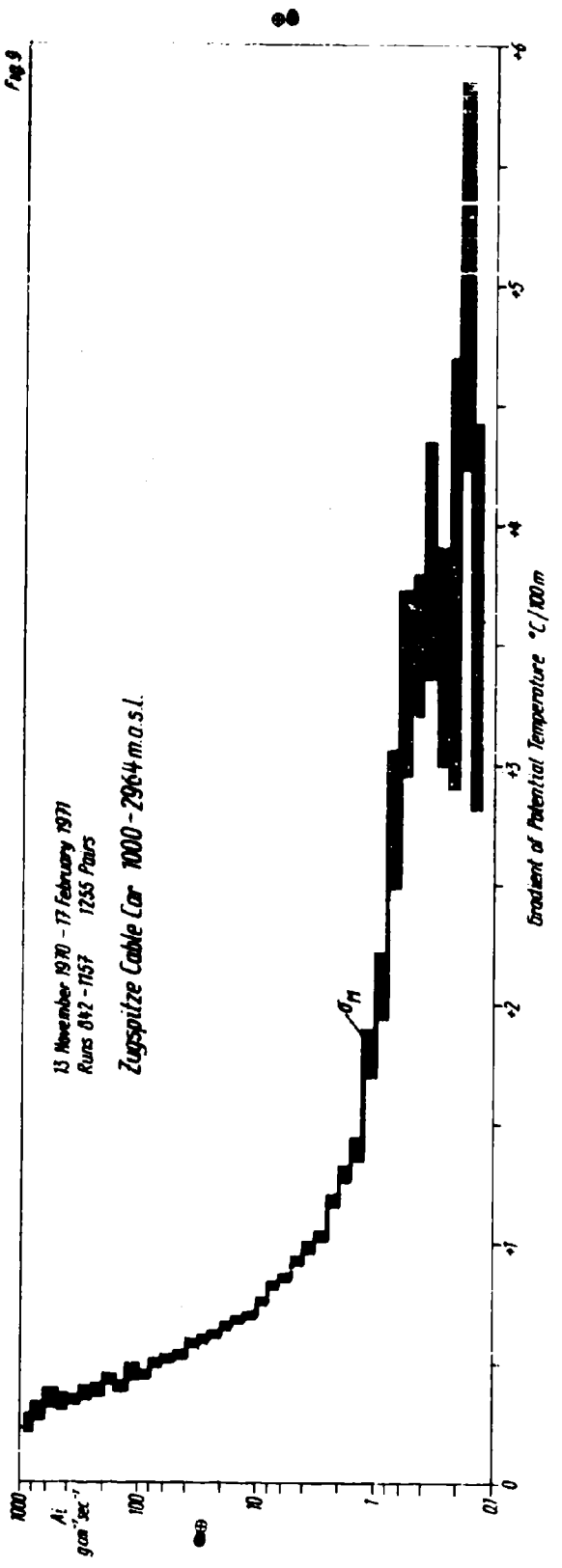
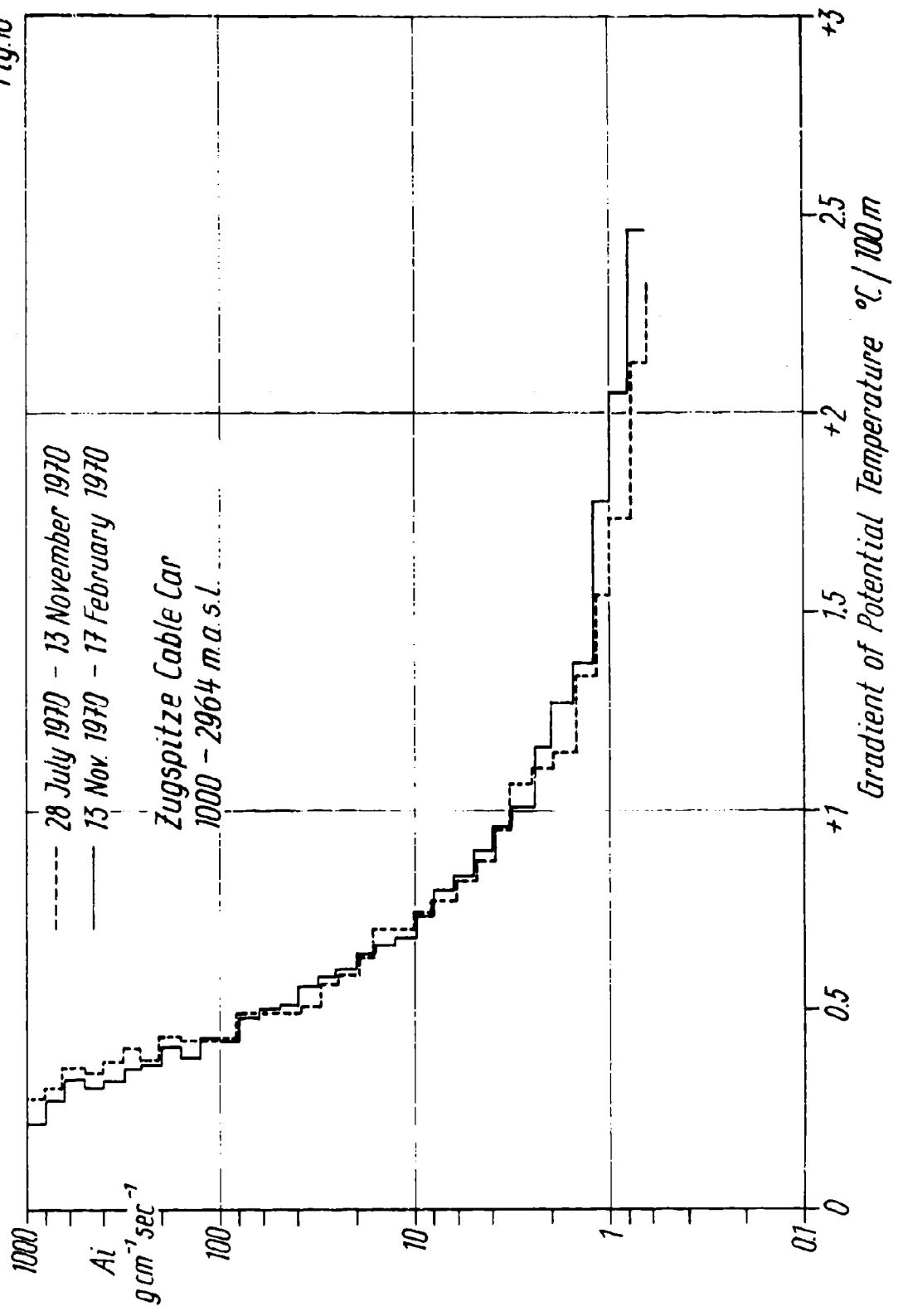
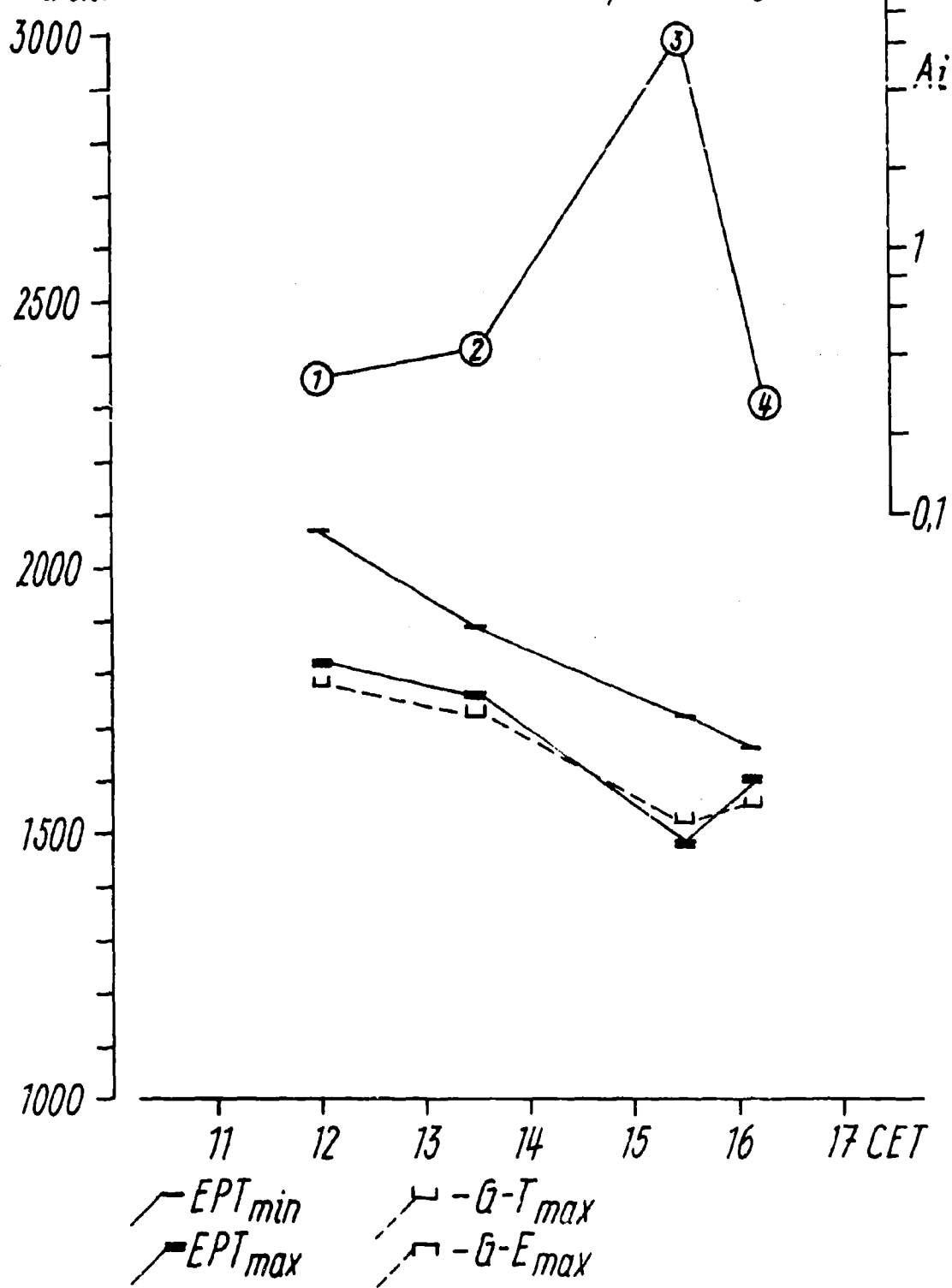


Fig. 10

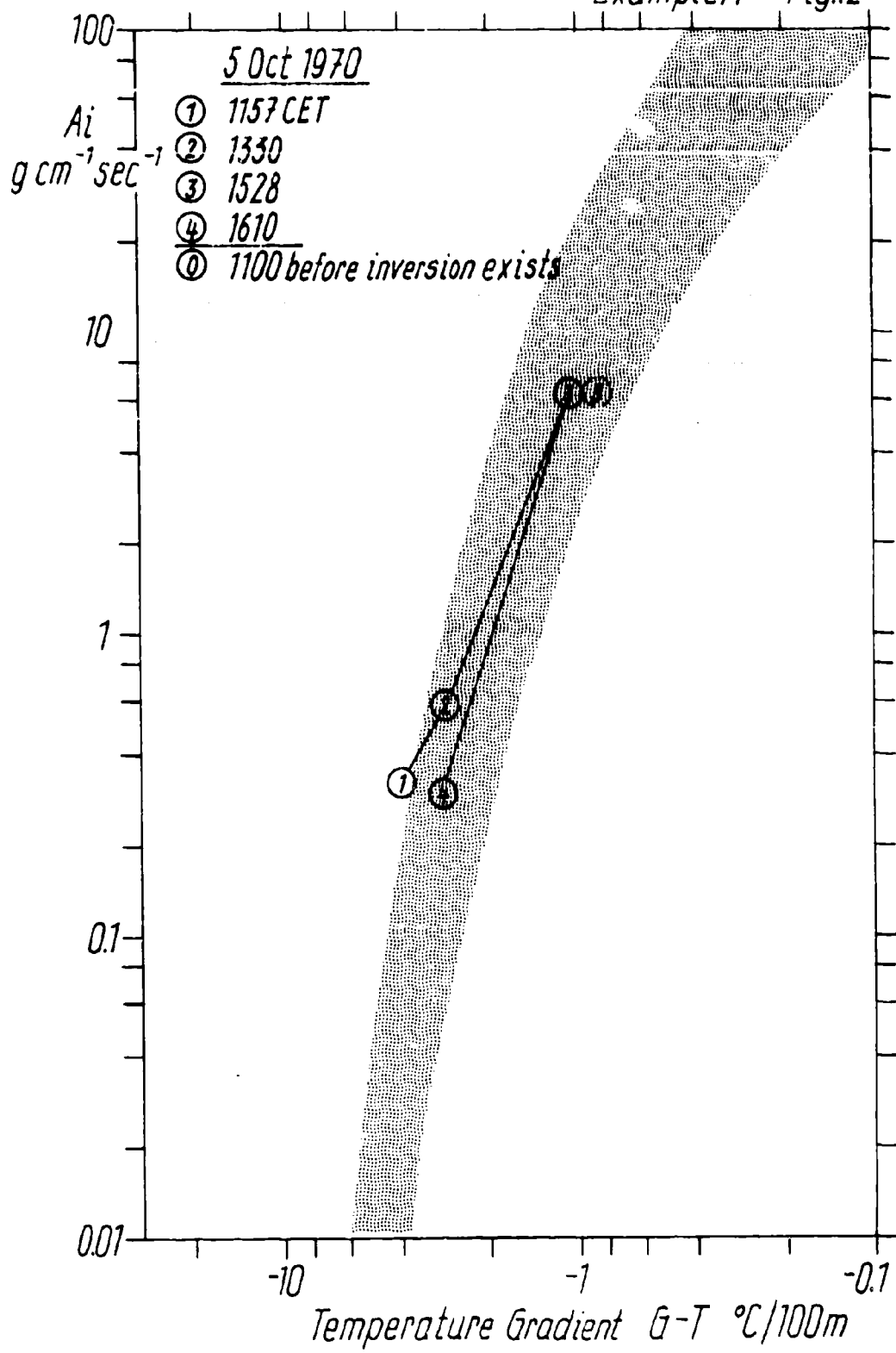


m.a.s.l.

5 Oct 1970 Example A Fig.11



Example A Fig.12



5 Oct 1970

Example A

Fig 13

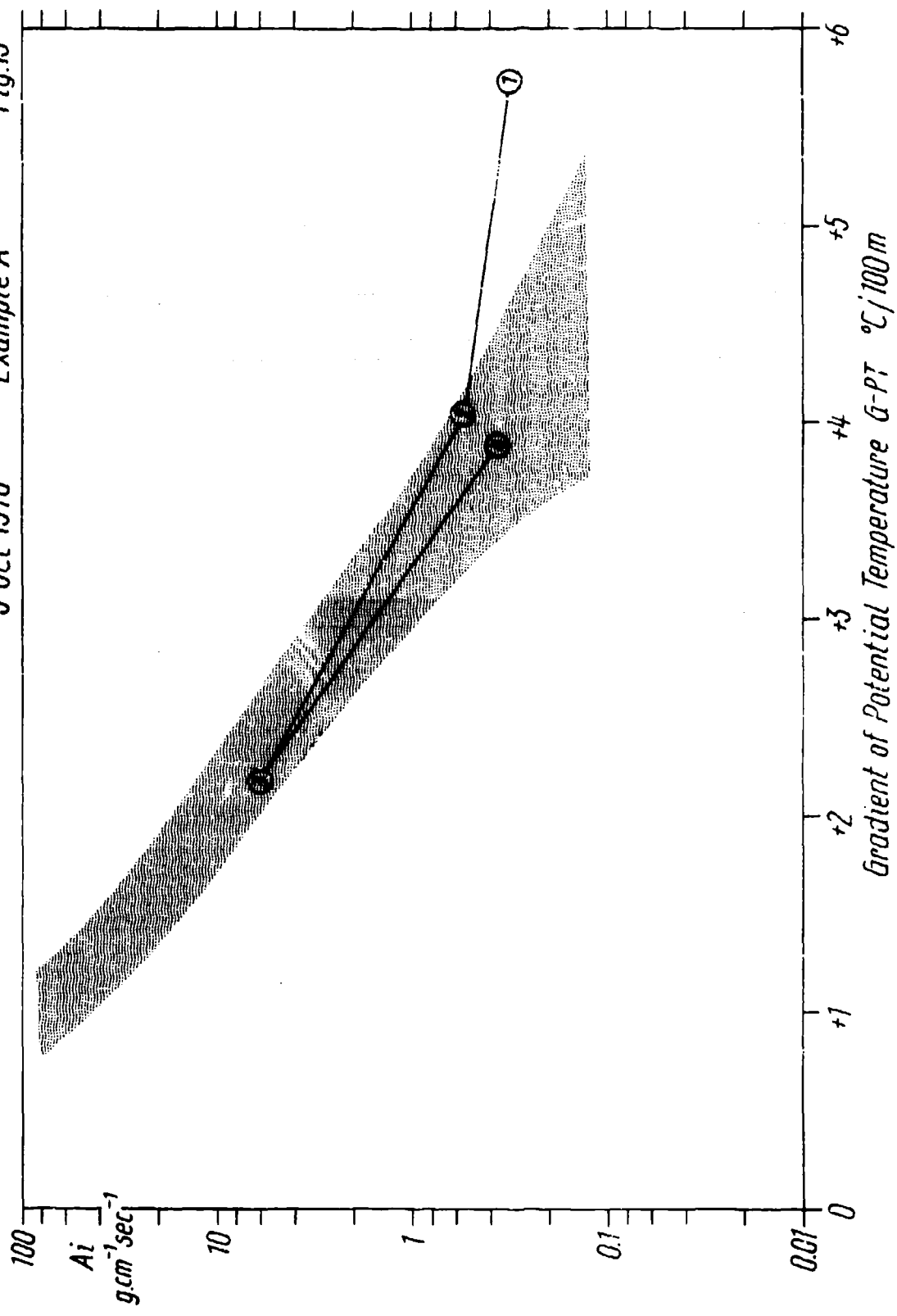
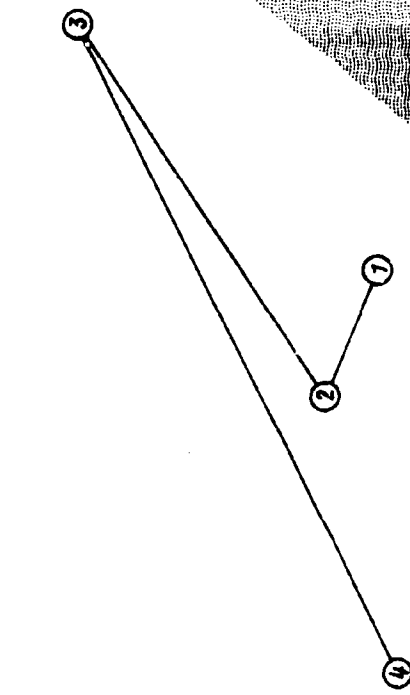


Fig. 14

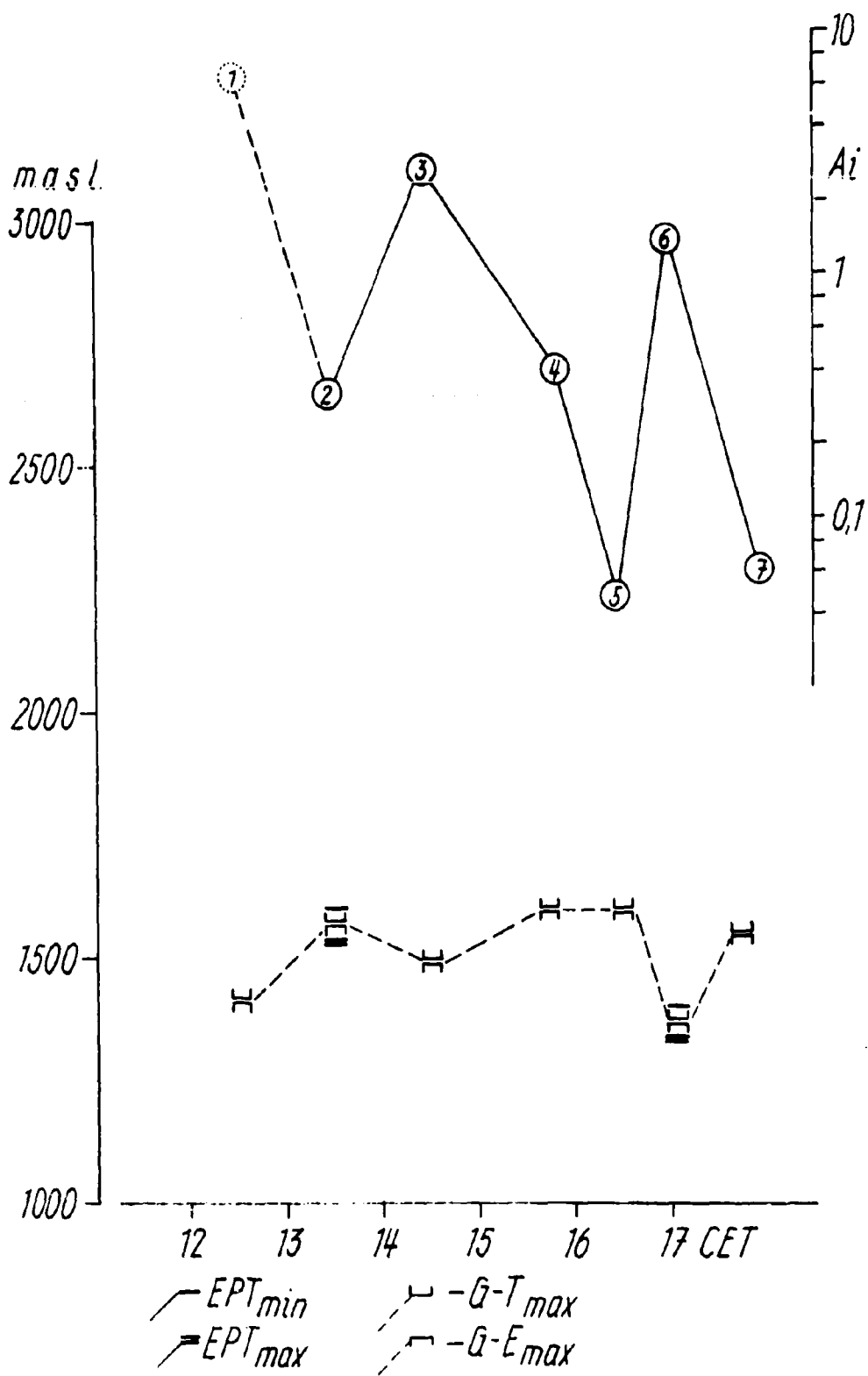
Example A

5 Oct 70

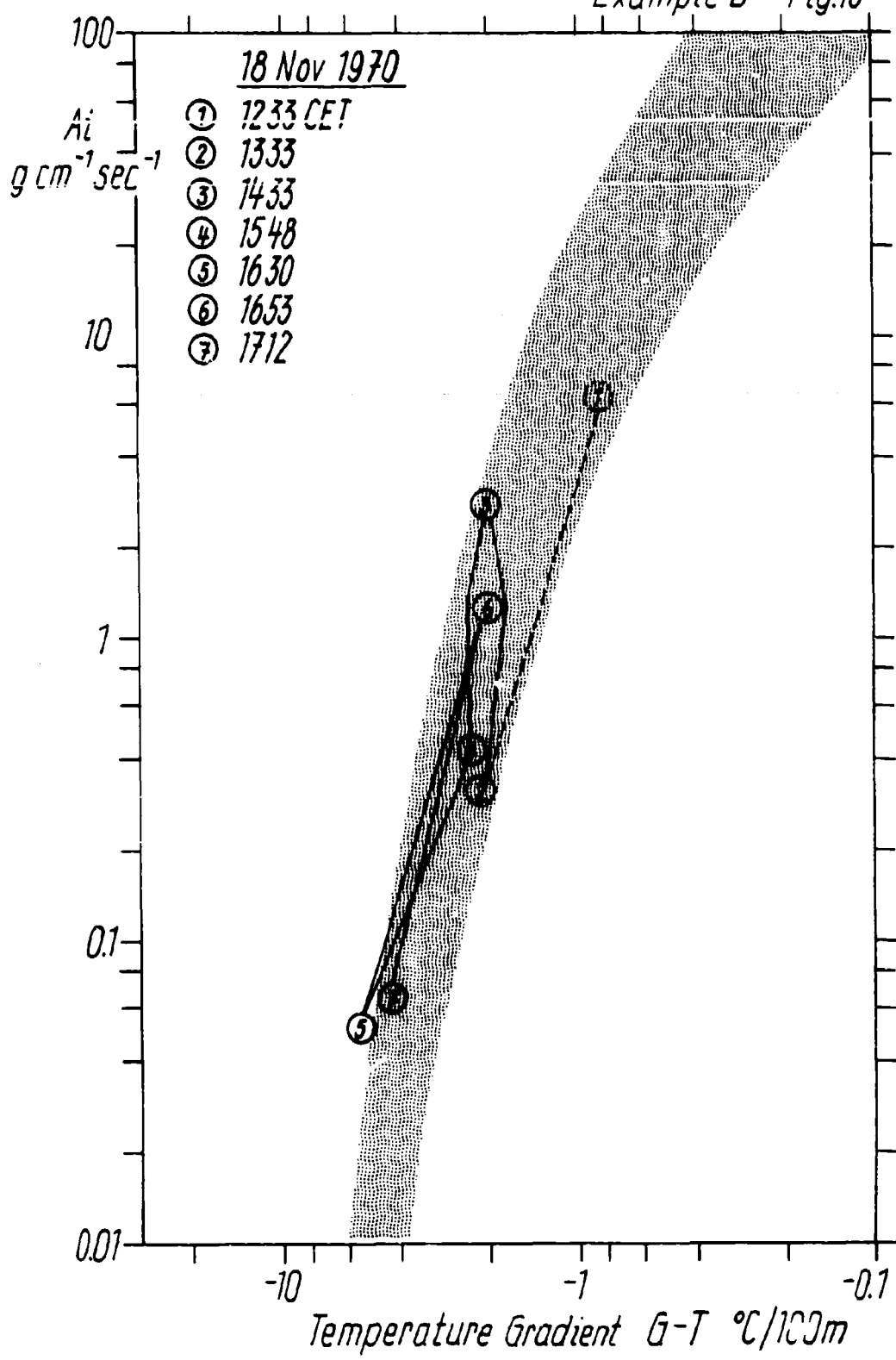
$A_i$   
 $g \text{ cm}^{-1} \text{ sec}^{-1}$



18 Nov 1970 Example B Fig. 15



Example B Fig.16



18 Nov 1970

Fig 17 Example B

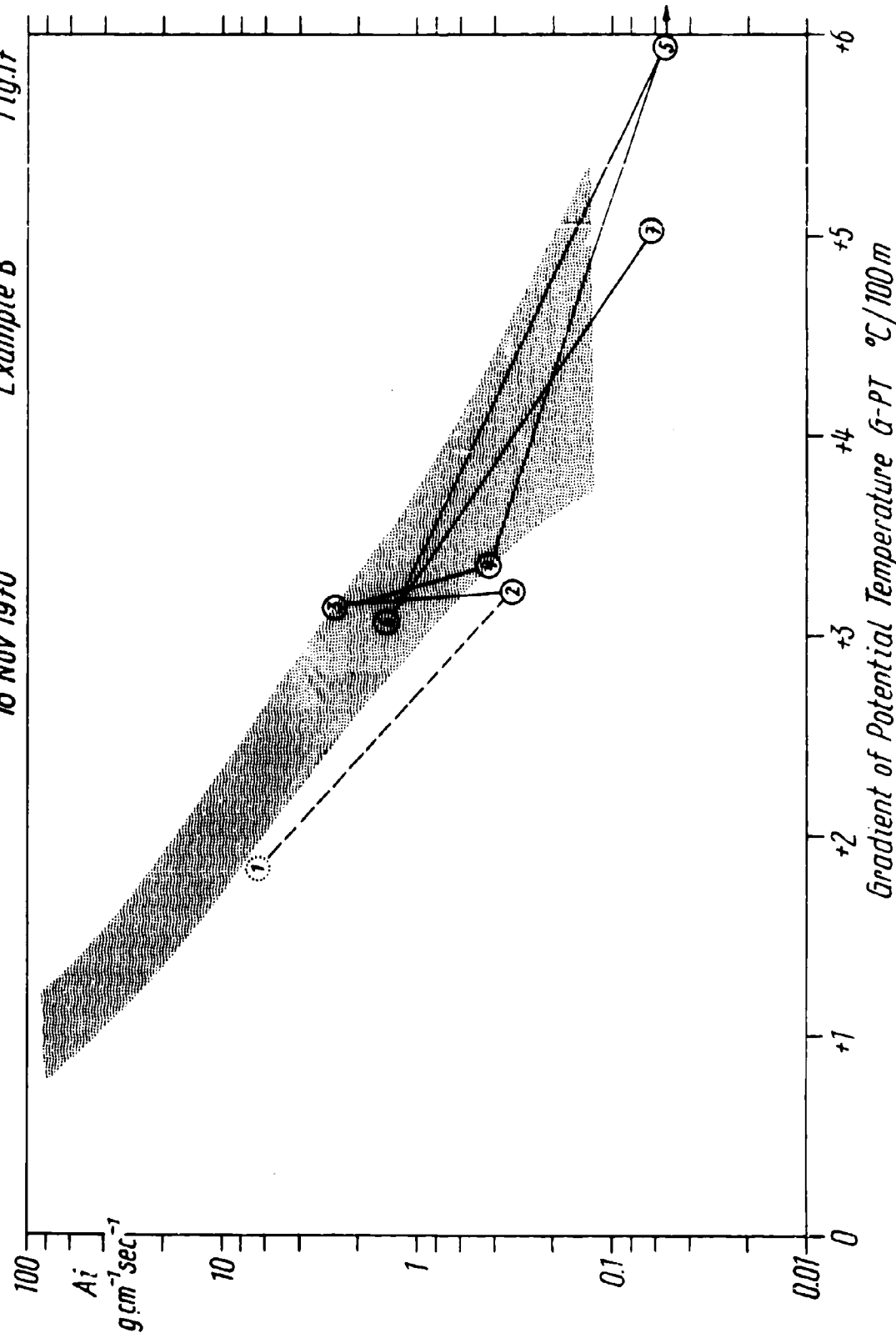
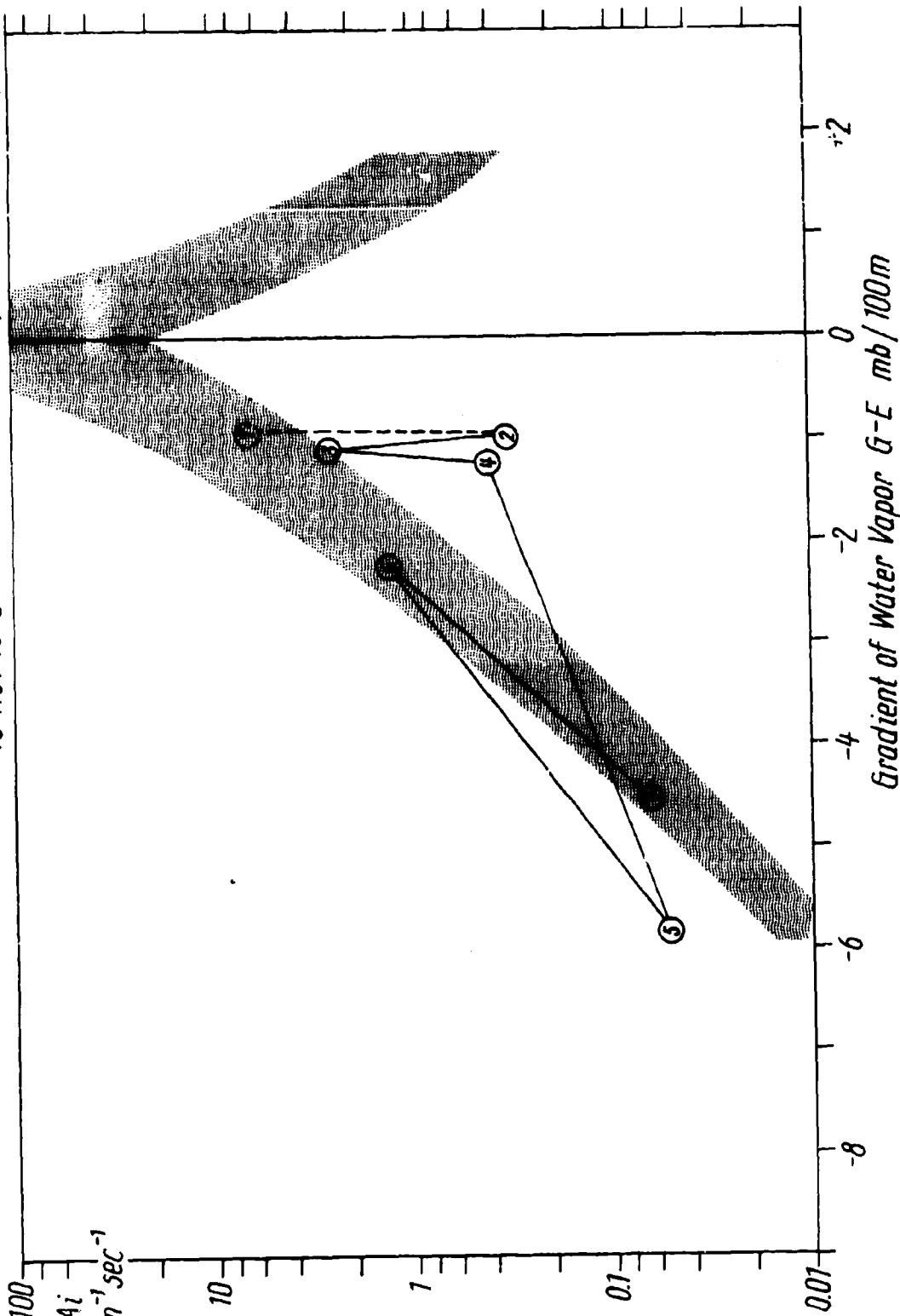


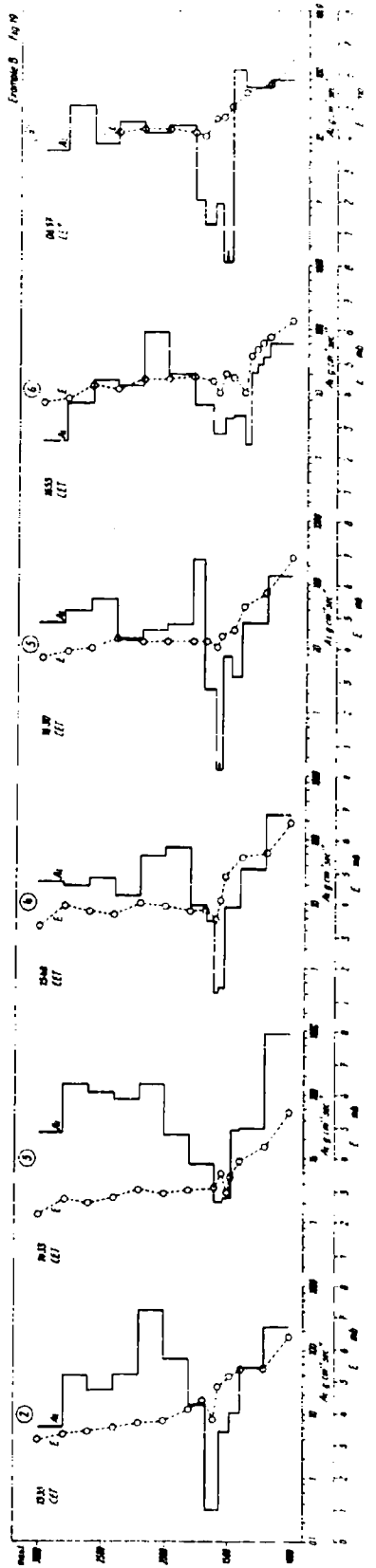
Fig. 18

Example B

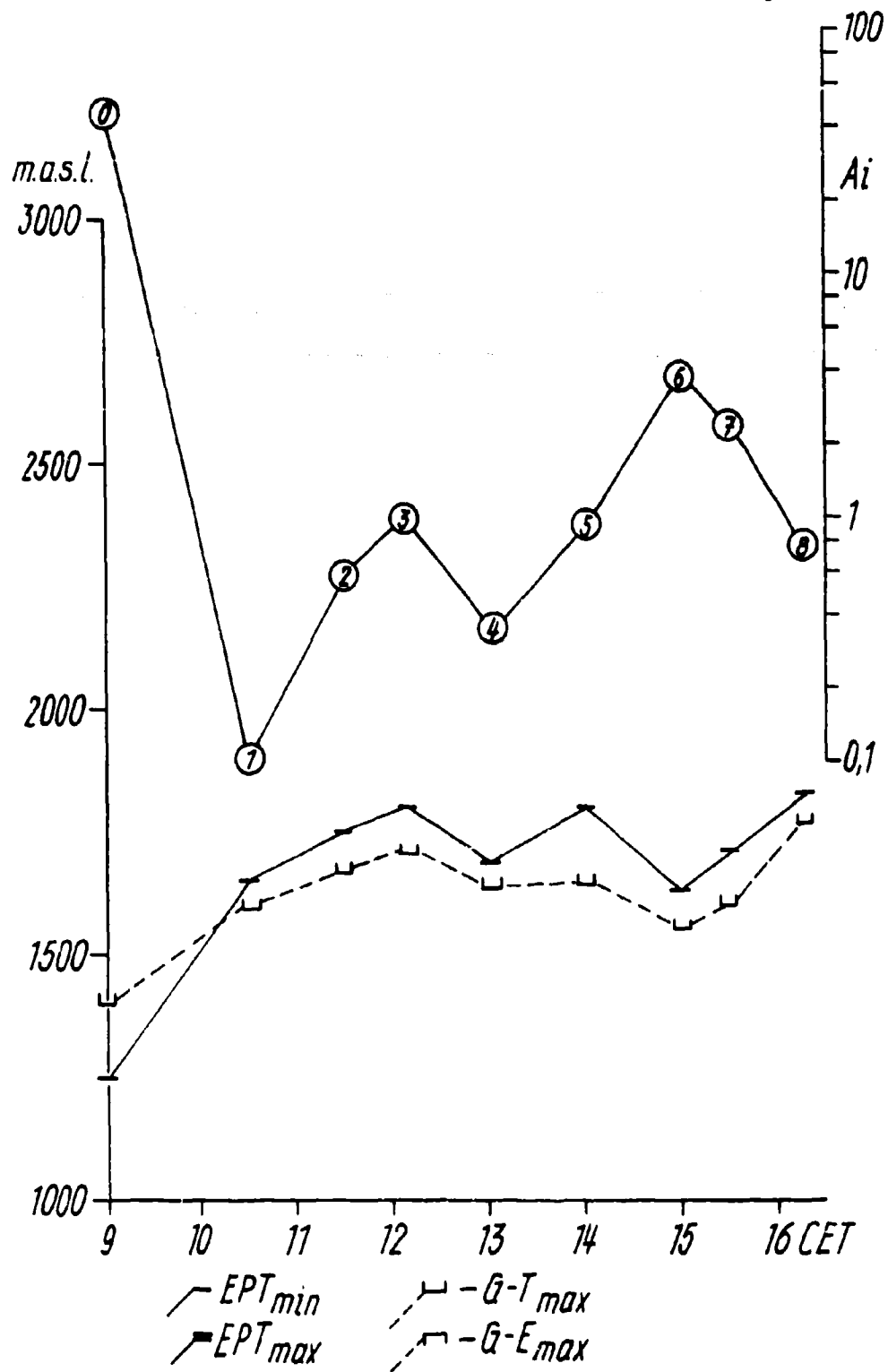
18 Nov 1930

100  
 $A_i$   
 $g cm^{-1} sec^{-1}$





14 Oct 1970 Example C Fig. 20



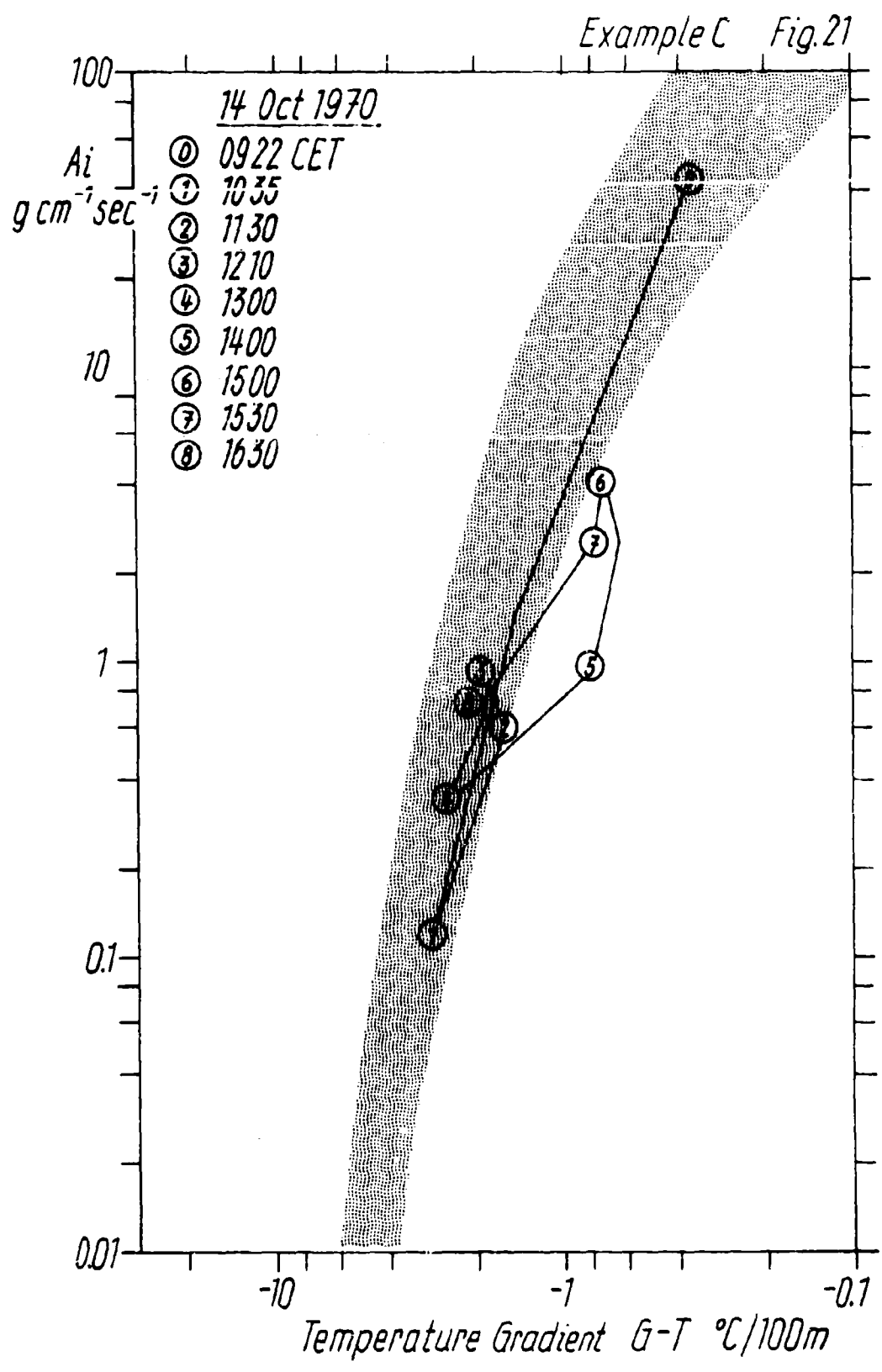
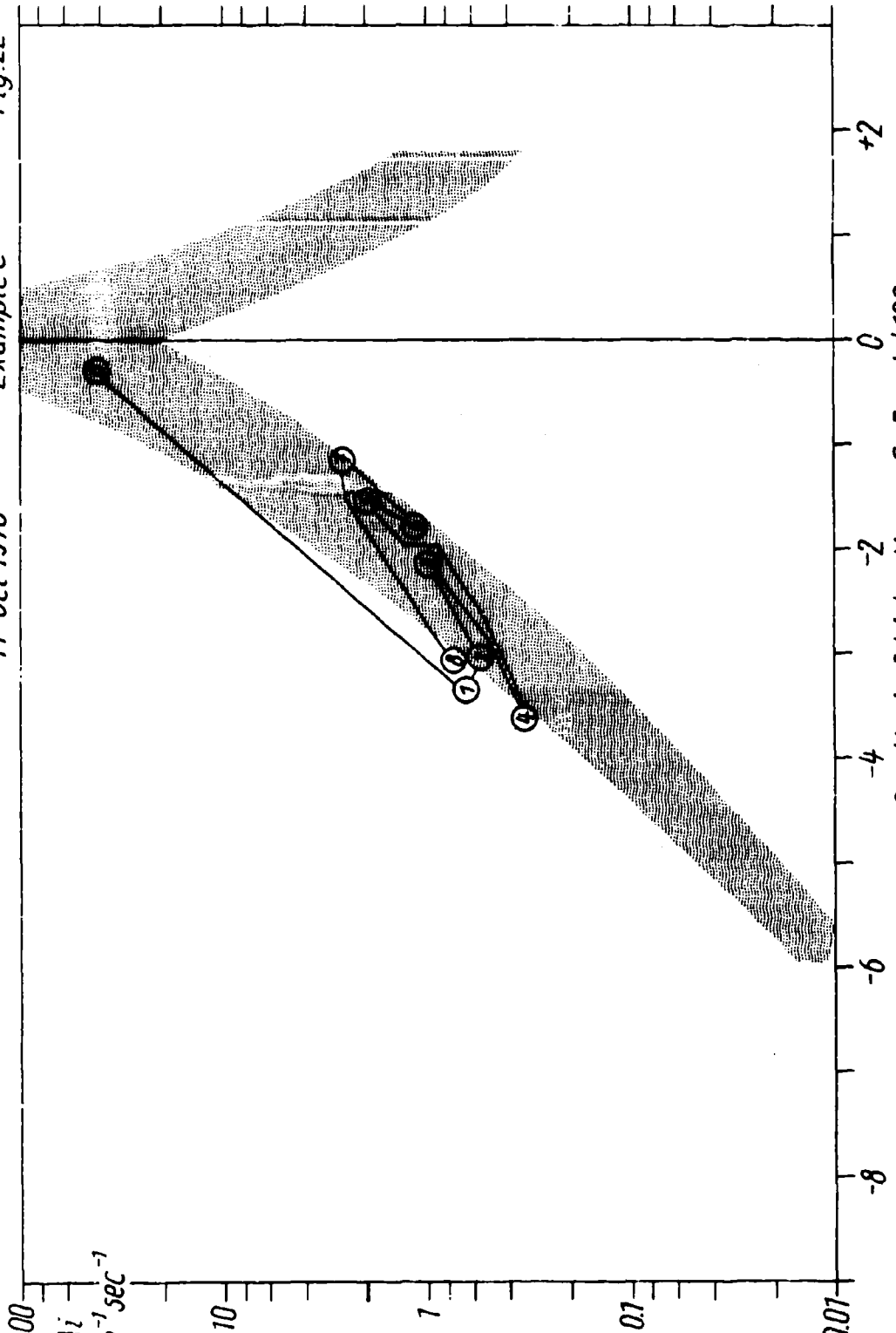


Fig. 22

Example C

14 Oct 1970

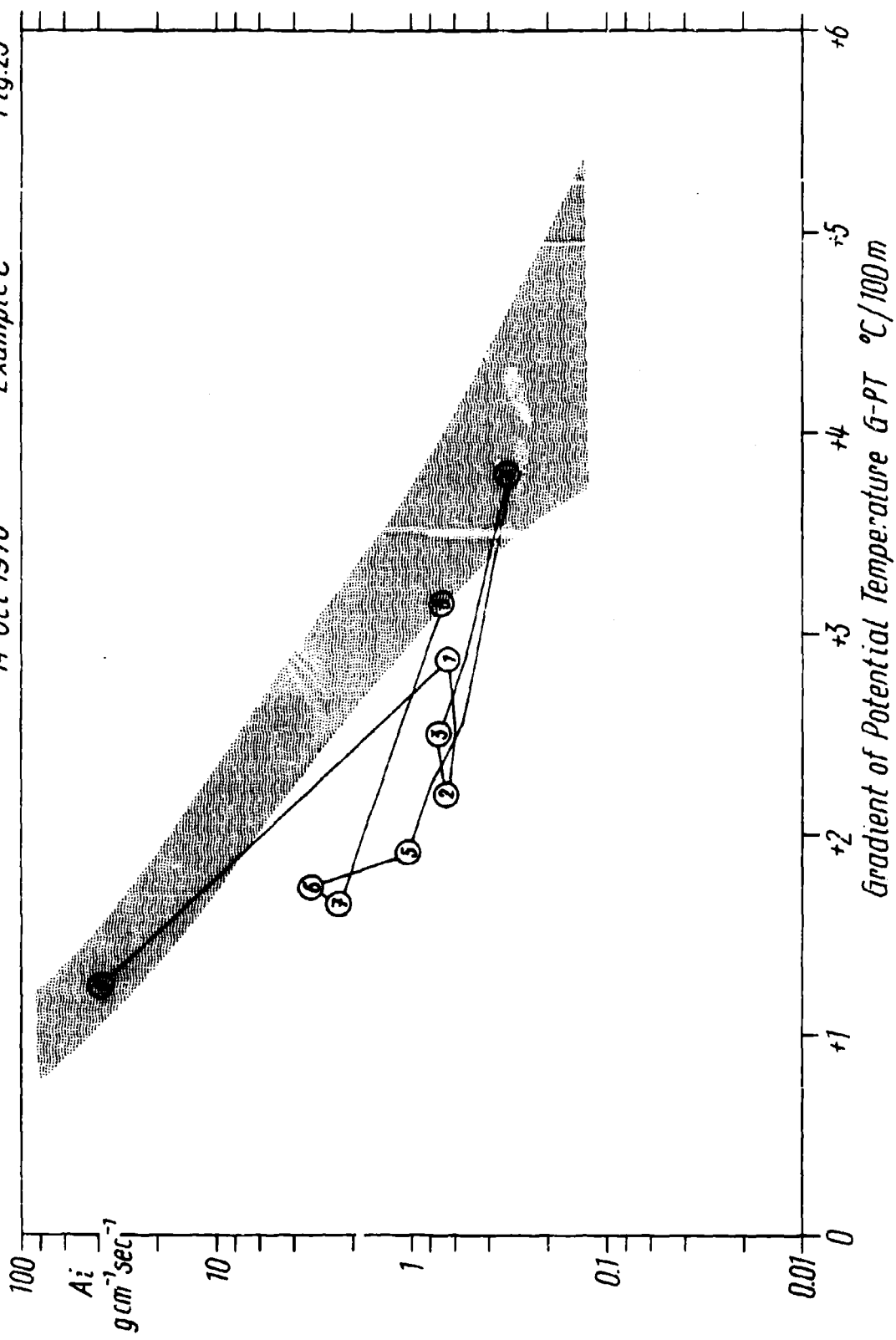
$A_i$   
 $g \text{ cm}^{-1} \text{ sec}^{-1}$



Gradient of Water Vapor G-F mb/100m

14 Oct 1970

Fig. 23  
Example C



Example D Fig. 24

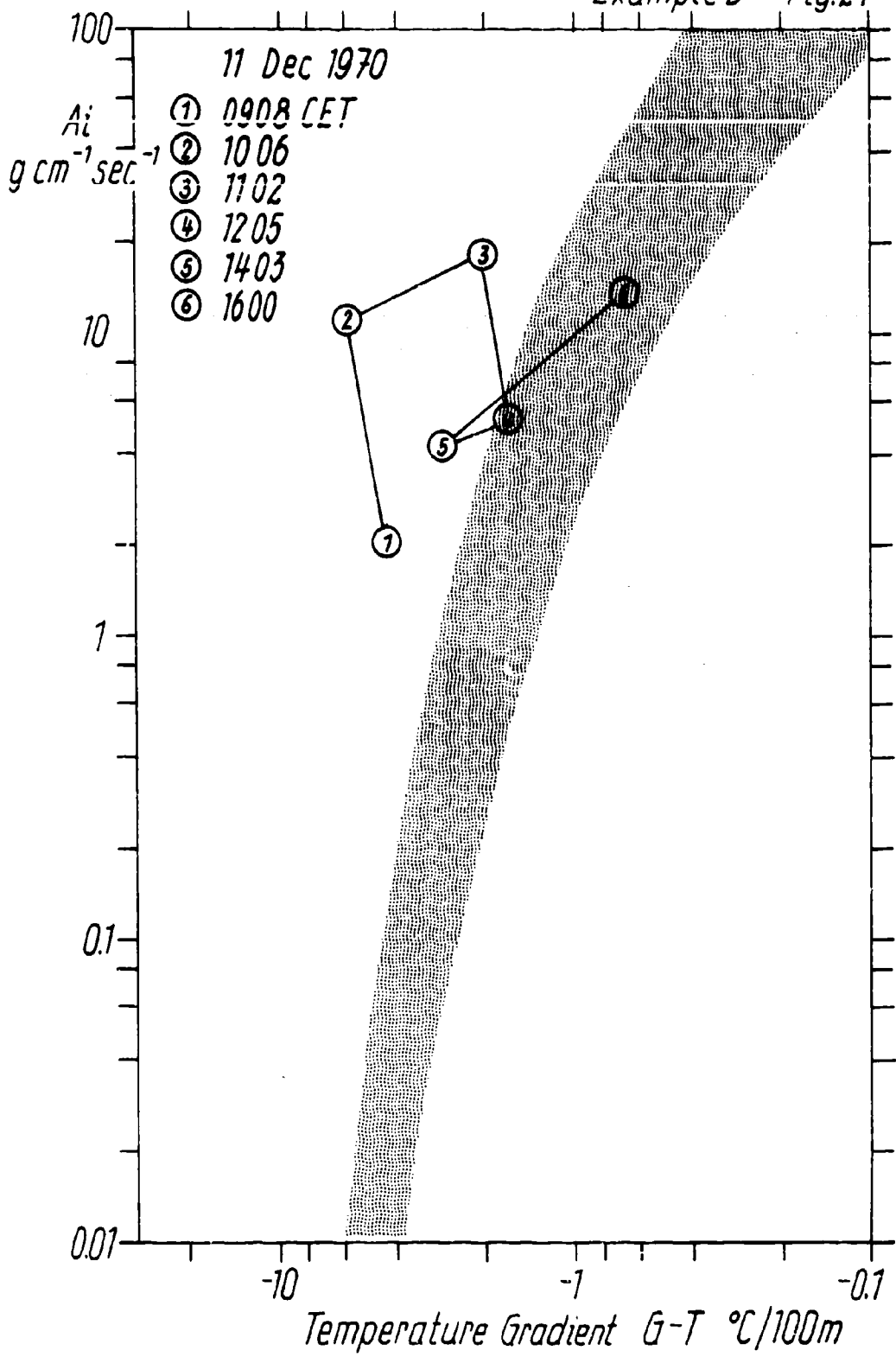
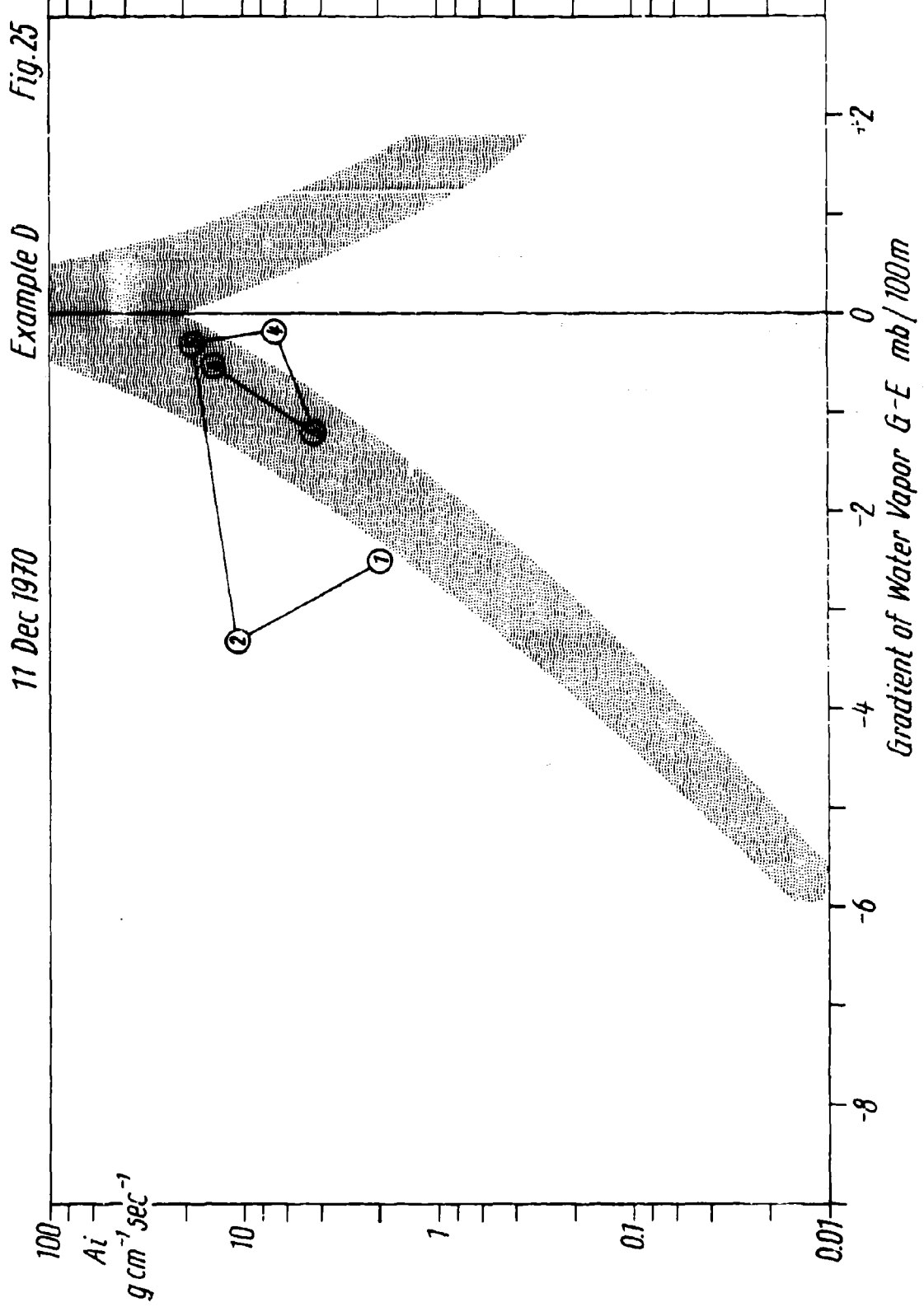


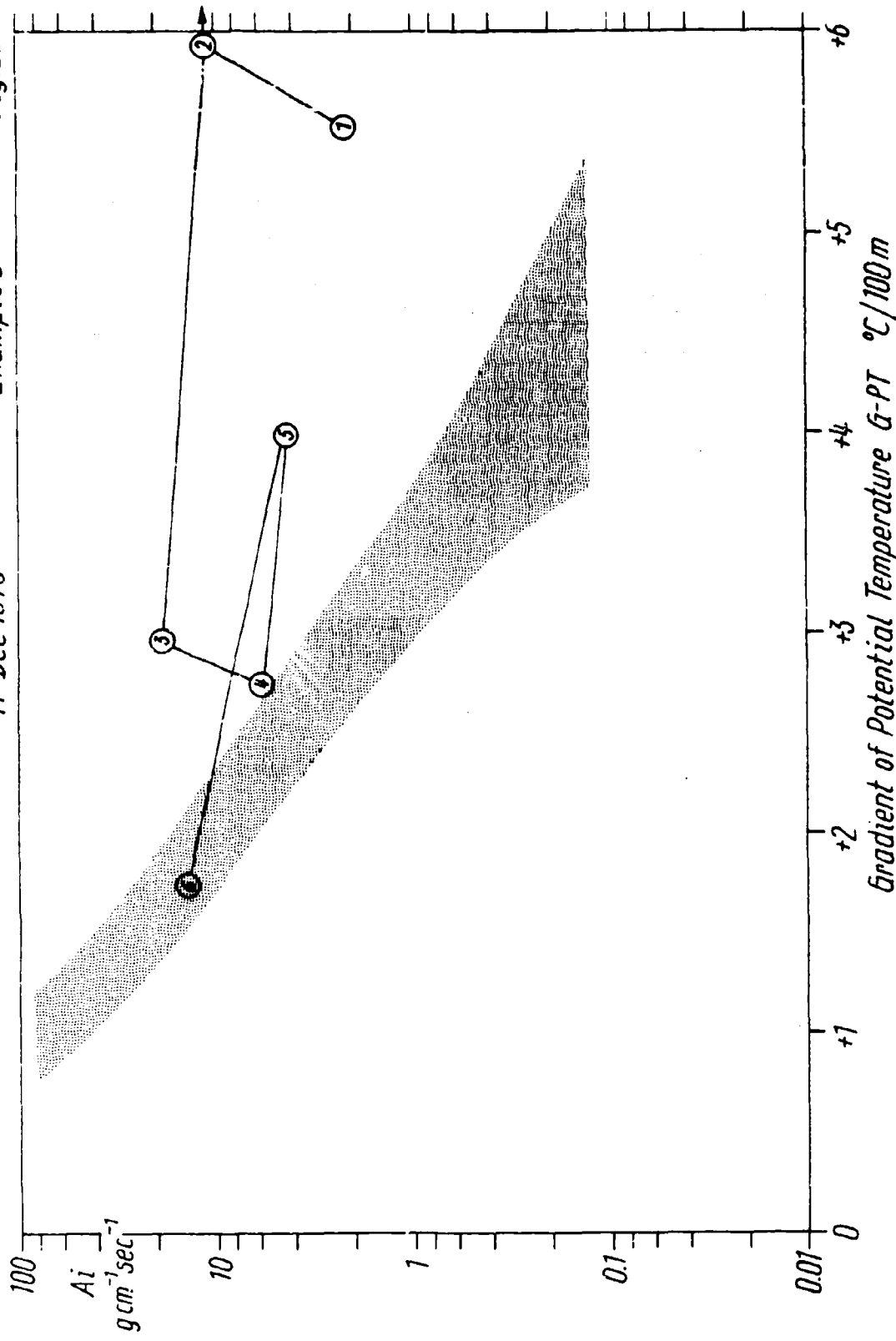
Fig. 25

11 Dec 1970

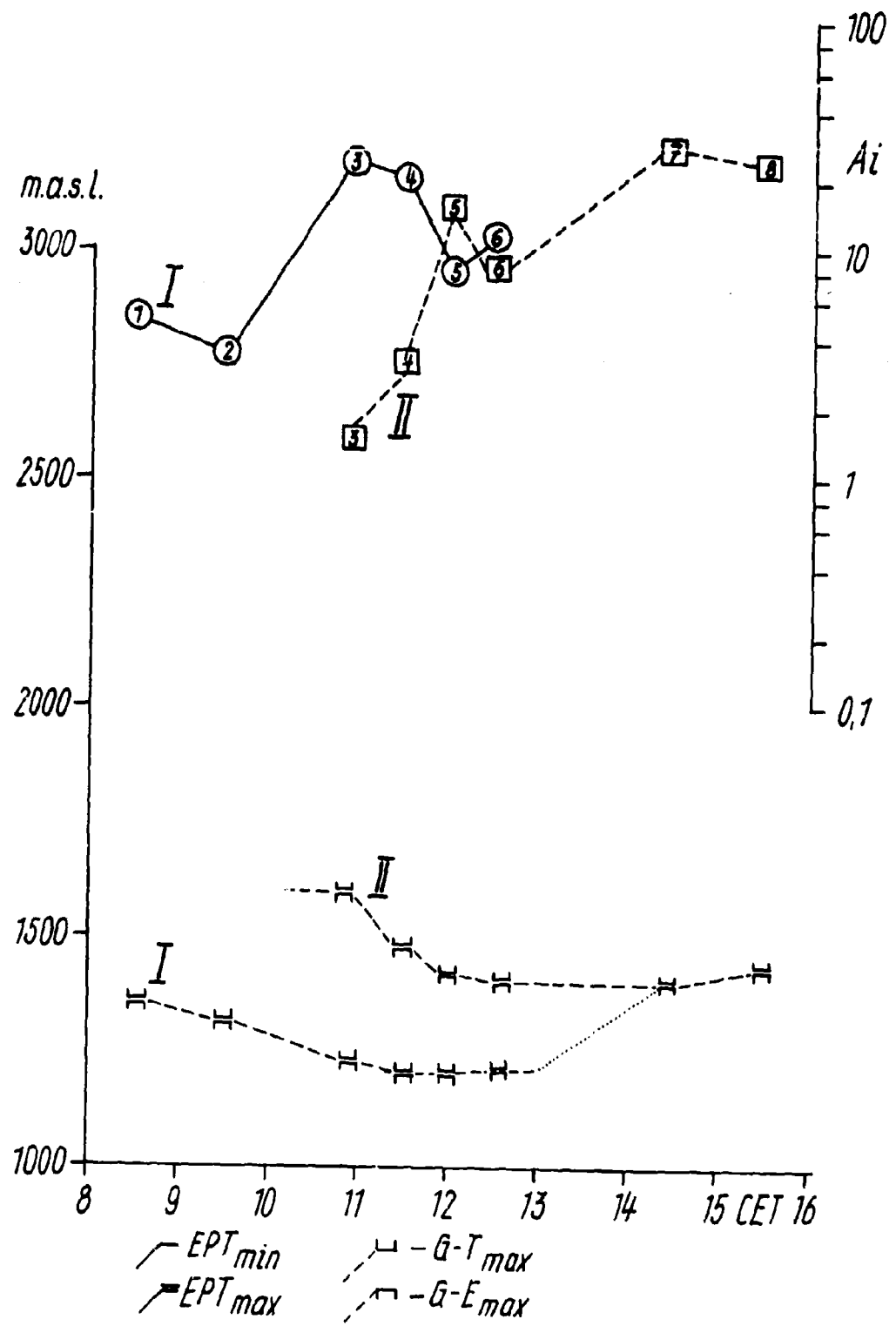


11 Dec 1970

Fig. 26  
Example D



17 Oct 1970 Example E Fig. 27



17 Oct 1970

Example E

Fig. 28

100

$A_i$   
 $g cm^{-3} sec^{-1}$

10

1

0.1

0.01

0

+6

+5

+4

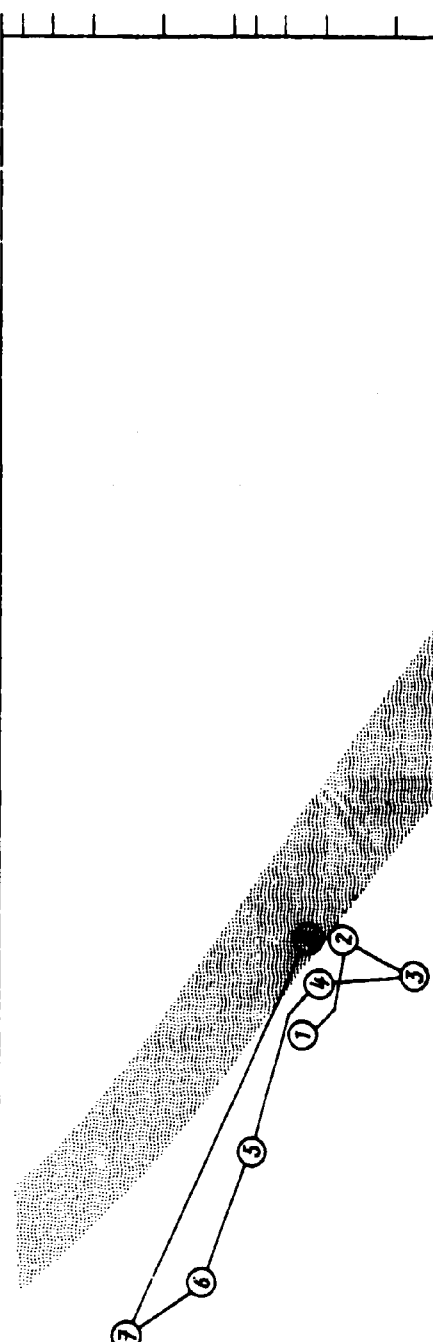
+3

+2

+1

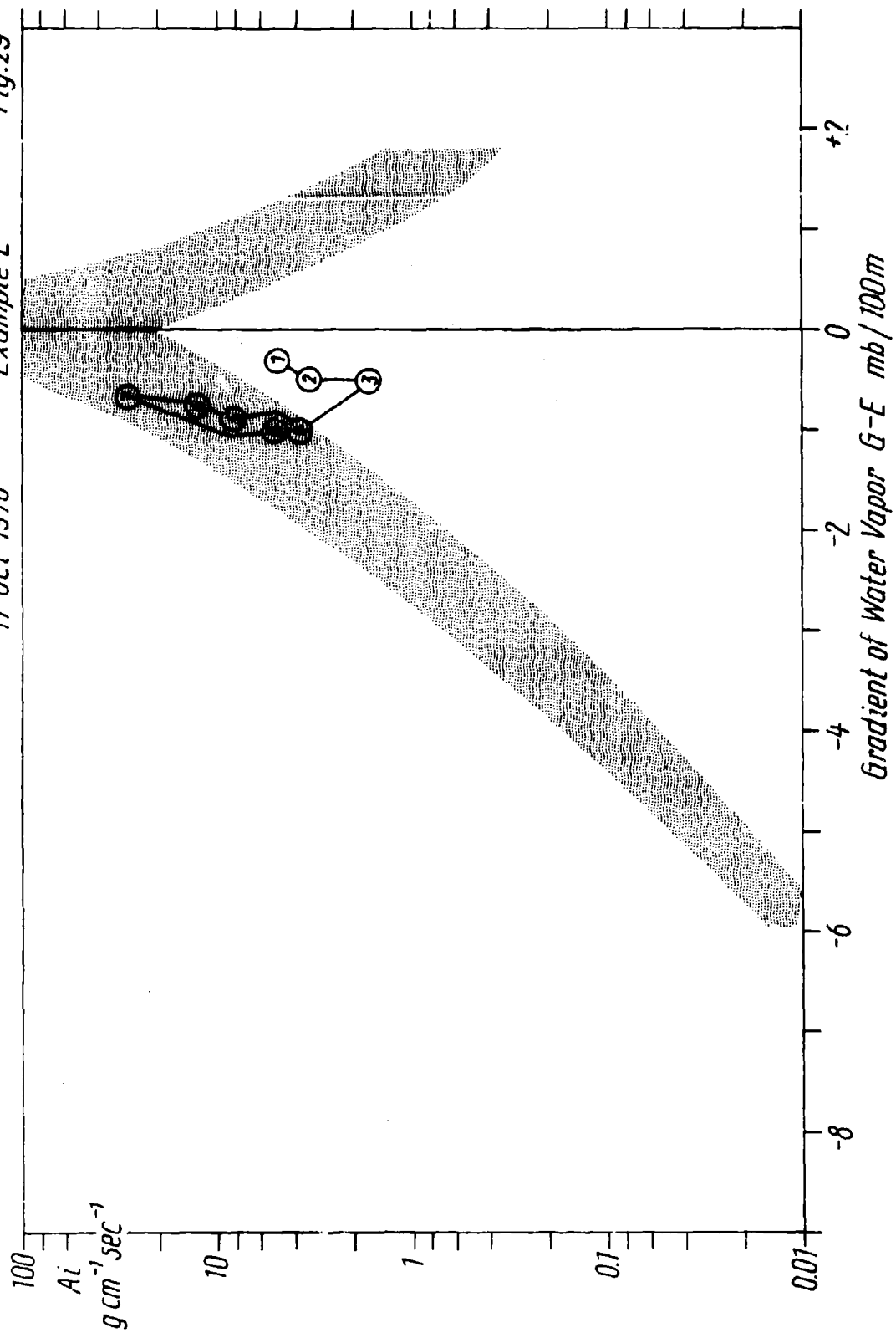
0

Gradient of Potential Temperature  $\delta - PT$   $^{\circ}C / 100m$

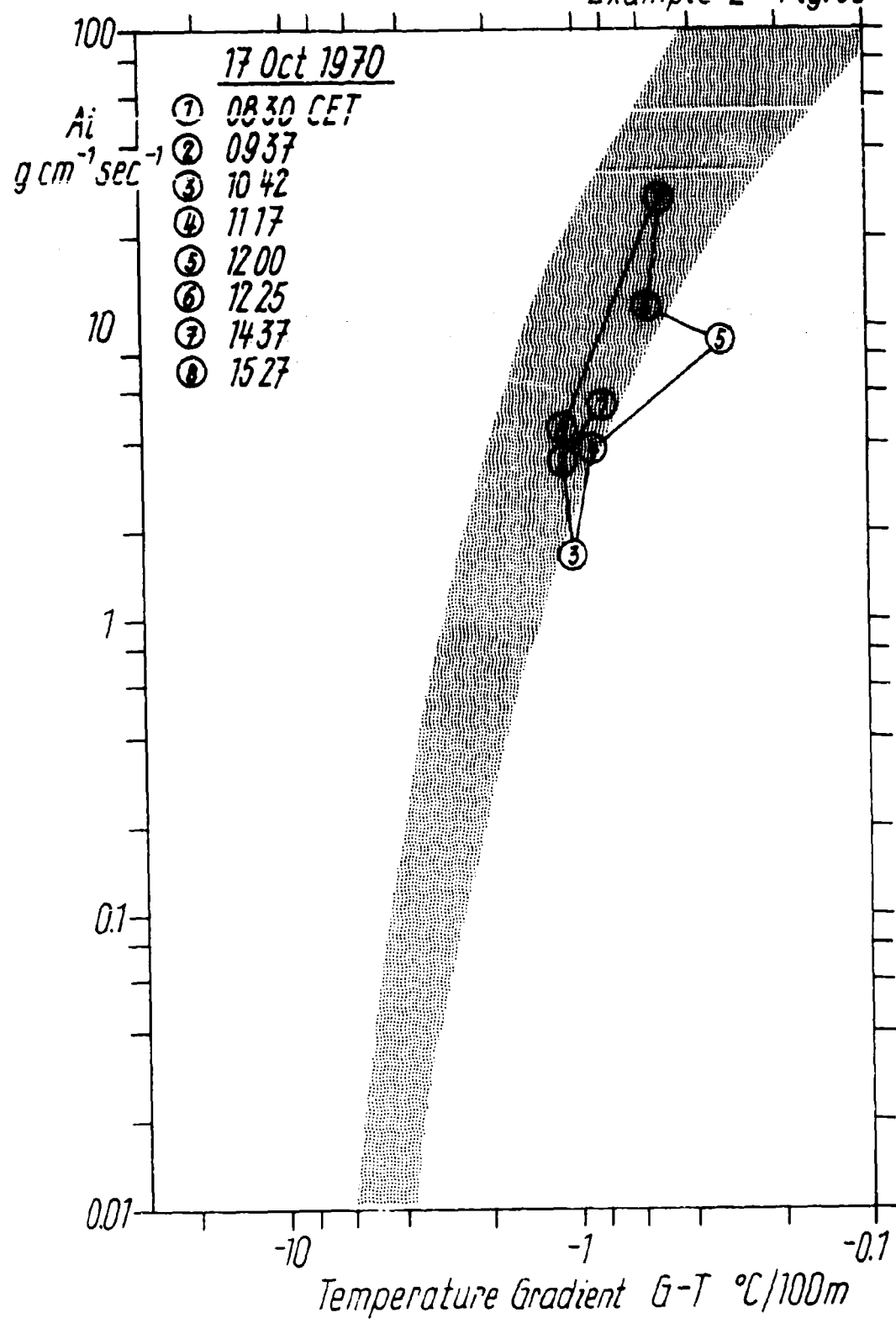


17 Oct 1970

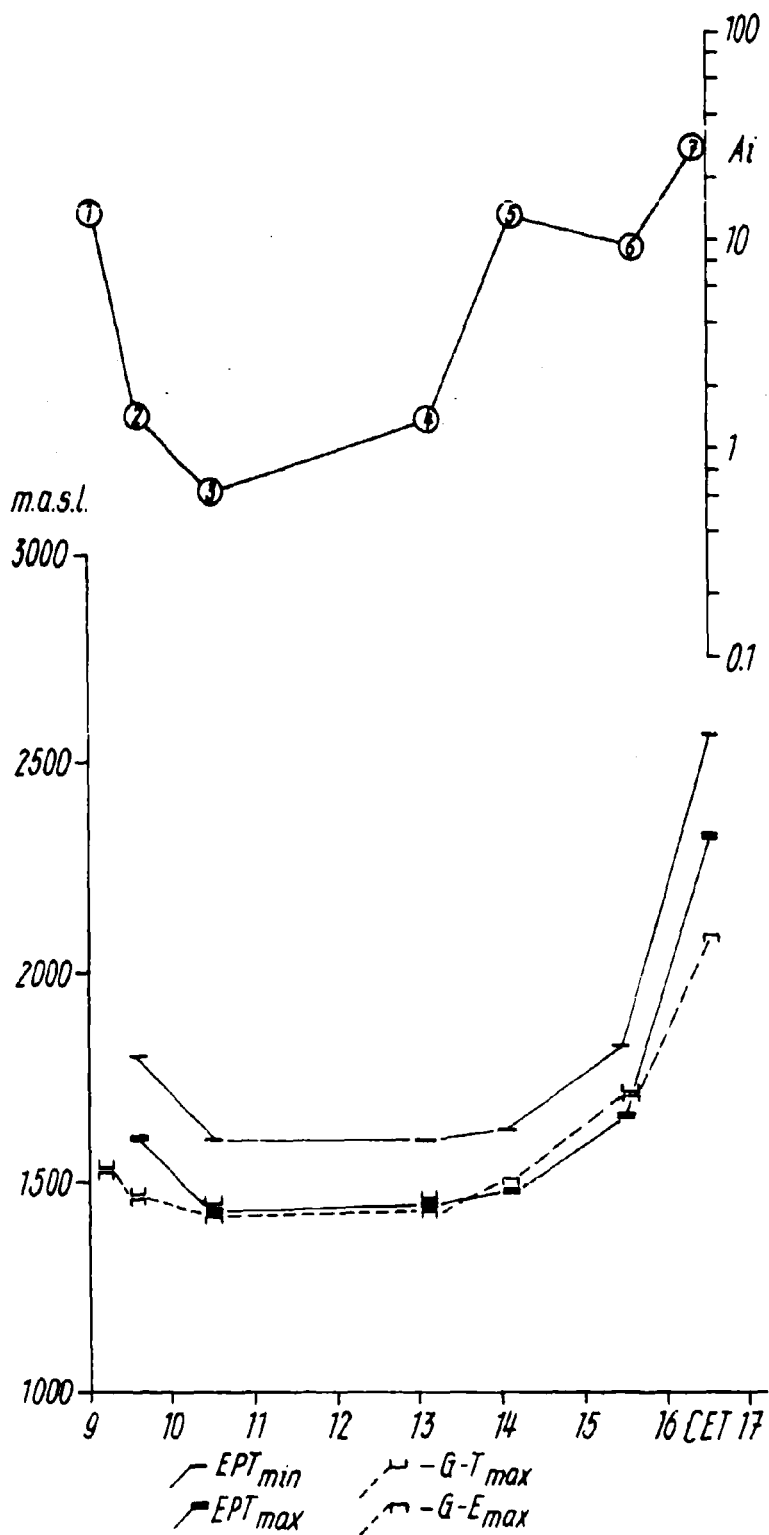
Fig. 29  
Example E



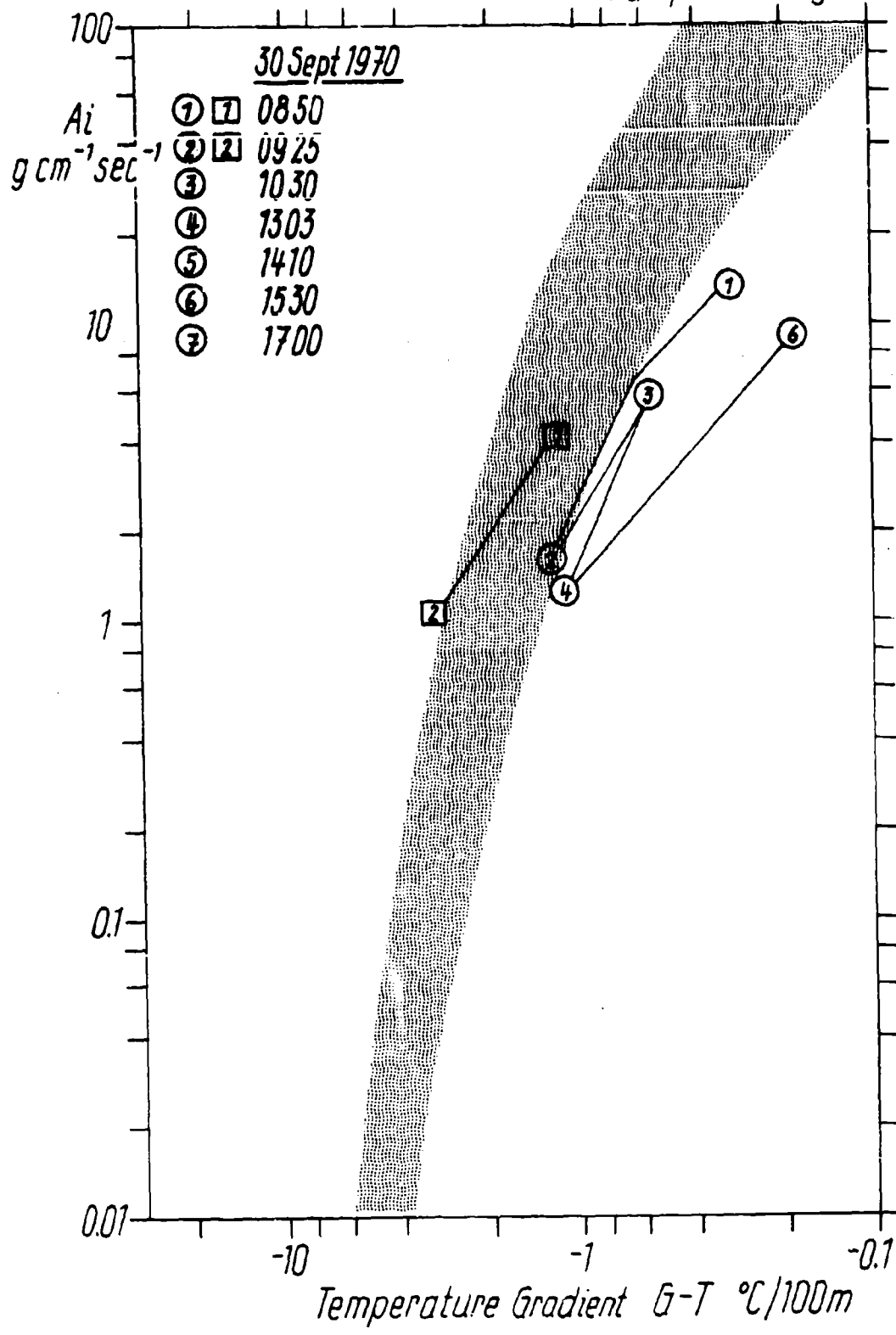
Example E Fig. 30



30 Sept. 1970 Example F Fig.31

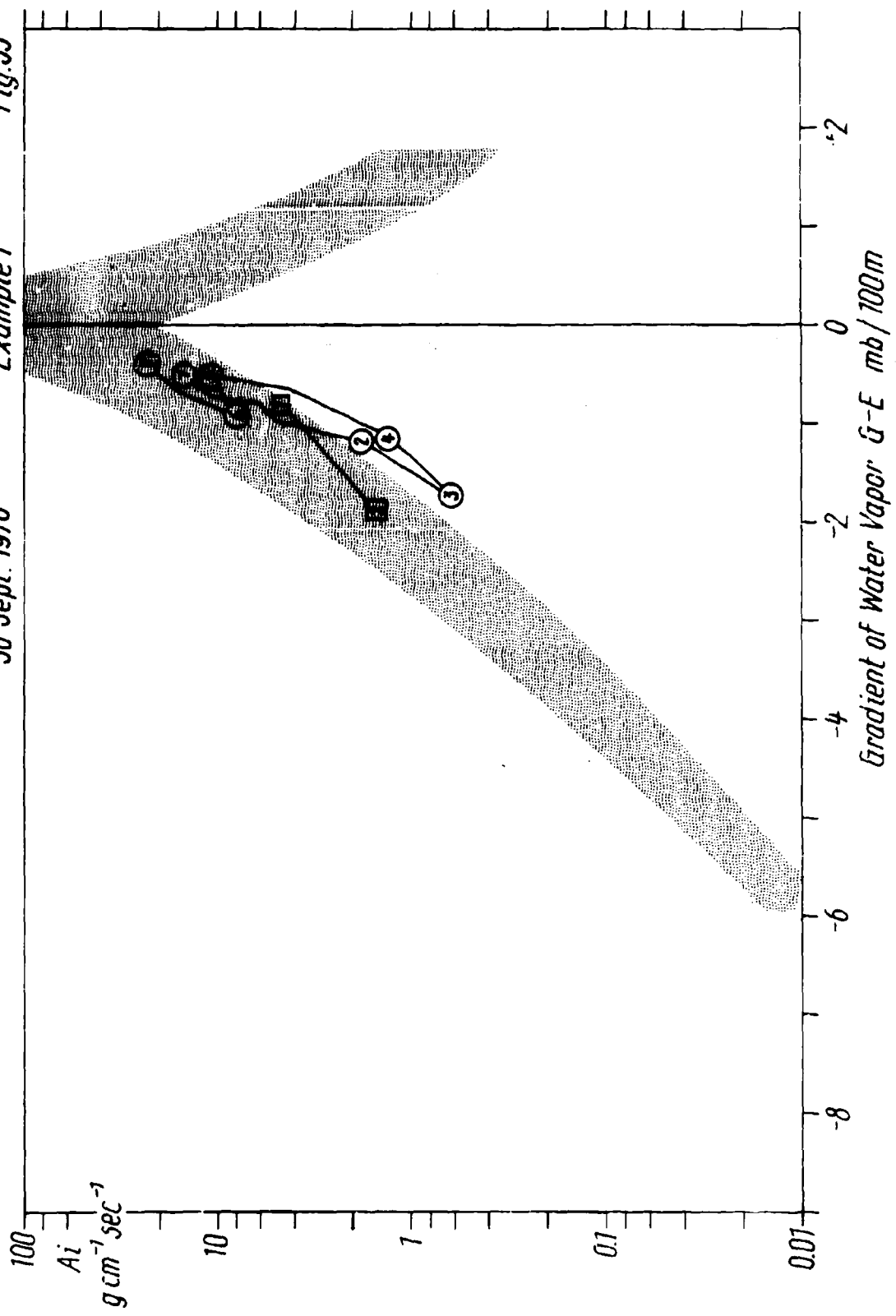


Example F Fig.32

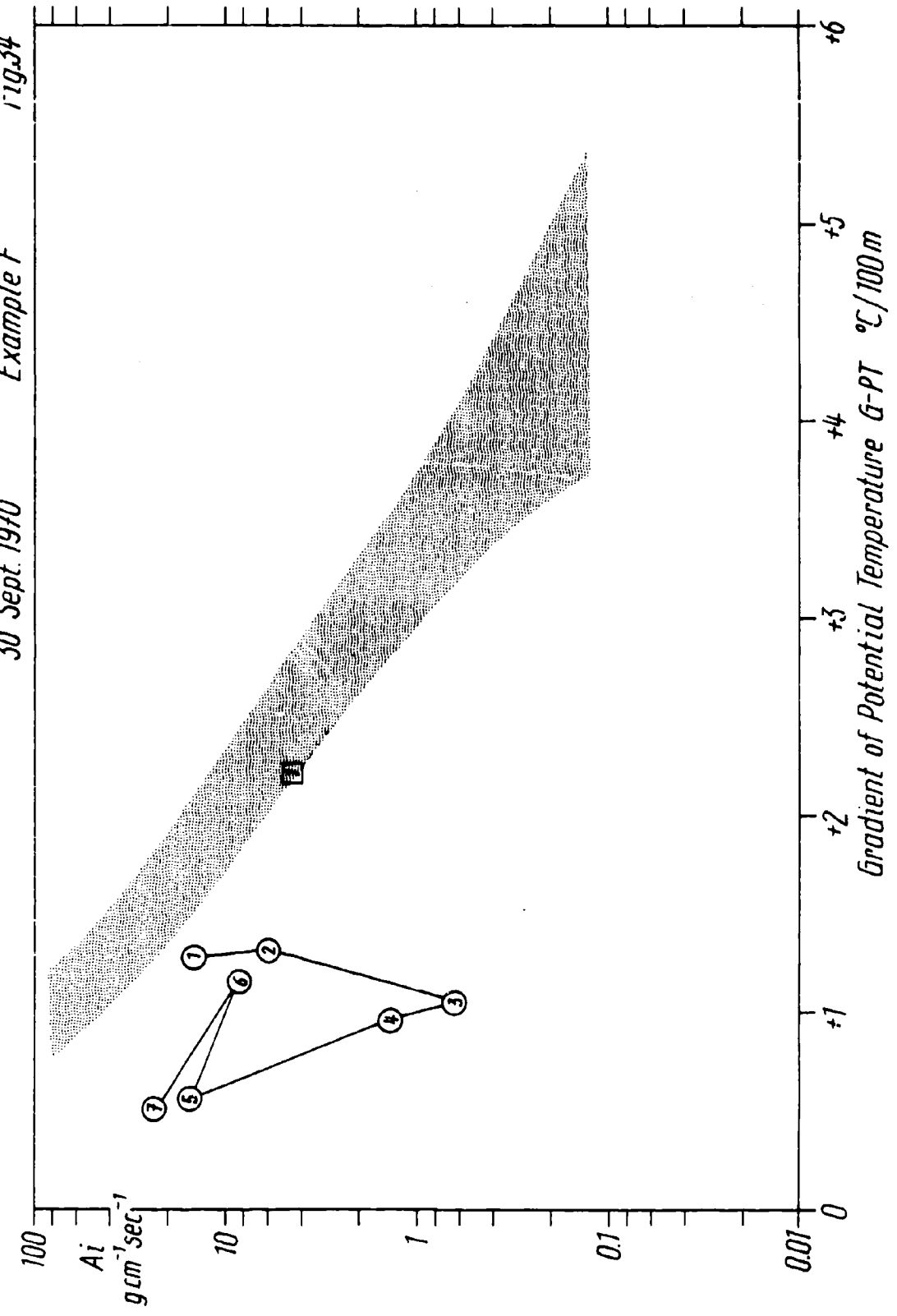


30 Sept. 1970

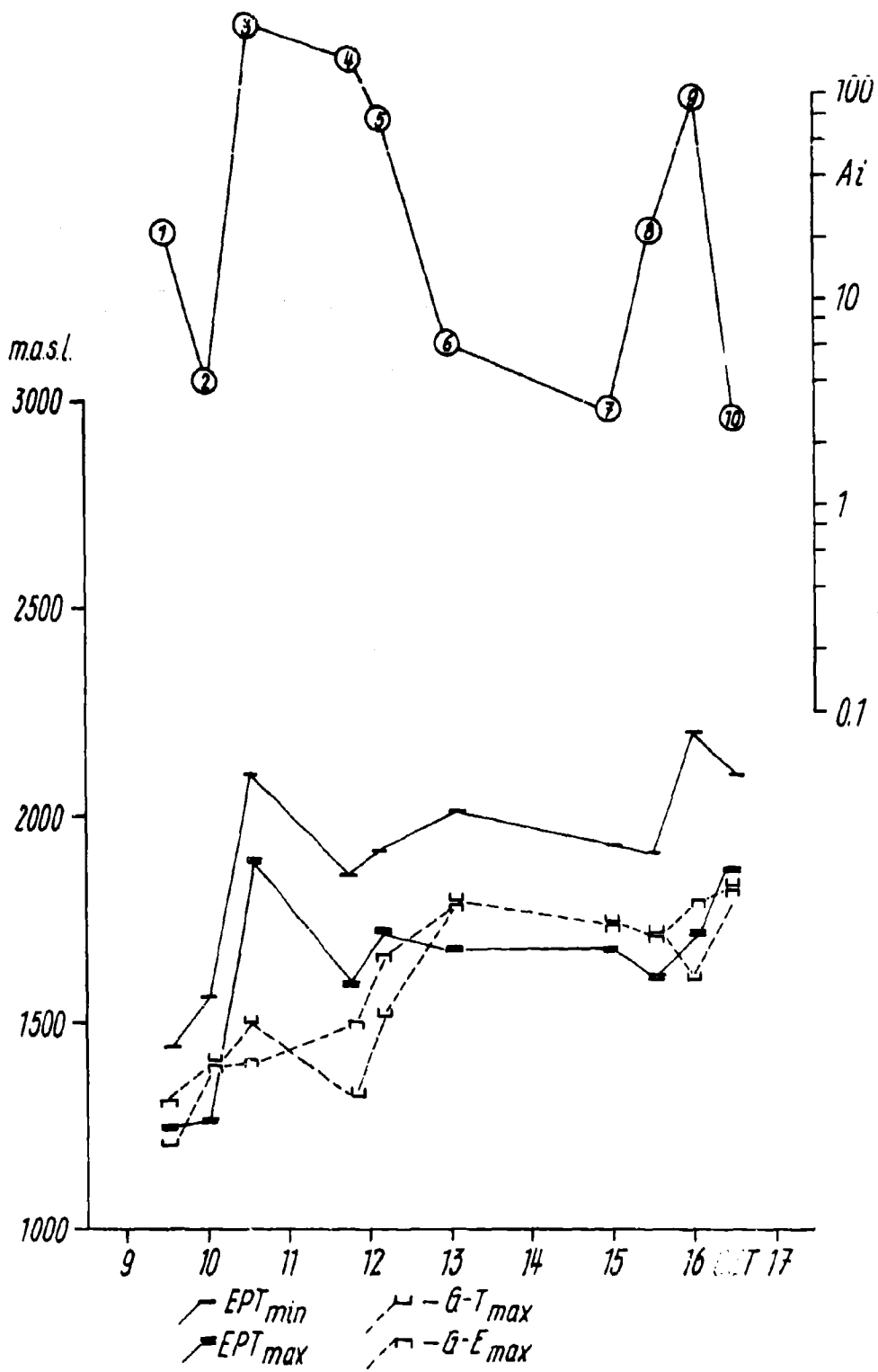
Fig. 33 Example F



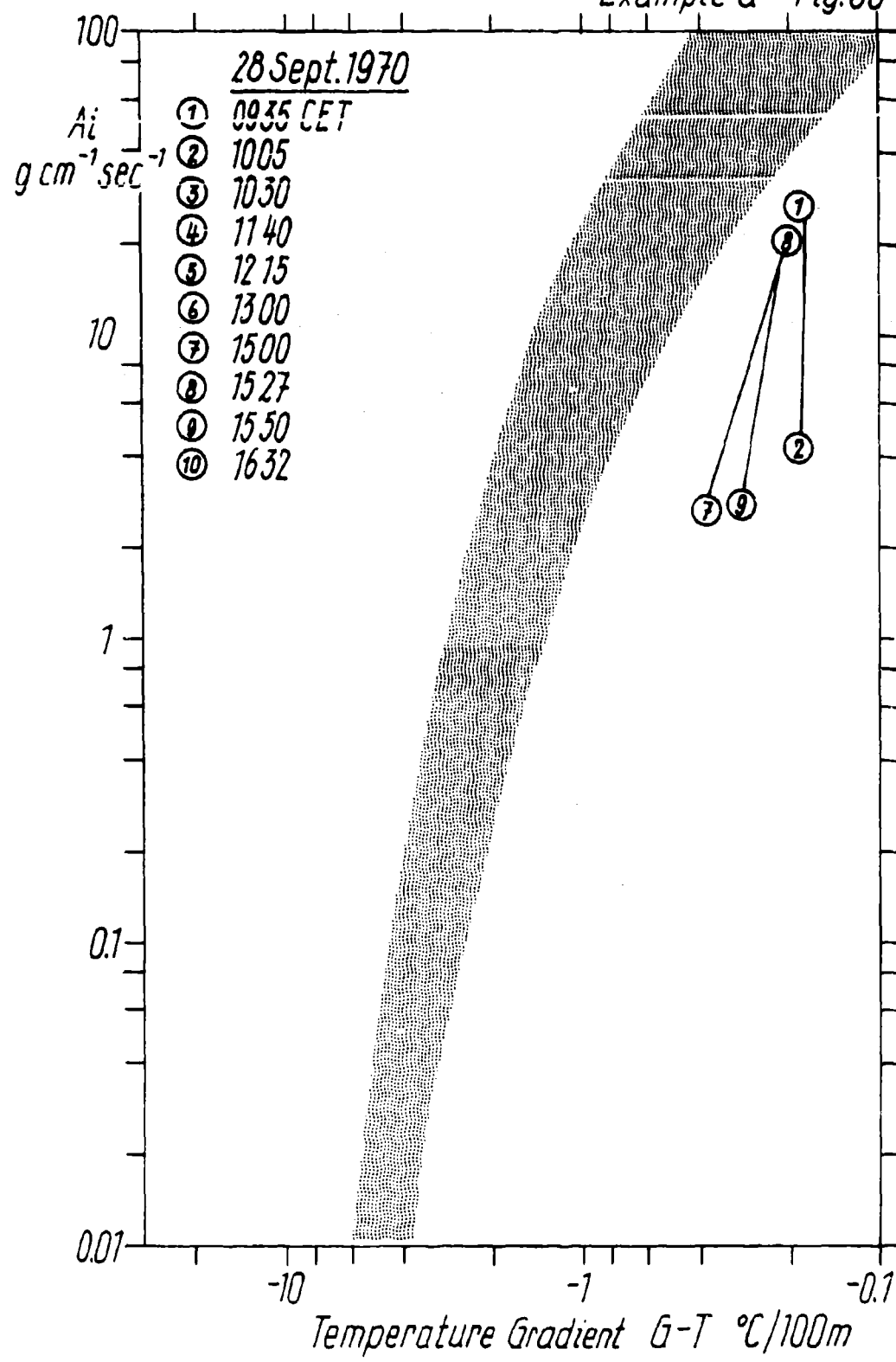
30 Sept. 1970      Example F      Fig. 34



28 Sept. 1970 Example G Fig. 35



Example 6 Fig. 36

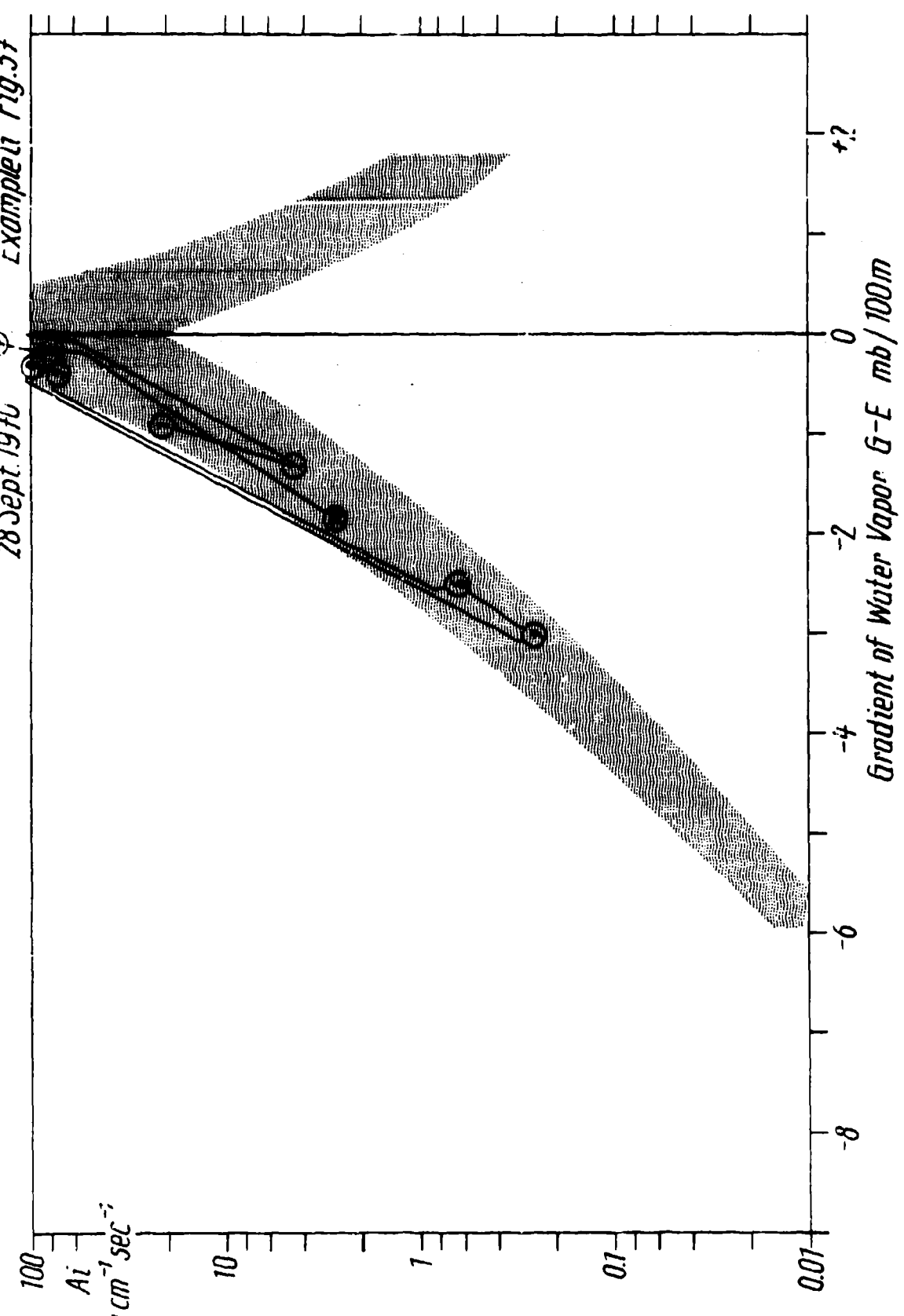


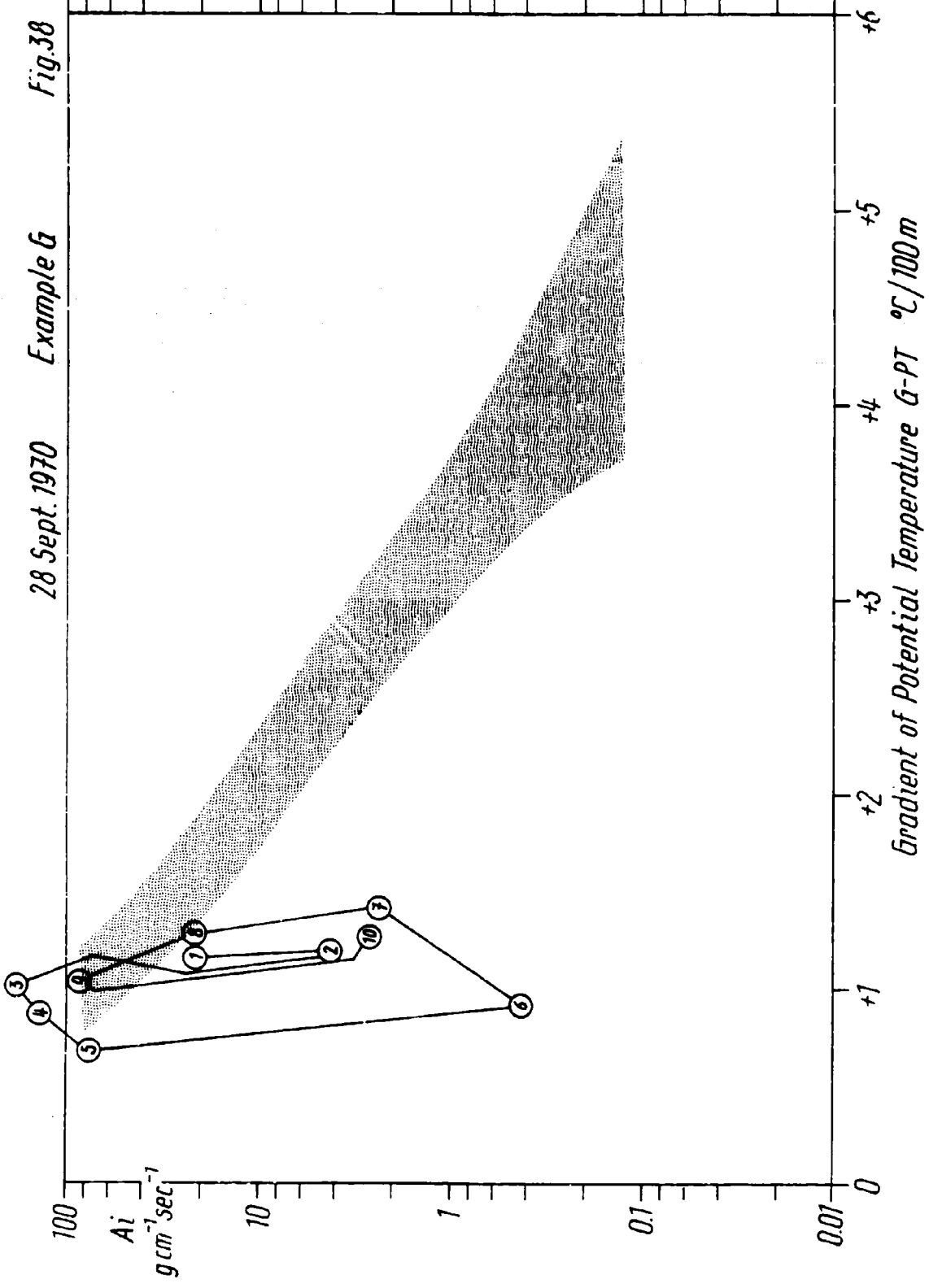
Exempli Fig. 37

③

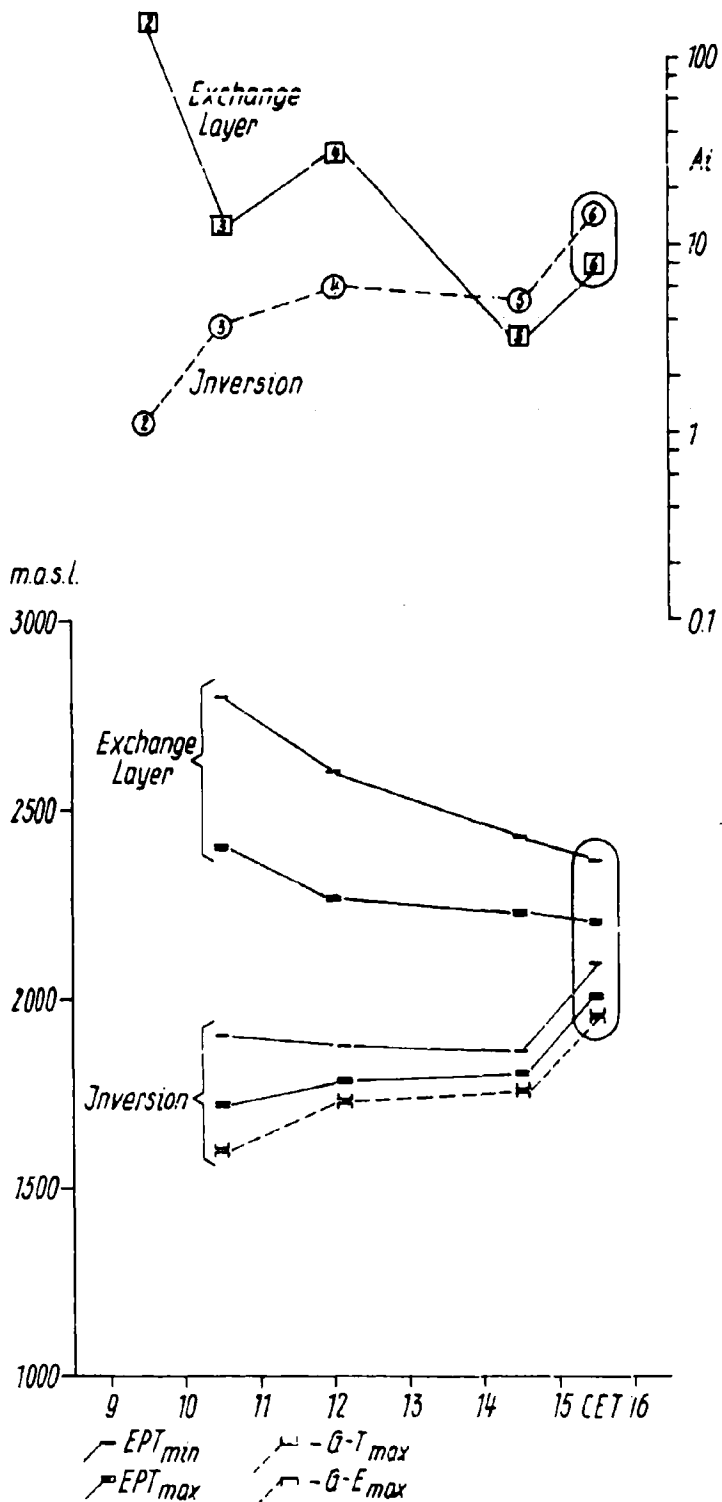
28 Sept. 1970

$Ai$   
 $g cm^{-1} sec^{-1}$

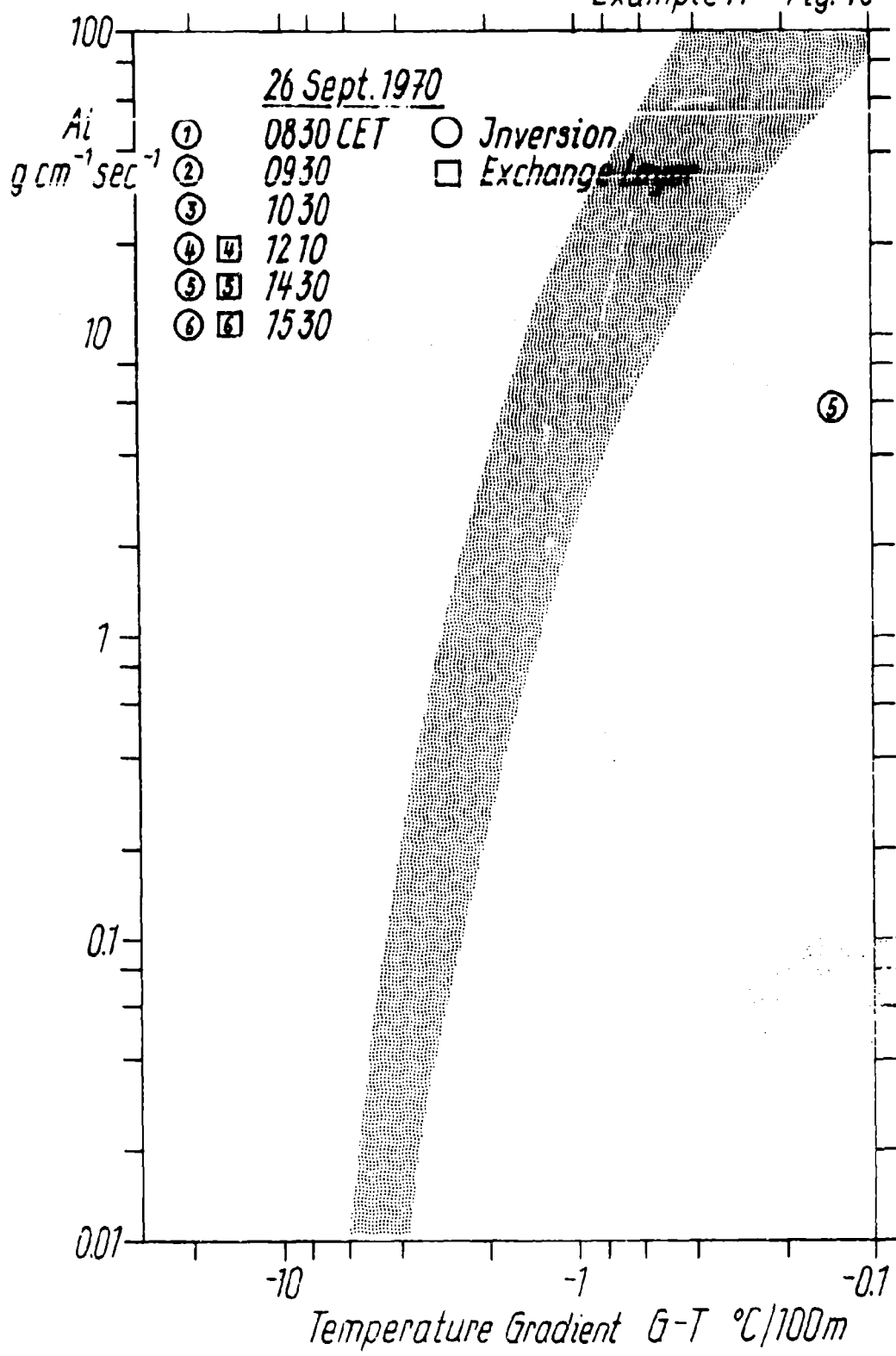




26 Sept. 1970 Example H Fig.39

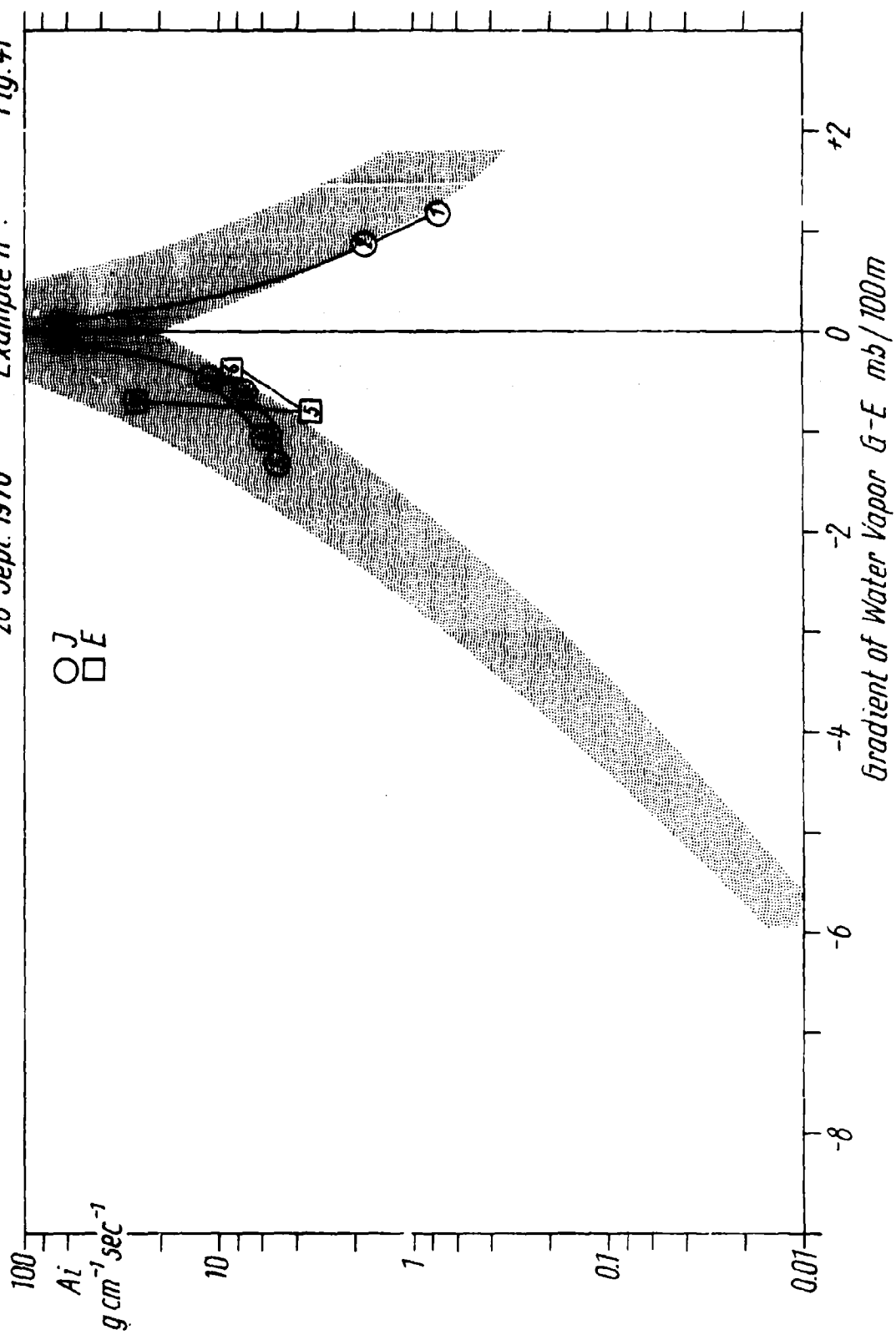


Example H Fig. 40



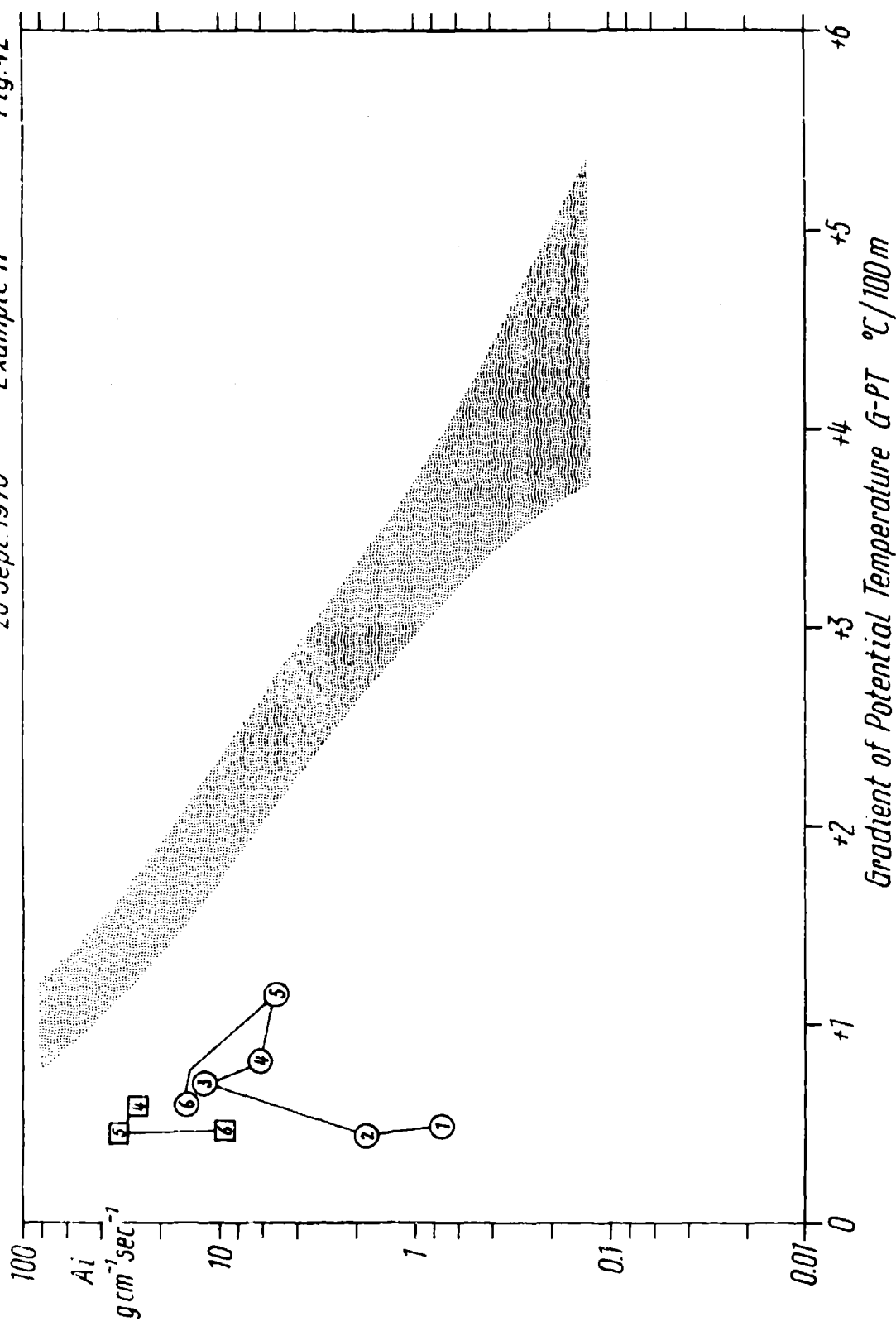
26 Sept 1970

Fig. 41  
Example H.

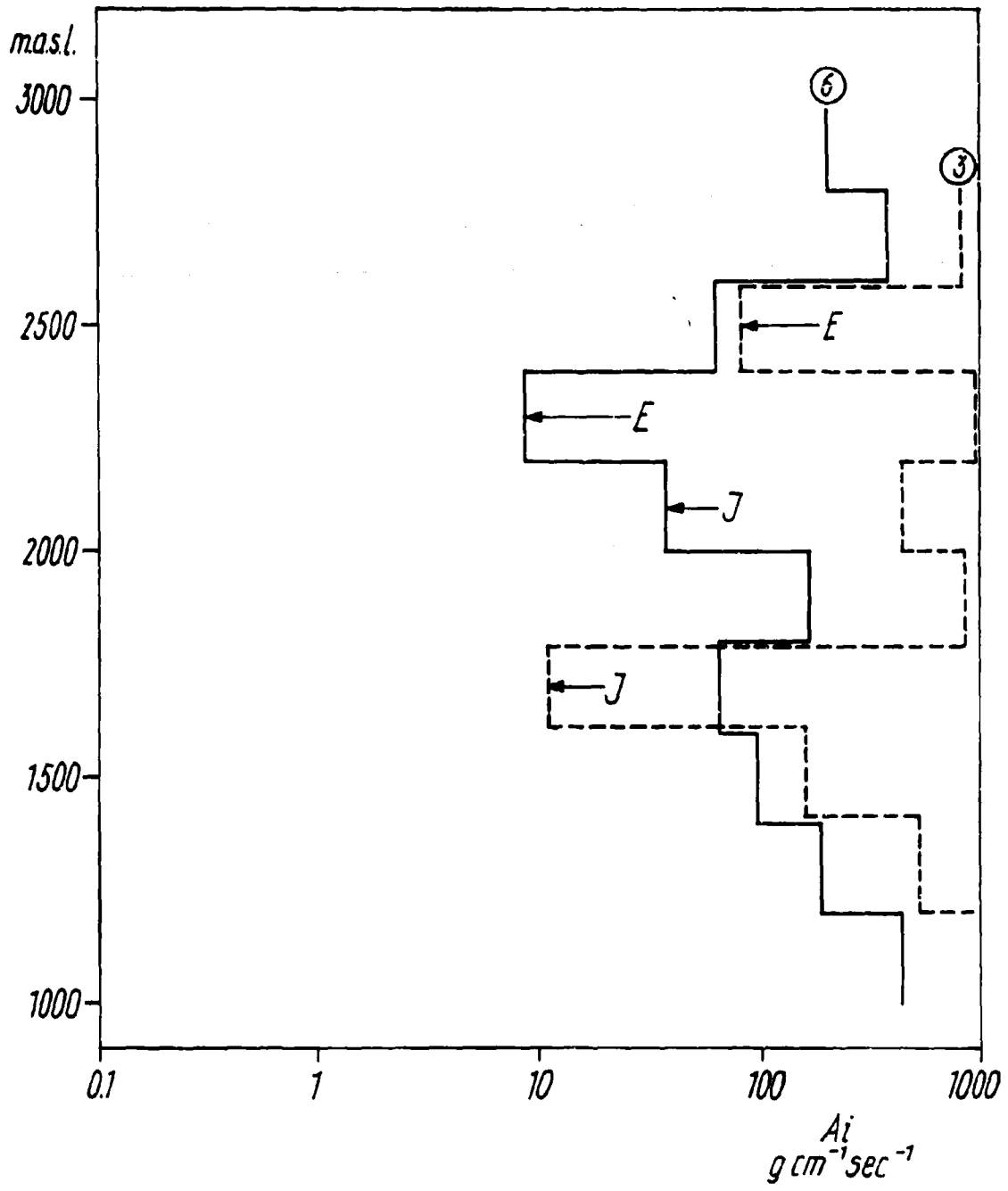


26 Sept. 1970 Example H

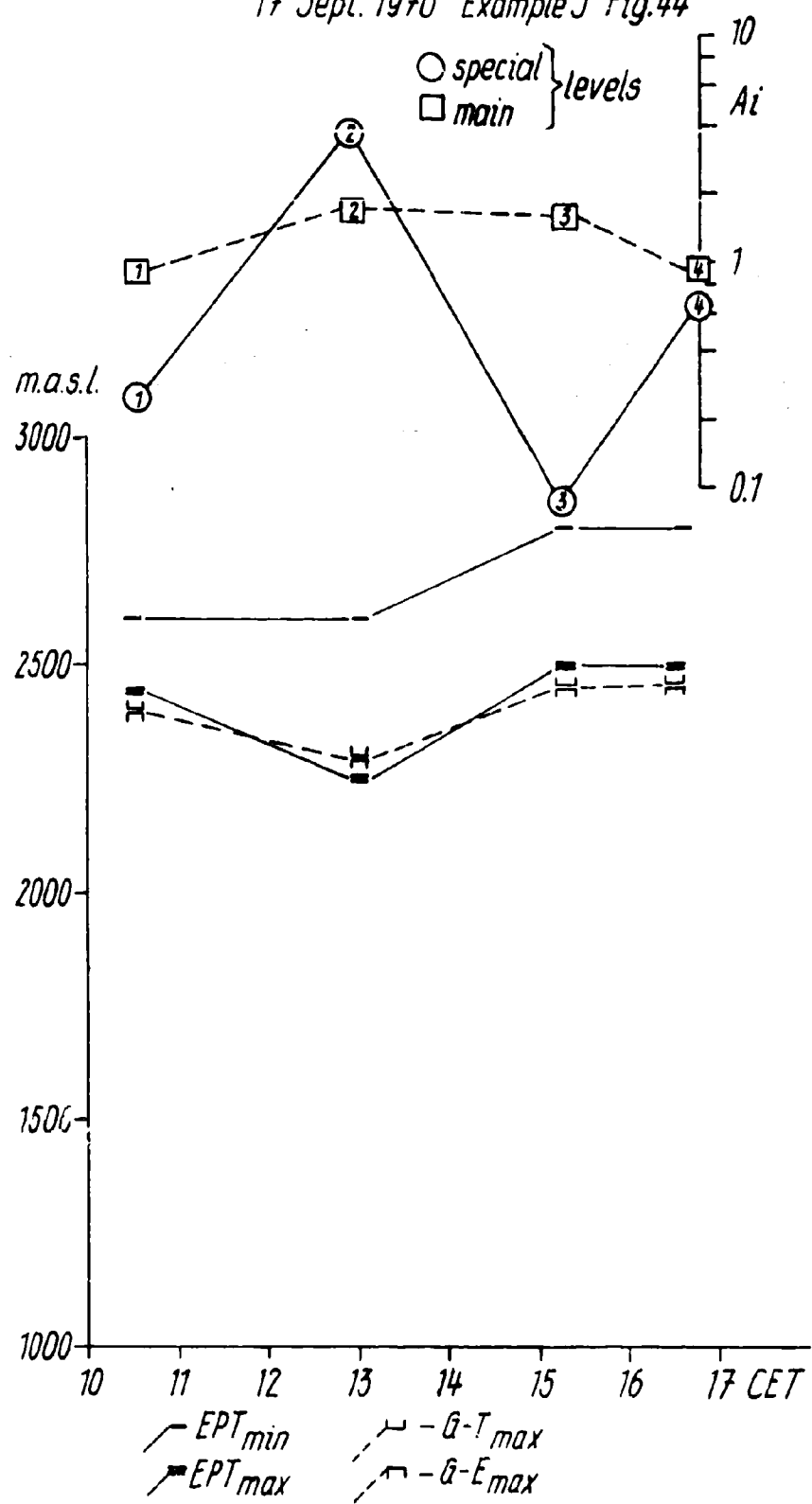
Fig. 42



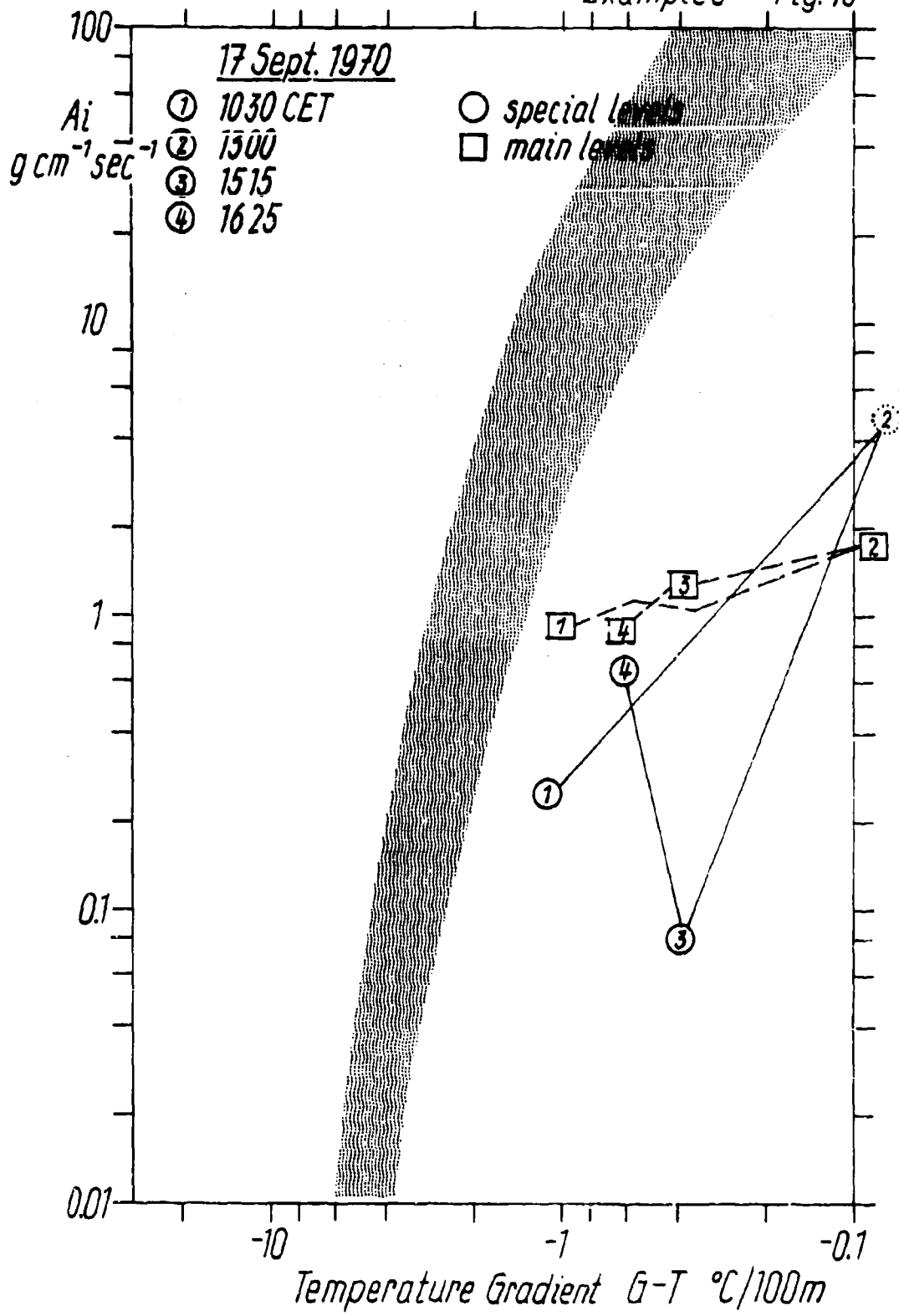
26 Sept. 1970 Example H Fig. 43



17 Sept. 1970 Example J Fig.44

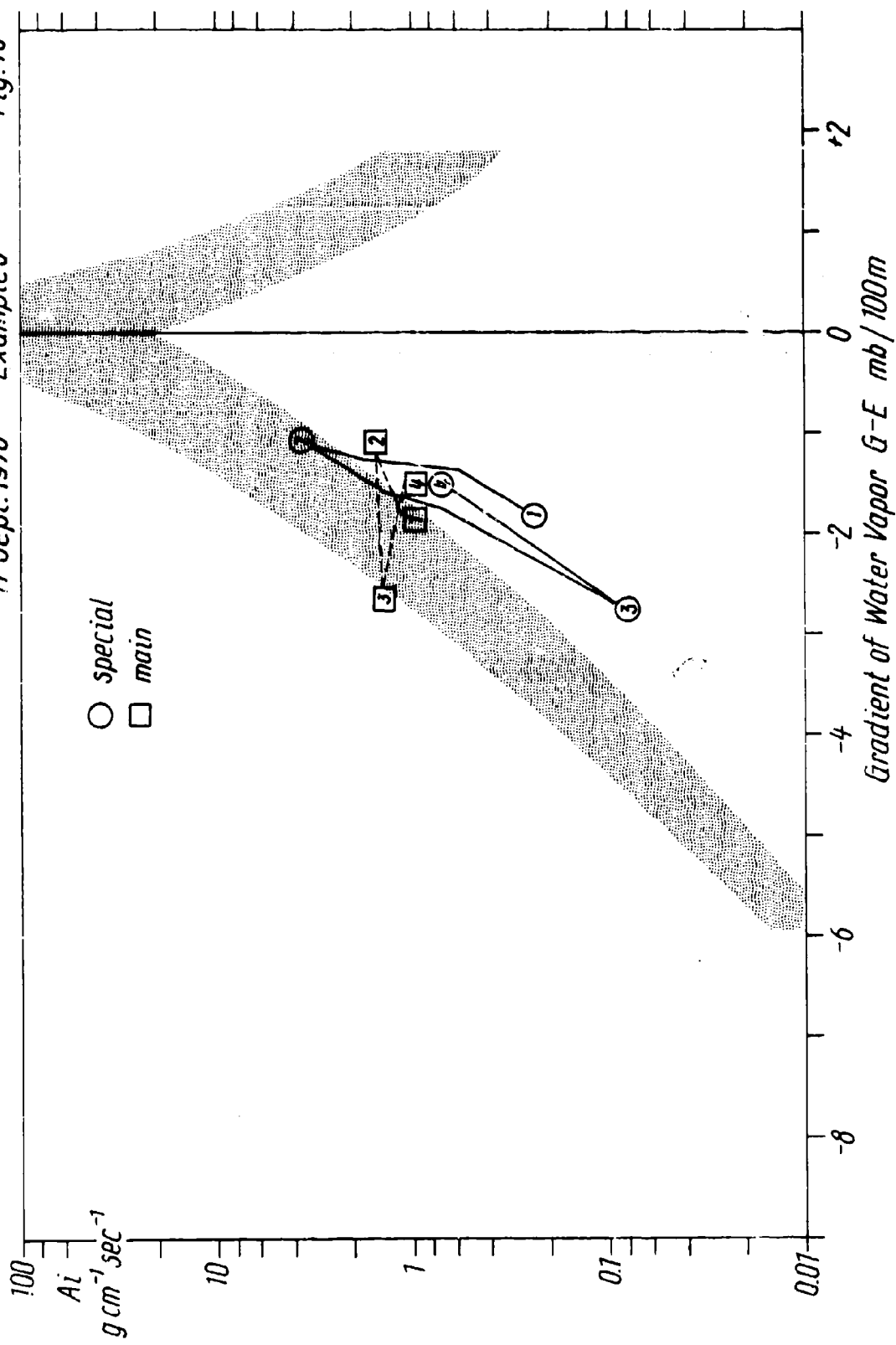


Example J Fig. 45



17 Sept. 1970      *Example J*

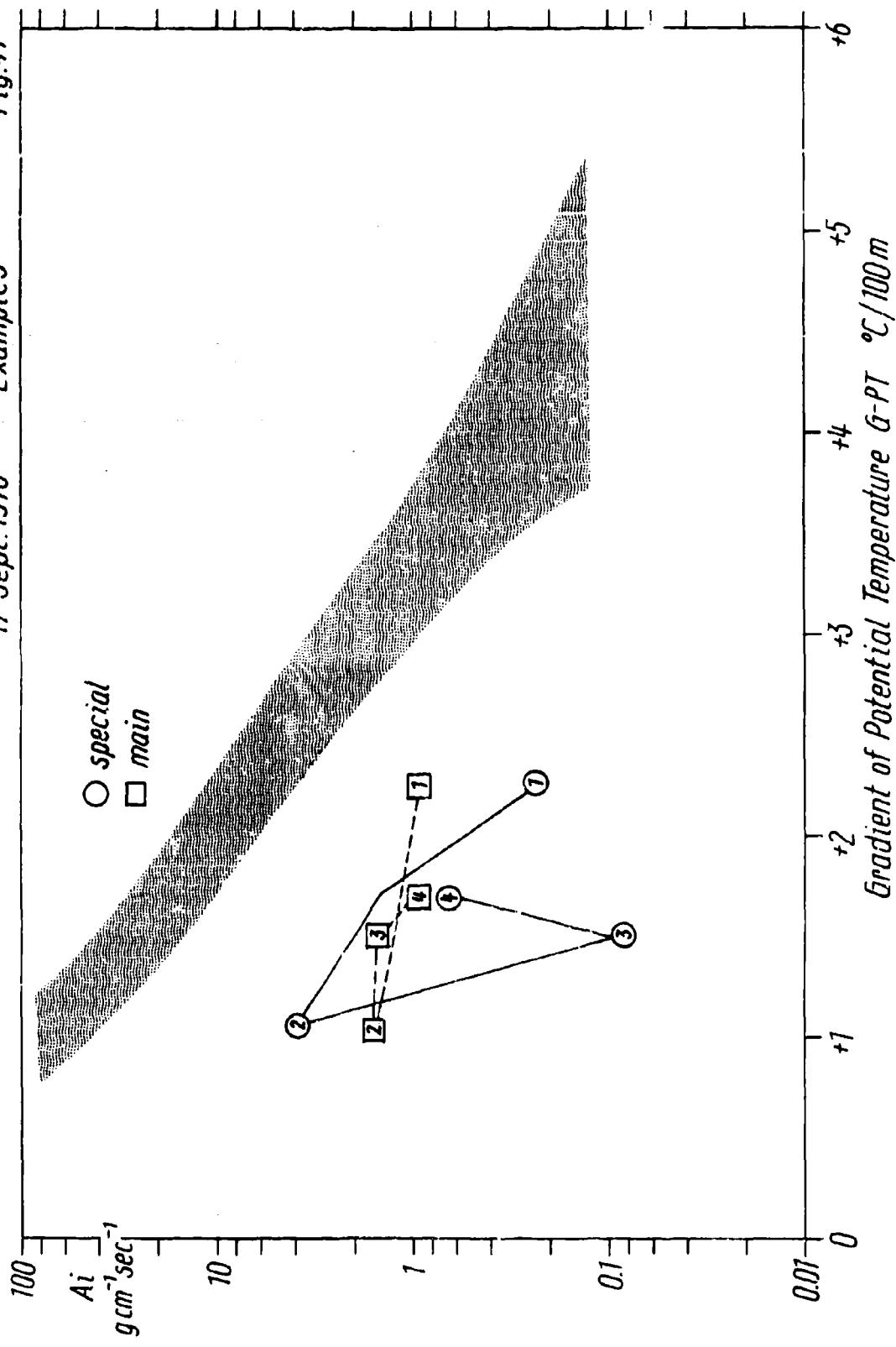
Fig. 46



17 Sept. 1970

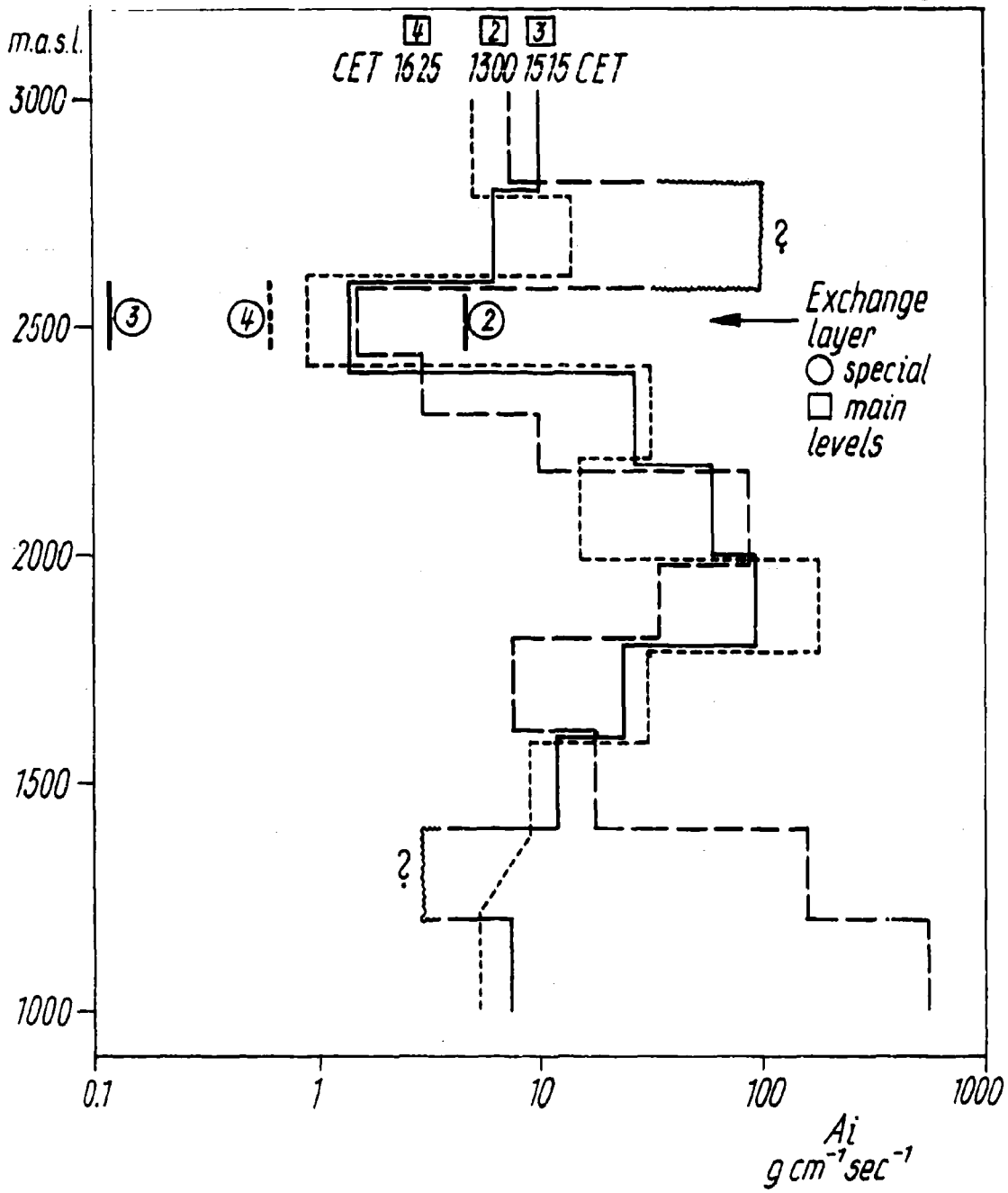
Example J

Fig. 47



### *Example J*

Fig. 48



2. Legends to the Figures 1 - 48

a

Legends to Figures

Fig. 1:

Chart on the processing of the recordings transmitted from the moving cable car, up to the final results: the completed tables printed out by teletype.

Fig. 2:

Relation between incremental exchange coefficient  $A_i$  and temperature gradient G-T. Representation of the relation by the individual pairs of values. The relation applies to real inversions exclusively (stationary equilibrium of the eddy diffusion).

Fig. 3:

Result of statistical analyses of Fig. 2 with indication of scatter (red).

Fig. 4:

Relation between incremental exchange coefficient  $A_i$  and gradient of potential temperature G-PT expressed in degrees centigrade per 100 m. Representation of the individual pairs of values. Valid for real inversions (stationary equilibrium of eddy diffusion).

Fig. 5:

Same as Fig. 4, however, result of statistical investigation with indication of scatter (red).

Fig. 6:

Relation between incremental exchange coefficient  $A_i$  and gradient of water vapor pressure G-E in mb/100m. Individual pairs of values. Valid for aerological structures having a G-T minimum with stationary equilibrium.

b

**Fig. 7:**

Same as Fig. 6, however, result of statistical investigation with indication of scatter (red).

**Fig. 8 and 9:**

Relation between incremental exchange coefficient  $A_i$  and gradient of potential temperature G-PT, divided into two intervals of time. Result of statistical investigation with indication of scatter. Relation of general applicability.

**Fig. 10:**

Mutual comparison of results from both intervals of time.

Re - Example A

**Fig. 11:**

Variations in space and time of important structural elements of the inversion newly formed at 1200 CET.

**Fig. 12:**

Time slope within the range of function  $A_i=f(G-T)$ . Numerals 1 through 4 identify the runs.

**Fig. 13:**

Same as Fig. 12, but relation  $A_i=f(G-PT)$ .

**Fig. 14:**

Same as Fig. 12, but function  $A_i=f(G-E)$ .

The following figures to Examples B trough H basically correspond to the figures of example A; hence separate legends are not needed.

**Fig. 19:**

Vertical profiles of the incremental exchange coefficients

c

$A_i$  and water vapor pressure E for runs 2 through 7.

Fig. 43:

Vertical profiles of the incremental exchange coefficients

$A_i$ , recorded during runs 3 and 6.

E: upper boundary of the exchange layer

I: level of inversion.

Fig. 48:

Vertical profile of the incremental exchange coefficients

$A_i$  for runs 2, 3 and 4.

3. Individual Runs and Data Tables

Examples A - J

Example

A

5 Oct 1970

①



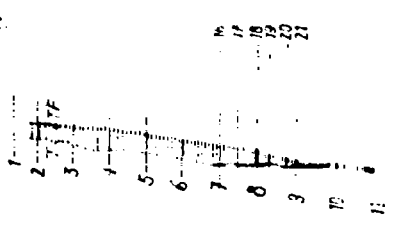
②



③



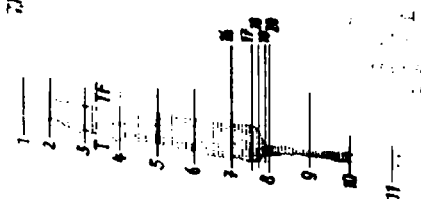
④



⑤



⑥



⑦



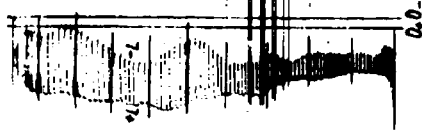
⑧



### *Example*

8

13 Nov 1970



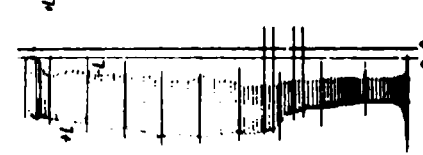
2

三



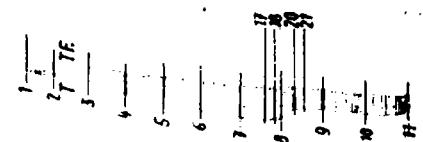
1

5	6	7	8	9	10	11
TF						
5	6	7	8	9	10	11
TF						
5	6	7	8	9	10	11



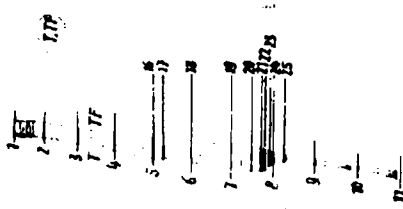
七

11

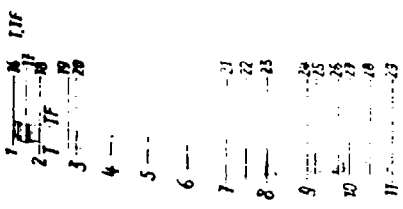


*Example*  
*C<sub>1</sub>*  
*14 Oct. 1970*

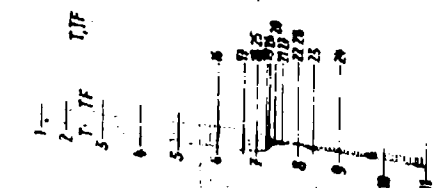
(1)



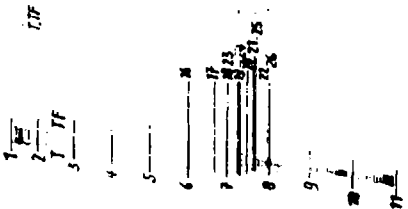
(0)



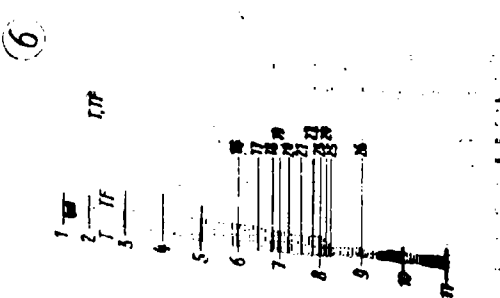
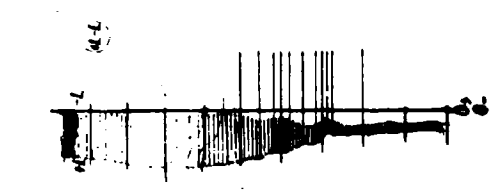
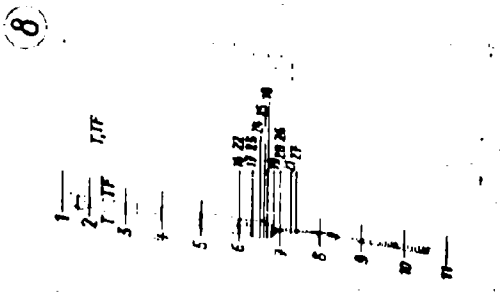
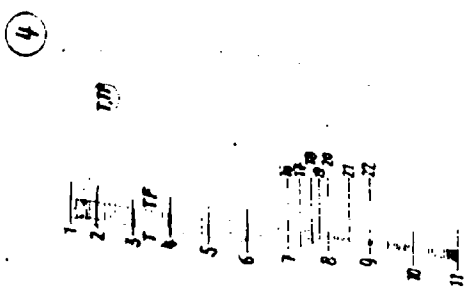
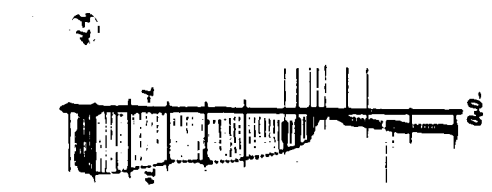
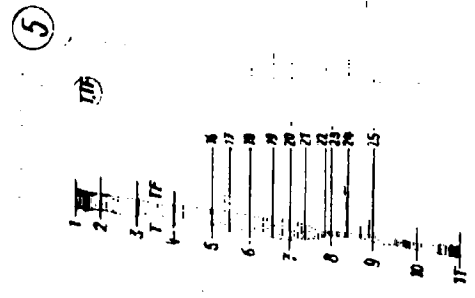
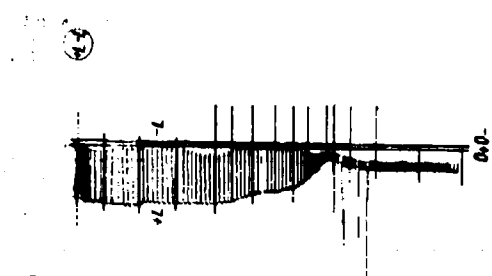
(3)



(2)

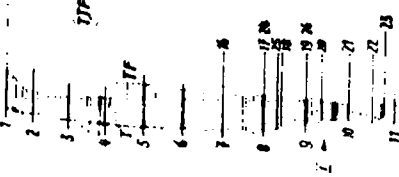


*Example*  
*C<sub>2</sub>*  
14 Oct 1970

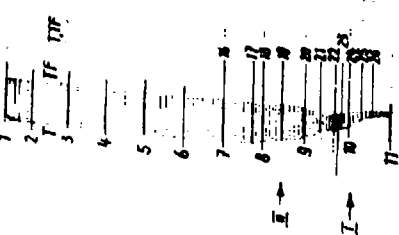


*Example*  
*E<sub>1</sub>*  
17 Oct 1970

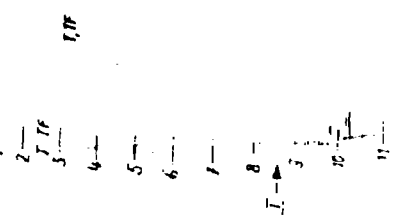
(2)



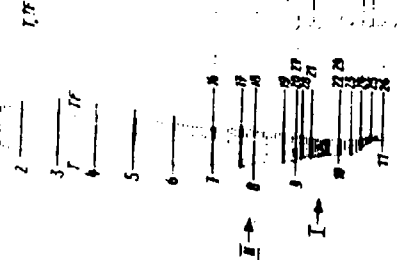
(4)



(1)



(3)



4.1

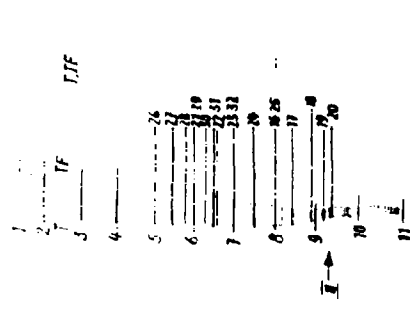
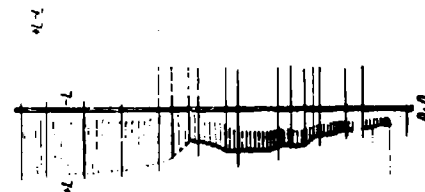
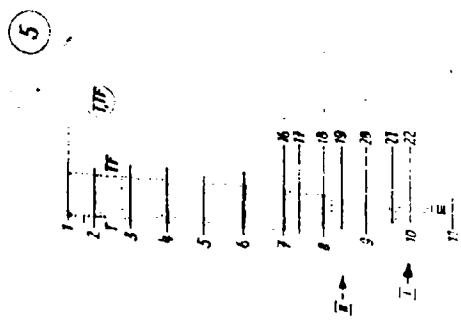
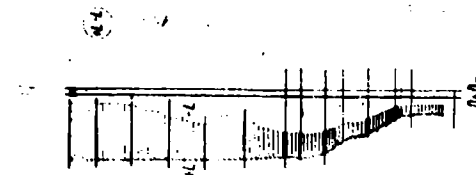
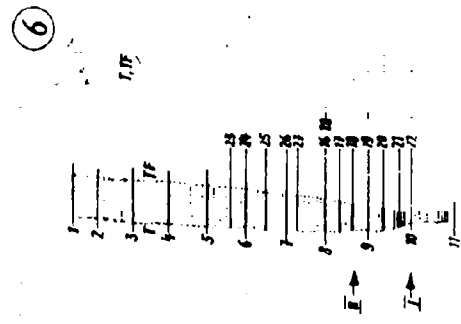
4.2

4.3

4.4

*Example*

*E<sub>2</sub>*  
17 Oct. 1970



*Example*

30 Sept 1970

(4)



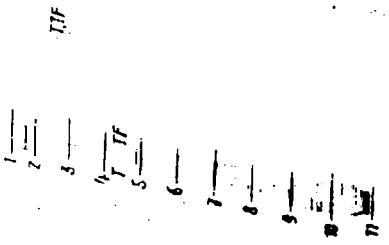
(5)



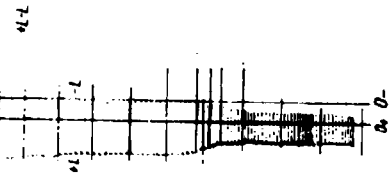
(4)



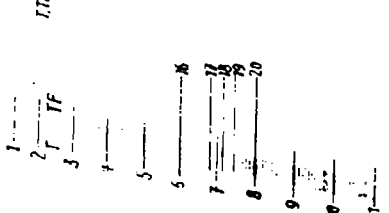
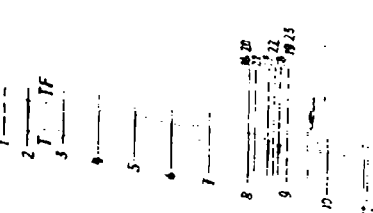
(7)



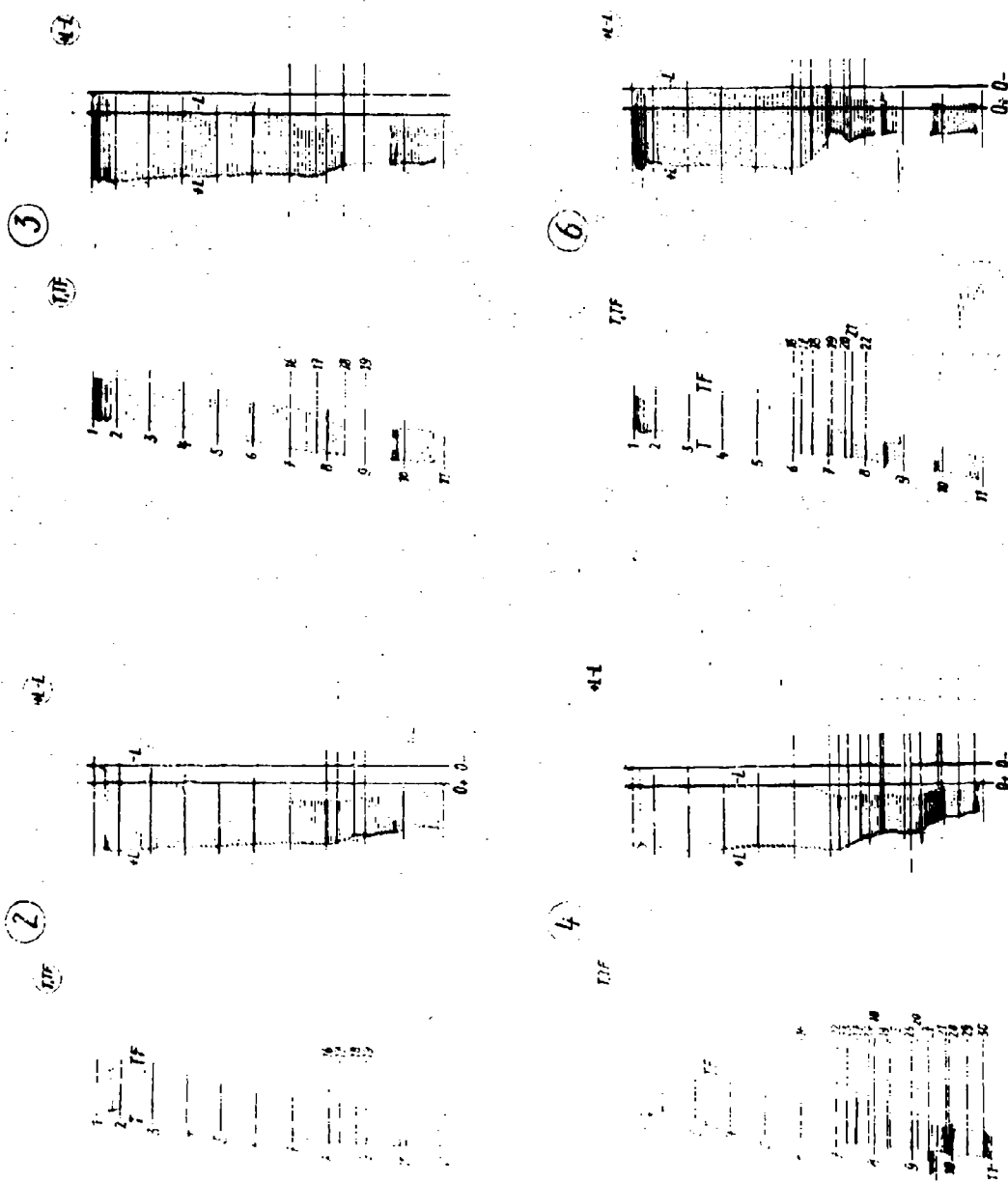
(4)



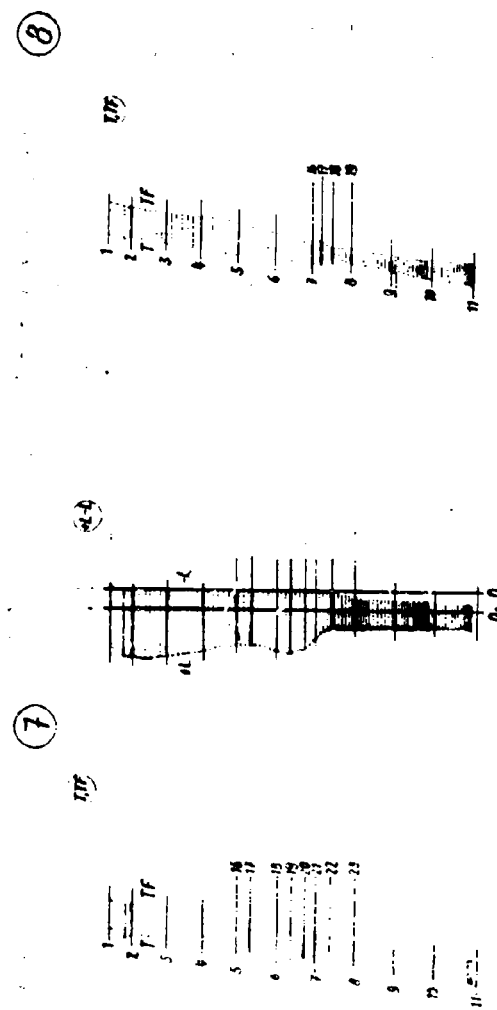
(6)



*Example*  
*G<sub>1</sub>*  
26 Sept. 1970



*Example*



*Example*

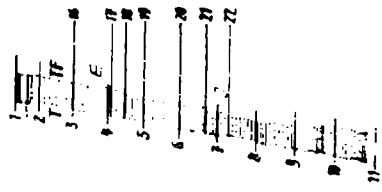
*H*

26 Sept. 1970

(1)



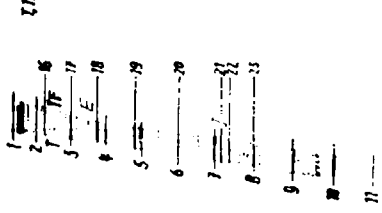
(4)



(2)



(3)



(5)



(2)



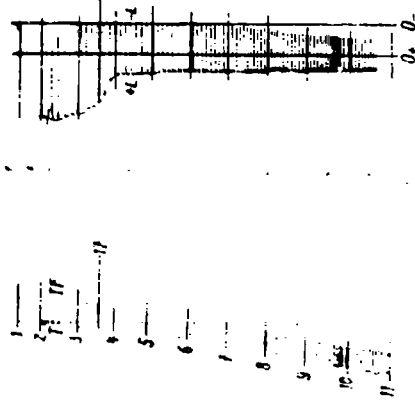
(6)



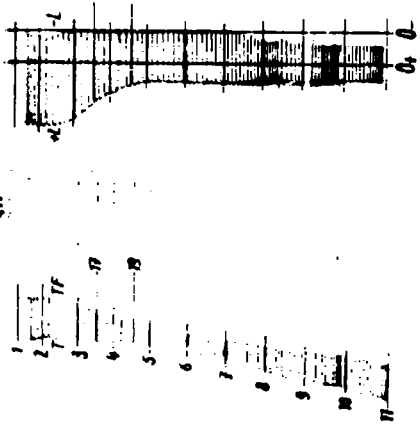
(4)



①



②



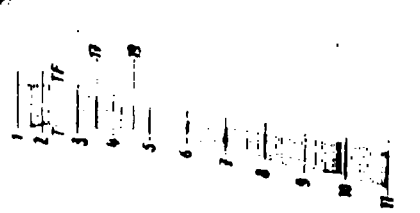
Example  
J

17 Sept. 1970

③



④



⑤



⑥



⑦





# Example B 18 Nov. 1970

Z-0651 18.11.1970

12:33 UHN

(1)

HALB-WECKEWE

NETS: WENDEL

E	N	P	T	TF	PT	EMT	E	S	HF	SL	L	W	L
+050.0	-	-	1040	1055	0313	0401	0321	-	-	-	-	03.3	
6	DN	IV	G-T	G-S	G-U	G-M	G-V	I	N	A	D	W	
+025	+000	-015	+010	+180	+018	+000	-	000.5	CODA	-	-	-	

E	N	P	T	TF	PT	EMT	E	S	HF	SL	L	W	L	
35	8800	7661	1	TP	PT	EMT	E	S	HF	SL	L	W	L	
02	2020	7661	+05.4	+00.6	2998	2084	0218	281.6	37.4	CB.5	/7/	1.43	04.4	
02	2020	7661	+05.5	+00.8	2988	2055	0313	43	38.7	37.4	CB.5	/7/	1.43	04.4
07	1600	8064	+05.3	+00.6	9950	3039	0318	47	CB.9	CB.3	/7/	1.43	04.5	
18	1600	8289	+05.1	+01.2	9816	3016	0311	31	37.5	36.4	CB.9	/7/	1.43	04.5
09	1000	8713	+05.7	+01.3	9813	3119	0311	31	37.5	36.4	CB.9	/7/	1.44	05.1
10	1600	8713	+05.7	+01.3	9813	0999	0315	32	37.5	36.4	CB.9	/7/	1.44	05.1
11	1000	8813	+04.3	+02.7	8861	2983	0317	47	04.58	77.9	01.1	00.8	1.33	31.9

E	N	P	T	TF	PT	EMT	E	S	HF	SL	L	W	L
05	1000	8041	+04.1	+01.1	9813	0981	0317	47	01.7	00.8	01.1	00.8	0.05
06	0959	+04.5	+01.2	+00.3	0917	+01.35	00.87	-	00.87	-	-	-	0.05
07	0958	+04.12	+01.2	+01.3	87.70	+1.17	01.39	00.33	0.65	67.98	07	-	-
08	+056	+04.10	+01.3	+01.3	87.70	+1.17	01.39	00.33	0.65	67.98	07	-	-
09	+055	+04.10	+01.3	+01.3	87.70	+1.17	01.39	00.33	0.65	67.98	07	-	-
10	+053	+04.10	+01.3	+01.3	87.70	+1.17	01.39	00.33	0.65	67.98	07	-	-
11	+050	+04.10	+01.3	+01.3	87.70	+1.17	01.39	00.33	0.65	67.98	07	-	-

NP-TEMPERATUR

E H P T T F PT EMT E S HF SL L W

E	H	P	T	T	F	PT	E	S	HF	SL	L	W	
16	1999	8969	+05.1	+01.8	8926	2088	04.52	02.40	51.4	08.0	01.8	1.41	03.4
17	1495	8313	+05.3	+01.4	8987	3017	04.59	03.41	51.5	01.9	01.9	1.42	03.4
18	1485	8450	+04.9	+01.6	9118	3019	03.50	03.70	57.6	01.9	01.9	1.42	03.4
09	1000	8966	+05.0	+01.5	8966	3024	03.07	03.66	56.9	01.8	00.9	1.43	03.0
10	1600	8840	+05.7	+01.8	9196	3021	03.04	03.63	51.0	01.7	01.1	1.40	03.0
11	1000	8823	+04.3	+02.7	8813	4999	03.48	33.74	57.3	01.1	01.2	1.40	03.9

12

DN IV G-T G-S G-U G-M I H A D A

+050

13

14

15

16

17

18

19

20

21

22

23

24

25

26

27

28

29

30

31

32

33

34

35

36

37

38

39

40

41

42

43

44

45

46

47

48

49

50

51

52

53

54

55

56

57

58

59

60

61

62

63

64

65

66

67

68

69

70

71

72

73

74

75

76

77

78

79

80

81

82

83

84

85

86

87

88

89

90

91

92

93

94

95

96

97

98

99

100

101

102

103

104

105

106

107

108

109

110

111

112

113

114

115

116

117

118

119

120

121

122

123

124

125

126

127

128

129

130

131

132

133

134

135

136

137

138

139

140

141

142

143

144

145

146

147

148

149

150

151

152

153

154

155

156

157

158

159

160

161

162

163

164

165

166

167

168

169

170

171

172

173

174

175

176

177

178

179

180

181

182

183

184

185

186

187

188

189

190

191

192

193

194

195

196

197

198

199

200

201

202

203

204

205

206







# Example E<sub>2</sub> 17 Oct. 1970

E-0436 17 Oct 1970

12:03 Uhr

(5)

HAUPT-NIVEAUS

Z	K	P	T	D	R	F	S	N	A	U	Z
01	1300	2100	+0.2	-0.1	1053	2047	-0.54	00.51	-07.5	-04.6	-01.3
02	0700	1300	+0.1	-0.1	1044	2046	-0.66	00.51	-07.7	-04.6	-01.3
03	0700	1700	+0.0	-0.1	1037	2045	-0.59	00.51	-07.7	-04.6	-01.3
04	2000	2400	+0.0	-0.1	1000	2044	-0.64	00.51	-07.7	-04.6	-01.3
05	2000	2100	+0.0	-0.1	1014	2043	-0.64	00.51	-07.7	-04.6	-01.3
06	0000	2000	+0.0	-0.1	1014	2042	-0.64	00.51	-07.7	-04.6	-01.3
07	0000	1800	+0.0	-0.1	2057	0958	-0.64	01.1	-07.7	-04.6	-01.3
08	0000	1600	+0.0	-0.1	1039	2057	-0.64	01.1	-07.7	-04.6	-01.3
09	0000	1400	+0.0	-0.1	1029	2056	-0.64	01.1	-07.7	-04.6	-01.3
10	0000	1200	+0.0	-0.1	1021	2055	-0.64	01.1	-07.7	-04.6	-01.3
11	0000	1000	+0.0	-0.1	1011	2054	-0.64	01.1	-07.7	-04.6	-01.3
Z	H	M	T	G	C	G	G	H	P	I	Z
01	1037	1037	1037	-0.1	-0.1	-0.1	-0.1	-0.1	-0.1	-0.1	01
02	-0.04	-0.04	-0.04	-0.16	-0.16	-0.16	-0.16	-0.16	-0.16	-0.16	01
03	-0.04	-0.04	-0.04	-0.16	-0.16	-0.16	-0.16	-0.16	-0.16	-0.16	01
04	-0.04	-0.04	-0.04	-0.16	-0.16	-0.16	-0.16	-0.16	-0.16	-0.16	01
05	-0.04	-0.04	-0.04	-0.16	-0.16	-0.16	-0.16	-0.16	-0.16	-0.16	01
06	-0.04	-0.04	-0.04	-0.16	-0.16	-0.16	-0.16	-0.16	-0.16	-0.16	01
07	-0.04	-0.04	-0.04	-0.16	-0.16	-0.16	-0.16	-0.16	-0.16	-0.16	01
08	-0.04	-0.04	-0.04	-0.16	-0.16	-0.16	-0.16	-0.16	-0.16	-0.16	01
09	-0.04	-0.04	-0.04	-0.16	-0.16	-0.16	-0.16	-0.16	-0.16	-0.16	01
10	-0.04	-0.04	-0.04	-0.16	-0.16	-0.16	-0.16	-0.16	-0.16	-0.16	01
11	-0.04	-0.04	-0.04	-0.16	-0.16	-0.16	-0.16	-0.16	-0.16	-0.16	01

WT-TEMPERATUR

Z	H	K	T	D	R	F	S	N	A	U	Z
16	1300	0103	10.3	-0.1	2057	0958	01.04	-04.04	-01.04	-07.04	-03.04
17	1317	0107	10.5	-0.1	2053	0952	01.04	-04.04	-01.04	-07.04	-03.04
18	1309	0109	10.5	-0.1	2051	0950	01.04	-04.04	-01.04	-07.04	-03.04
19	1315	0114	10.5	-0.1	2050	0948	01.04	-04.04	-01.04	-07.04	-03.04
20	1300	0116	10.5	-0.1	2049	0946	01.04	-04.04	-01.04	-07.04	-03.04
21	1300	0117	10.5	-0.1	2048	0945	01.04	-04.04	-01.04	-07.04	-03.04
22	1300	0118	10.5	-0.1	2047	0944	01.04	-04.04	-01.04	-07.04	-03.04
23	1300	0119	10.5	-0.1	2046	0943	01.04	-04.04	-01.04	-07.04	-03.04
24	1300	0120	10.5	-0.1	2045	0942	01.04	-04.04	-01.04	-07.04	-03.04
25	1300	0121	10.5	-0.1	2044	0941	01.04	-04.04	-01.04	-07.04	-03.04
26	1300	0122	10.5	-0.1	2043	0940	01.04	-04.04	-01.04	-07.04	-03.04
27	1300	0123	10.5	-0.1	2042	0939	01.04	-04.04	-01.04	-07.04	-03.04
28	1300	0124	10.5	-0.1	2041	0938	01.04	-04.04	-01.04	-07.04	-03.04
29	1300	0125	10.5	-0.1	2040	0937	01.04	-04.04	-01.04	-07.04	-03.04
30	1300	0126	10.5	-0.1	2039	0936	01.04	-04.04	-01.04	-07.04	-03.04
31	1300	0127	10.5	-0.1	2038	0935	01.04	-04.04	-01.04	-07.04	-03.04
32	1300	0128	10.5	-0.1	2037	0934	01.04	-04.04	-01.04	-07.04	-03.04
33	1300	0129	10.5	-0.1	2036	0933	01.04	-04.04	-01.04	-07.04	-03.04
34	1300	0130	10.5	-0.1	2035	0932	01.04	-04.04	-01.04	-07.04	-03.04
35	1300	0131	10.5	-0.1	2034	0931	01.04	-04.04	-01.04	-07.04	-03.04
36	1300	0132	10.5	-0.1	2033	0930	01.04	-04.04	-01.04	-07.04	-03.04
37	1300	0133	10.5	-0.1	2032	0929	01.04	-04.04	-01.04	-07.04	-03.04
38	1300	0134	10.5	-0.1	2031	0928	01.04	-04.04	-01.04	-07.04	-03.04
39	1300	0135	10.5	-0.1	2030	0927	01.04	-04.04	-01.04	-07.04	-03.04
40	1300	0136	10.5	-0.1	2029	0926	01.04	-04.04	-01.04	-07.04	-03.04
41	1300	0137	10.5	-0.1	2028	0925	01.04	-04.04	-01.04	-07.04	-03.04
42	1300	0138	10.5	-0.1	2027	0924	01.04	-04.04	-01.04	-07.04	-03.04
43	1300	0139	10.5	-0.1	2026	0923	01.04	-04.04	-01.04	-07.04	-03.04
44	1300	0140	10.5	-0.1	2025	0922	01.04	-04.04	-01.04	-07.04	-03.04
45	1300	0141	10.5	-0.1	2024	0921	01.04	-04.04	-01.04	-07.04	-03.04
46	1300	0142	10.5	-0.1	2023	0920	01.04	-04.04	-01.04	-07.04	-03.04
47	1300	0143	10.5	-0.1	2022	0919	01.04	-04.04	-01.04	-07.04	-03.04
48	1300	0144	10.5	-0.1	2021	0918	01.04	-04.04	-01.04	-07.04	-03.04
49	1300	0145	10.5	-0.1	2020	0917	01.04	-04.04	-01.04	-07.04	-03.04
50	1300	0146	10.5	-0.1	2019	0916	01.04	-04.04	-01.04	-07.04	-03.04
51	1300	0147	10.5	-0.1	2018	0915	01.04	-04.04	-01.04	-07.04	-03.04
52	1300	0148	10.5	-0.1	2017	0914	01.04	-04.04	-01.04	-07.04	-03.04
53	1300	0149	10.5	-0.1	2016	0913	01.04	-04.04	-01.04	-07.04	-03.04
54	1300	0150	10.5	-0.1	2015	0912	01.04	-04.04	-01.04	-07.04	-03.04
55	1300	0151	10.5	-0.1	2014	0911	01.04	-04.04	-01.04	-07.04	-03.04
56	1300	0152	10.5	-0.1	2013	0910	01.04	-04.04	-01.04	-07.04	-03.04
57	1300	0153	10.5	-0.1	2012	0909	01.04	-04.04	-01.04	-07.04	-03.04
58	1300	0154	10.5	-0.1	2011	0908	01.04	-04.04	-01.04	-07.04	-03.04
59	1300	0155	10.5	-0.1	2010	0907	01.04	-04.04	-01.04	-07.04	-03.04
60	1300	0156	10.5	-0.1	2009	0906	01.04	-04.04	-01.04	-07.04	-03.04
61	1300	0157	10.5	-0.1	2008	0905	01.04	-04.04	-01.04	-07.04	-03.04
62	1300	0158	10.5	-0.1	2007	0904	01.04	-04.04	-01.04	-07.04	-03.04
63	1300	0159	10.5	-0.1	2006	0903	01.04	-04.04	-01.04	-07.04	-03.04
64	1300	0150	10.5	-0.1	2005	0902	01.04	-04.04	-01.04	-07.04	-03.04
65	1300	0151	10.5	-0.1	2004	0901	01.04	-04.04	-01.04	-07.04	-03.04
66	1300	0152	10.5	-0.1	2003	0900	01.04	-04.04	-01.04	-07.04	-03.04
67	1300	0153	10.5	-0.1	2002	0899	01.04	-04.04	-01.04	-07.04	-03.04
68	1300	0154	10.5	-0.1	2001	0898	01.04	-04.04	-01.04	-07.04	-03.04
69	1300	0155	10.5	-0.1	2000	0897	01.04	-04.04	-01.04	-07.04	-03.04
70	1300	0156	10.5	-0.1	1999	0896	01.04	-04.04	-01.04	-07.04	-03.04
71	1300	0157	10.5	-0.1	1998	0895	01.04	-04.04	-01.04	-07.04	-03.04
72	1300	0158	10.5	-0.1	1997	0894	01.04	-04.04	-01.04	-07.04	-03.04
73	1300	0159	10.5	-0.1	1996	0893	01.04	-04.04	-01.04	-07.04	-03.04
74	1300	0150	10.5	-0.1	1995	0892	01.04	-04.04	-01.04	-07.04	-03.04
75	1300	0151	10.5	-0.1	1994	0891	01.04	-04.04	-01.04	-07.04	-03.04
76	1300	0152	10.5	-0.1	1993	0890	01.04	-04.04	-01.04	-07.04	-03.04
77	1300	0153	10.5	-0.1	1992	0889	01.04	-04.04	-01.04	-07.04	-03.04
78	1300	0154	10.5	-0.1	1991	0888	01.04	-04.04	-01.04	-07.04	-03.04
79	1300	0155	10.5	-0.1	1990	0887	01.04	-04.04	-01.04	-07.04	-03.04
80	1300	0156	10.5	-0.1	1989	0886	01.04	-04.04	-01.04	-07.04	-03.04
81	1300	0157	10.5	-0.1	1988	0885	01.04	-04.04	-01.04	-07.04	-03.04
82	1300	0158	10.5	-0.1	1987	0884	01.04	-04.04	-01.04	-07.04	-03.04
83	1300	0159	10.5	-0.1	1986	0883	01.04	-04.04	-01.04	-07.04	-03.04
84	1300	0150	10.5	-0.1	1985	0882	01.04	-04.04	-01.04	-07.04	-03.04
85	1300	0151	10.5	-0.1	1984	0881	01.04	-04.04	-01.04	-07.04	-03.04
86	1300	0152	10.5	-0.1	1983	0880	01.04	-04			

# Example F 30 Sept. 1970

E-0784 30.09.1970 13:03 UN:

(4)

## HAUPT-BEVALES:

C	N	P	T	IP	PT	E	R	A	D	L	U	Z
01	3003	5130	+03.8	051.8	3073	3104	023.2	43.6	01.5	/	130	02.8
02	8800	7030	+02.3	050.8	3073	3104	01.5	03.8	01.5	/	130	01.5
03	8800	7030	+02.3	050.8	3073	3104	01.5	03.8	01.5	/	130	01.5
04	8400	7501	+02.6	051.3	3056	3104	04.7	02.9	02.6	/	130	01.5
05	8800	7501	+02.6	051.3	3056	3104	04.7	02.9	02.6	/	130	01.5
06	8800	7501	+02.6	051.3	3056	3104	04.7	02.9	02.6	/	130	01.5
07	1850	6133	+16.7	050.0	3020	3147	05.9	39.0	01.7	/	130	01.5
08	1800	6147	+13.9	050.6	3023	3126	05.7	39.9	01.7	/	130	01.5
09	1800	6147	+13.9	050.6	3023	3126	05.7	39.9	01.7	/	130	01.5
10	1800	6744	+15.2	052.7	0998	3104	06.5	06.5	02.9	01.5	130	01.5
11	1800	6744	+15.2	052.7	0998	3104	06.5	06.5	02.9	01.5	130	01.5

CHARTS 30.09.1970 14:15 UN:

(5)

## HAUPT-BEVALES:

C	N	P	T	IP	PT	E	R	A	D	L	U	Z	
01	064					024.8	08.9						
02	079	+10.5	+01.1	+00.3	+3.81	C-11.0	-09.49	09.81	37.3	30	48007	CB	
03	+064	+01.5	+01.1	+00.3	+3.81	024.8	08.9						
04	+119	+04.0	+11.7	+00.3	+3.81	024.8	08.9						
05	+119	+04.0	+11.7	+00.3	+3.81	024.8	08.9						
06	+184	+05.9	+0.34	+0.88	-11.17	+02.4	-01.58	01.48	4816.74	00	00		
07	+134	+05.9	+0.34	+0.88	-11.17	+02.4	-01.58	01.48	56.16	57671	07		
08	+184	+06.0	+0.34	+0.88	-11.17	+02.4	-01.58	01.48	78.31	78044	04		
09	+184	+06.0	+0.34	+0.88	-11.17	+02.4	-01.58	01.48	80.39	24815	08		
10	+183	+07.0	+0.34	+0.88	-11.16	+02.4	-01.58	01.48	78.36	35.73	34806	10	
11	+178	+04.0	+0.65	+0.38	+0.31	+0.65	-0.64	07.81	3201.87	00	11		

## HP-TOPOMORPHEN:

C	N	P	T	IP	PT	E	R	A	D	L	U	Z
14	1801	8347	+13.9	050.6	3083	3128	04.7	04.7	01.7	02.4	01.7	
15	1800	8350	+16.8	050.3	3218	3154	07.6	08.8	03.8	01.3	02.4	
16	1800	8409	+12.8	+11.7	3204	3166	06.8	02.16	02.1	01.0	02.5	
17	1800	8544	+13.0	+0.5	3209	3166	06.8	02.16	02.1	01.0	02.5	

## HP-FREQUENZIMETRIE:

C	N	P	T	IP	PT	E	R	A	D	L	U	Z
01	105	0181	+0.89	+1.63	+1.32	+0.02	+0.70	+0.18	4.87	4.87	4806	17
02	049	+0.89	+1.63	+1.32	+0.02	+0.70	+0.18	4.87	4.87	4806	17	
03	049	+0.89	+1.63	+1.32	+0.02	+0.70	+0.18	4.87	4.87	4806	17	
04	1800	8344	+13.6	+0.6	3063	3165	06.8	02.0	02.0	02.5	01.5	

## HP-FREQUENZIMETRIE:

C	N	P	T	IP	PT	E	R	A	D	L	U	Z
01	1801	8347	+13.9	+0.6	3083	3128	04.7	04.7	01.7	02.4	01.7	
02	1800	8350	+16.8	+0.3	3218	3154	07.6	08.8	03.8	01.3	02.4	
03	1800	8409	+12.8	+11.7	3204	3166	06.8	02.16	02.1	01.0	02.5	
04	1800	8544	+13.0	+0.5	3209	3166	06.8	02.16	02.1	01.0	02.5	

## HP-FREQUENZIMETRIE:

C	N	P	T	IP	PT	E	R	A	D	L	U	Z
01	034	1146	+0.83	+0.33	-0.19	-0.78	+0.42	+0.01	4.83	4.83	83570	11
02	093	+150	+0.10	+0.06	-0.23	-0.73	+0.44	+0.01	4.83	4.83	83720	10
03	070	+146	+0.10	+0.07	-0.24	-0.73	+0.44	+0.01	4.83	4.83	83720	10

## HP-FREQUENZIMETRIE:

C	N	P	T	IP	PT	E	R	A	D	L	U	Z
01	034	1146	+0.83	+0.33	-0.19	-0.78	+0.42	+0.01	4.83	4.83	83570	11
02	093	+150	+0.10	+0.06	-0.23	-0.73	+0.44	+0.01	4.83	4.83	83720	10
03	070	+146	+0.10	+0.07	-0.24	-0.73	+0.44	+0.01	4.83	4.83	83720	10

## HP-FREQUENZIMETRIE:

C	N	P	T	IP	PT	E	R	A	D	L	U	Z
01	034	1146	+0.83	+0.33	-0.19	-0.78	+0.42	+0.01	4.83	4.83	83570	11
02	093	+150	+0.10	+0.06	-0.23	-0.73	+0.44	+0.01	4.83	4.83	83720	10
03	070	+146	+0.10	+0.07	-0.24	-0.73	+0.44	+0.01	4.83	4.83	83720	10

## HP-FREQUENZIMETRIE:

C	N	P	T	IP	PT	E	R	A	D	L	U	Z
01	034	1146	+0.83	+0.33	-0.19	-0.78	+0.42	+0.01	4.83	4.83	83570	11
02	093	+150	+0.10	+0.06	-0.23	-0.73	+0.44	+0.01	4.83	4.83	83720	10
03	070	+146	+0.10	+0.07	-0.24	-0.73	+0.44	+0.01	4.83	4.83	83720	10

## HP-FREQUENZIMETRIE:

C	N	P	T	IP	PT	E	R	A	D	L	U	Z
01	034	1146	+0.83	+0.33	-0.19	-0.78	+0.42	+0.01	4.83	4.83	83570	11
02	093	+150	+0.10	+0.06	-0.23	-0.73	+0.44	+0.01	4.83	4.83	83720	10
03	070	+146	+0.10	+0.07	-0.24	-0.73	+0.44	+0.01	4.83	4.83	83720	10

## HP-FREQUENZIMETRIE:

C	N	P	T	IP	PT	E	R	A	D	L	U	Z
01	034	1146	+0.83	+0.33	-0.19	-0.78	+0.42	+0.01	4.83	4.83	83570	11
02	093	+150	+0.10	+0.06	-0.23	-0.73	+0.44	+0.01	4.83	4.83	83720	10
03	070	+146	+0.10	+0.07	-0.24	-0.73	+0.44	+0.01	4.83	4.83	83720	10

## HP-FREQUENZIMETRIE:

C	N	P	T	IP	PT	E	R	A	D	L	U	Z
01	034	1146	+0.83	+0.33	-0.19	-0.7						









4. Tables I - XII

**TABLE I**  
**RaB in air; units:  $10^{-12} \mu\text{c}/\text{cm}^3$**

**Station designations:** Z Zugspitze                            2964 m a.s.l.  
                           W Wank                                    1780 m a.s.l.  
                           G Garmisch-Partenkirchen            730 m a.s.l.

**Measurement periods :** a = 2150 - 0920, b = 0950 - 1220,  
                           c = 1250 - 1620. (Central European Time)

**Month:** July 1970      ("No measurement" is denoted by: - )

	a			b			c		
	Z	W	G	Z	W	G	Z	W	G
1.	8,5	7	130	14,2	16	82	7,9	61	85
2.	-	57	233	12,2	24	64	14,8	-	58
3.	8,1	28	108	8,8	16	43	7,1	10	37
4.	3,3	18	130	1,9	11	46	3,9	17	57
5.	-	-	171	-	-	54	-	-	-
6.	4,2	-	263	4,9	57	145	17,5	64	92
7.	4,1	49	299	20,4	109	160	60,6	108	150
8.	5,8	116	256	71,7	145	237	90,3	154	229
9.	-	75	194	55,9	76	128	31,8	11	57
10.	32,7	90	304	58,7	81	116	62,9	81	86
11.	100,3	135	333	86,5	146	151	92,8	90	129
12.	-	-	268	-	-	115	-	-	-
13.	49,7	150	-	80,9	171	228	96,2	141	189
14.	65,5	87	313	68,2	113	180	66,9	103	131
15.	3,7	4	35	2,5	7	39	1,5	10	53
16.	3,2	7	80	1,3	4	58	0,8	-	38
17.	1,7	2	54	0,5	4	50	0,6	-	46
18.	2,6	15	180	7,7	35	93	5,4	21	53
19.	-	-	172	-	-	88	-	-	-
20.	75,1	-	306	99,9	157	208	93,2	168	153
21.	63,7	63	148	79,3	77	135	55,9	86	89
22.	69,7	156	336	64,0	150	200	55,1	113	138
23.	68,3	107	320	78,3	157	291	114,2	105	147
24.	75,8	75	200	84,4	126	-	88,2	104	133
25.	1,6	14	-	1,6	9	-	1,2	14	38
26.	-	-	-	-	-	38	-	-	-
27.	1,4	15	173	2,1	15	128	3,4	23	113
28.	5,2	74	316	13,3	46	190	69,3	108	186
29.	77,4	68	307	111,4	110	131	17,6	32	96
30.	49,3	97	304	58,1	150	213	73,1	118	152
31.	44,2	89	240	55,2	126	184	65,4	46	-

**TABLE II**  
RaB in air; units:  $10^{-12} \mu\text{c}/\text{cm}^3$

**Station Designations:** Z Zugspitze 2964 m a.s.l.  
 W Wank 1780 m a.s.l.  
 G Garmisch-Partenkirchen 730 m a.s.l.  
**Measurement periods :** a = 2150 - 0920, b = 0950 - 1220,  
 c = 1250 - 1620. (Central European Time)  
**Month:** August 1970 ("No measurement" is denoted by: - )

	a			b			c		
	Z	W	G	Z	W	G	Z	W	G
1.	22,1	49	297	40,5	112	246	51,2	44	65
2.	-	-	-	-	-	174	-	-	-
3.	31,8	101	-	63,2	111	-	67,2	77	-
4.	38,8	69	286	41,0	36	148	70,4	108	145
5.	110,3	147	359	99,8	125	143	89,7	82	-
6.	71,3	160	333	76,2	166	268	97,0	137	191
7.	142,6	107	349	87,5	95	188	73,0	94	-
8.	50,4	49	242	45,6	87	120	25,2	48	96
9.	-	-	161	-	-	130	-	-	-
10.	1,5	-	569	1,6	4	338	-	7	431
11.	0,3	32	466	-	58	174	-	26	112
12.	2,7	18	165	10,7	50	107	46,6	56	-
13.	28,4	98	-	39,8	105	-	78,5	122	132
14.	83,7	107	388	73,5	136	200	53,4	77	100
15.	-	-	-	-	-	-	-	-	-
16.	-	-	-	-	-	-	-	-	-
17.	28,3	98	268	0,8	17	153	3,6	18	109
18.	15,6	67	215	13,3	103	169	40,0	99	133
19.	70,5	172	426	85,6	232	295	105,0	154	134
20.	77,8	110	449	101,7	132	150	53,7	23	110
21.	3,8	10	90	4,4	9	66	-	9	61
22.	5,1	25	151	7,8	35	93	28,6	41	68
23.	-	-	258	-	-	109	-	-	-
24.	-	-	194	1,7	20	243	1,2	19	102
25.	21,9	62	304	19,9	91	158	35,3	76	93
26.	15,5	101	306	24,1	128	207	82,2	86	117
27.	72,0	100	382	78,3	104	203	86,3	125	189
28.	28,3	48	217	50,7	58	130	82,6	70	153
29.	75,2	115	318	94,5	140	240	87,4	156	210
30.	-	-	503	-	-	174	-	-	-
31.	33,1	-	306	36,0	121	198	39,5	101	133

TABLE III

RaB in air; units:  $10^{-12} \mu\text{c}/\text{cm}^3$ 

Station Designations: Z Zugspitze 2964 m a.s.l.  
 W Wall 1780 m a.s.l.  
 G Garmisch-Partenkirchen 730 m a.s.l.

Measurement periods : a = 2150 - 0920, b = 0950 - 1220,  
 c = 1250 - 1620. (Central European Time)

Month: September 1970 ("No measurement" is denoted by: - )

	a			b			c		
	Z	W	G	Z	W	G	Z	W	G
1.	8,3	56	535	3,7	33	117	4,8	85	198
2.	38,4	80	167	45,5	114	154	88,5	129	120
3.	76,4	124	448	104,4	127	250	60,8	123	247
4.	2,4	41	279	3,7	22	67	13,2	30	59
5.	2,7	22	342	-	4	114	1,4	16	61
6.	-	-	92	-	-	57	-	-	-
7.	3,1	40	136	10,4	54	115	26,4	82	81
8.	65,6	120	276	44,5	131	230	84,7	153	160
9.	67,9	136	279	69,7	181	255	121,5	163	158
10.	54,0	112	301	59,7	101	157	50,9	91	181
11.	63,2	91	326	62,8	65	105	15,4	12	75
12.	37,8	20	88	51,8	35	104	65,3	47	99
13.	-	-	107	-	-	44	-	-	-
14.	29,4	58	258	26,3	153	160	63,4	101	103
15.	83,7	-	394	124,8	131	208	138,7	156	159
16.	4,3	16	74	2,3	11	84	1,8	12	37
17.	6,3	38	235	3,5	28	53	1,7	33	59
18.	5,5	26	275	11,1	53	184	24,0	83	124
19.	27,3	108	380	26,9	177	376	43,9	193	318
20.	-	-	504	-	-	237	-	-	-
21.	8,0	46	527	1,6	92	150	-	91	134
22.	1,6	48	697	12,4	143	201	36,8	94	119
23.	4,8	89	273	5,9	117	153	56,3	84	122
24.	8,4	84	410	0,9	109	201	24,3	132	167
25.	2,6	10	331	5,6	70	175	14,3	61	133
26.	5,4	41	401	3,2	138	230	31,2	170	164
27.	-	-	419	-	-	257	-	-	-
28.	5,8	19	311	6,6	74	265	22,3	144	211
29.	13,6	64	384	36,2	109	315	64,3	200	333
30.	5,9	44	329	12,8	50	200	41,6	146	226

TABLE IV

RaB in air; units  $10^{-12} \mu\text{c}/\text{cm}^3$ 

Station Designations: Z Zugspitze 2964 m a.s.l.  
 W Wank 1780 m a.s.l.  
 G Garmisch-Partenkirchen 730 m a.s.l.

Measurement periods : a = 2150 - 0920, b = 0950 - 1220,  
 c = 1250 - 1620. (Central European Time)

Month: October 1970 ("No measurement" is denoted by: - )

	a			b			c		
	Z	W	G	Z	W	G	Z	W	G
1.	-	4	130	-	6	47	-	2	53
2.	1,7	16	99	0,2	9	96	0,1	8	34
3.	2,7	3	45	0,9	-	35	2,4	2	15
4.	-	-	59	-	-	56	-	-	-
5.	1,1	11	175	0,6	11	145	0,9	27	126
6.	15,5	22	190	20,6	74	143	50,3	103	174
7.	24,8	86	210	29,3	77	107	65,6	80	109
8.	40,3	43	251	26,3	61	245	34,8	50	294
9.	40,7	49	631	40,5	40	410	45,9	74	401
10.	27,7	71	276	28,6	74	123	52,8	103	392
11.	-	-	359	-	-	653	-	-	-
12.	12,4	51	238	9,9	124	431	14,0	155	399
13.	8,8	84	407	7,0	112	382	15,9	168	270
14.	16,4	65	727	20,2	232	373	46,4	192	392
15.	4,7	78	268	5,4	150	200	5,7	34	141
16.	7,4	61	412	9,9	82	322	16,7	78	141
17.	6,8	61	700	4,4	79	361	16,6	145	554
18.	-	-	395	-	-	464	-	-	-
19.	11,8	18	297	13,6	31	282	19,6	69	203
20.	13,1	11	71	6,0	4	136	8,7	3	171
21.	18,9	25	159	5,2	21	74	4,1	20	74
22.	11,1	32	226	14,7	19	63	13,4	40	36
23.	-	7	129	3,5	3	57	3,2	4	18
24.	14,2	23	175	9,6	61	112	12,9	69	102
25.	-	-	221	-	-	117	-	-	-
26.	-	9	-	2,3	10	345	6,6	36	200
27.	13,3	44	493	13,4	33	345	16,4	105	193
28.	7,2	38	487	6,0	66	264	16,1	60	169
29.	3,4	17	302	0,8	9	138	2,0	7	149
30.	6,5	15	286	2,5	35	208	8,4	25	205
31.	7,6	13	208	7,3	18	305	14,6	21	252

TABLE V

Station Designations: Z Zugspitze 2964 m a.s.l.  
 W Wank 1780 m a.s.l.  
 G Garmisch-Partenkirchen 730 m a.s.l.

Measurement periods : a = 2150 - 0920, b = 0950 - 1220,  
 c = 1250 - 1620. (Central European Time)

Month: November 1970 ("No measurement" is denoted by: - )

	a			b			c		
	Z	W	G	Z	W	G	Z	W	G
1.	-	-	221	-	-	145	-	-	-
2.	4,8	10	271	9,8	7	82	12,0	10	56
3.	14,4	22	276	11,6	9	35	12,2	11	34
4.	26,9	51	319	19,4	65	129	24,8	77	134
5.	7,0	15	416	8,3	10	196	4,2	5	36
6.	14,2	9	54	4,5	8	41	9,3	16	58
7.	20,1	65	384	19,7	125	320	49,5	193	289
8.	-	-	446	-	-	383	-	-	-
9.	35,2	48	484	15,2	47	373	13,5	29	91
10.	10,8	17	64	8,6	14	45	7,8	13	46
11.	4,7	28	334	2,6	25	196	2,3	6	270
12.	11,0	30	366	11,4	41	222	17,7	83	177
13.	82,9	83	415	80,1	136	241	86,8	116	183
14.	65,3	88	521	61,1	136	310	67,8	26	263
15.	-	-	211	-	-	91	-	-	-
16.	7,9	5	109	10,3	4	78	17,0	7	79
17.	3,3	21	315	1,3	10	228	0,7	2	227
18.	16,6	36	327	18,5	70	291	28,1	78	245
19.	32,2	32	302	39,4	29	209	48,1	70	146
20.	11,7	10	193	10,6	7	189	9,3	28	99
21.	45,8	-	384	57,9	-	174	44,3	-	61
22.	-	-	194	-	-	86	-	-	-
23.	3,4	19	306	2,9	14	145	-	23	146
24.	2,8	7	236	1,9	5	188	1,3	5	209
25.	4,7	22	245	3,6	16	189	1,3	83	294
26.	5,9	11	285	0,3	25	271	-	47	247
27.	3,4	24	551	0,7	40	308	0,4	61	403
28.	2,9	-	202	2,1	-	187	23,5	-	158
29.	-	-	197	-	-	340	-	-	-
30.	57,7	33	546	7,6	5	620	7,2	14	261

TABLE VI

Station Designation: Z Zugspitze 2964 m a.s.l.  
 W Wank 1780 m a.s.l.  
 G Garmisch-Partenkirchen 730 m a.s.l.

Measurement periods: a = 2150 - 0920, b = 0950 - 1220.  
 b = 1250 - 1620. (Central European Time)

Month: December 1970 ("No measurement" is denoted by: - )

	a			b			c		
	Z	W	G	Z	W	G	Z	W	G
1.	22,9	70	350	24,9	85	292	55,4	92	315
2.	6,7	9	285	7,5	18	175	7,5	22	146
3.	10,9	27	279	-	21	224	-	4	135
4.	-	11	233	4,1	15	250	-	-	181
5.	15,0	-	317	4,7	-	371	2,1	-	59
6.	-	-	343	-	-	183	-	-	-
7.	57,0	-	505	73,9	85	648	74,6	226	333
8.	42,0	23	187	38,7	23	205	9,4	72	233
9.	3,2	17	513	1,3	10	397	1,5	10	401
10.	2,9	6	746	0,2	12	672	-	38	551
11.	3,1	16	1045	1,6	13	557	1,4	36	509
12.	6,8	49	239	6,1	23	228	9,7	33	344
13.	-	-	317	-	-	570	-	-	-
14.	17,6	142	824	14,2	148	825	30,7	140	750
15.	32,3	10	173	5,4	12	108	16,3	15	102
16.	-	11	257	2,1	16	332	3,2	27	234
17.	2,4	7	804	0,9	9	830	-	50	630
18.	7,8	16	686	5,6	17	670	7,4	33	430
19.	5,8	54	429	5,3	74	378	3,6	105	280
20.	-	-	554	-	-	715	-	-	-
21.	2,7	15	555	1,4	26	685	6,5	16	485
22.	11,3	6	88	8,9	14	84	18,7	16	102
23.	20,4	44	436	21,7	21	260	15,9	28	152
24.	11,2	28	-	13,8	43	598	-	-	272
25.	-	-	490	-	-	495	-	-	-
26.	-	-	-	-	-	750	-	-	-
27.	-	-	328	-	-	850	-	-	-
28.	52,0	52	559	47,4	57	510	62,2	79	546
29.	34,8	88	504	31,9	93	466	25,3	38	434
30.	39,3	113	430	63,9	168	488	71,1	68	494
31.	78,5	61	713	54,2	103	292	-	-	278

TABLE VII

RaB in air; units  $10^{-12} \mu\text{c}/\text{cm}^3$

Station Designations: Z Zugspitze 2964 m a.s.l.  
W Wank 1780 m a.s.l.  
G Garmisch-Partenkirchen 730 m a.s.l.

Measurement periods : a = 2150 - 0920, b = 0950 - 1220,  
c = 1250 - 1620, (Central European Time)

Month: January 1971 ("No measurement" is denoted by: - )

	a			b			c		
	Z	W	G	Z	W	G	Z	W	G
1.	-	-	182	-	-	120	-	-	-
2.	3,2	12	444	2,3	8	415	3,1	10	459
3.	-	-	1150	-	-	721	-	-	-
4.	17,6	6	514	31,5	54	368	34,6	133	330
5.	25,1	74	650	12,5	79	1006	11,0	120	844
6.	-	-	402	-	-	481	-	-	-
7.	8,6	51	347	6,7	19	319	7,4	45	331
8.	4,4	8	247	3,0	13	291	0,7	13	399
9.	1,9	5	256	0,1	4	350	5,2	22	345
10.	-	-	279	-	-	413	-	-	-
11.	30,8	30	290	32,5	30	292	25,5	30	287
12.	34,1	85	508	25,6	111	445	31,4	186	344
13.	21,4	124	661	14,3	145	880	17,1	160	509
14.	26,4	36	334	30,6	26	371	32,5	30	558
15.	84,1	198	516	63,4	195	536	109,2	128	150
16.	30,2	127	588	25,3	151	599	25,5	147	304
17.	-	-	560	-	-	420	-	-	-
18.	12,8	107	434	10,2	79	445	25,9	217	443
19.	57,5	81	441	52,6	73	497	48,3	95	327
20.	52,9	91	480	35,1	77	511	34,9	107	431
21.	31,2	53	388	27,2	25	498	36,4	22	369
22.	11,7	31	-	11,7	19	403	19,4	24	416
23.	30,9	91	400	23,8	119	342	21,1	124	213
24.	-	-	314	-	-	139	-	-	-
25.	17,3	-	321	32,9	62	348	36,3	37	198
26.	11,3	27	350	9,9	12	338	9,0	22	291
27.	32,7	59	330	27,5	77	297	35,1	71	160
28.	11,7	11	176	11,7	12	207	12,3	17	109
29.	10,3	119	467	7,4	122	278	12,6	145	184
30.	26,5	99	336	29,4	86	294	24,2	61	198
31.	-	-	144	-	-	78	-	-	-

TABLE VIII

RaB in air; units  $10^{-12} \mu\text{c}/\text{cm}^3$ 

Station Designations: Z Zugspitze 2964 m a.s.l.

W Wank 1780 m a.s.l.

G Ermisch-Partenkirchen 730 m a.s.l.

Measurement periods : a = 2150 - 0920, b = 0950 - 1220,  
c = 1250 - 1620. (Central European Time)Month: February 1971 ("No measurement" is denoted by: - )

	a			b			c		
	Z	W	G	Z	W	G	Z	W	G
1.	20,5	26	498	41,8	102	390	45,5	72	235
2.	4,1	27	57	2,0	26	60	5,7	86	74
3.	3,0	7	430	2,1	10	333	0,2	12	352
4.	11,9	3	65	16,1	4	64	11,1	15	85
5.	5,2	5	388	1,0	10	308	-	26	305
6.	8,6	2	224	-	6	445	0,8	26	392
7.	-	-	772	-	-	283	-	-	-
8.	2,8	5	414	0,3	22	212	1,0	34	134
9.	3,1	31	457	0,5	66	415	-	121	298
10.	2,0	91	635	-	117	644	-	192	478
11.	2,4	156	677	0,8	158	910	0,1	170	592
12.	5,1	76	487	-	31	364	24,3	26	135
13.	8,1	64	388	9,1	67	425	33,6	153	184
14.	-	-	615	-	-	277	-	-	-
15.	103,7	85	362	75,4	149	-	104,3	185	362
16.	54,7	56	281	35,2	34	184	53,5	16	33
17.	7,1	20	264	5,3	12	-	6,6	22	-
18.	7,3	17	-	4,1	8	280	9,9	21	275
19.	12,3	20	339	11,6	21	367	24,5	22	141
20.	12,1	7	47	12,9	20	79	12,1	16	66
21.	-	-	348	-	-	210	-	-	-
22.	8,6	23	388	3,0	15	96	6,0	7	38
23.	5,1	7	47	4,6	7	25	5,5	5	36
24.	5,7	15	236	1,5	29	117	1,1	78	93
25.	1,8	19	367	6,1	14	203	6,2	7	63
26.	-	-	46	8,6	7	34	12,0	6	40
27.	-	14	33	-	17	48	22,5	21	63
28.	-	-	338	-	-	109	-	-	-

TABLE IX

RnR in air; units  $10^{-12} \mu\text{C}/\text{cm}^3$

Station Designations: Z Zugspitze 2964 m a.s.l.  
W Wank 1780 m a.s.l.  
G Garmisch-Partenkirchen 730 m a.s.l.

Measurement periods : a = 2150 - 0920, b = 0950 - 1220,  
c = 1250 - 1620. (Central European Time)

Month: March 1971 ("No measurement" is denoted by: - )

	a			b			c		
	Z	W	G	Z	W	G	Z	W	G
1.	58,9	72	85	57,4	73	117	65,2	70	128
2.	14,6	90	482	22,9	128	255	6,0	133	210
3.	41,1	71	470	-	113	349	98,4	112	215
4.	62,9	133	147	45,6	117	170	13,9	107	130
5.	49,2	75	553	51,2	109	209	69,6	-	129
6.	45,4	95	461	52,9	169	420	55,8	176	230
7.	-	-	613	-	-	198	-	-	-
8.	28,9	136	470	16,7	136	312	16,4	182	320
9.	11,3	130	756	19,9	192	544	14,7	101	266
10.	5,8	27	272	34,3	13	137	18,7	18	54
11.	-	18	101	9,2	15	87	-	13	64
12.	5,5	19	124	1,5	12	79	7,1	16	101
13.	4,4	16	266	1,7	35	207	5,0	65	189
14.	-	-	336	-	-	242	-	-	-
15.	23,1	180	407	17,1	169	334	62,9	157	196
16.	64,2	12	128	23,0	6	69	24,1	8	58
17.	10,2	18	232	0,8	38	125	22,4	24	138
18.	27,1	90	270	29,8	79	221	100,3	69	162
19.	24,6	30	292	22,2	37	176	41,2	47	158
20.	32,8	37	201	42,7	35	105	31,3	23	63
21.	-	-	93	-	-	41	-	-	-
22.	16,4	28	195	13,4	39	165	85,8	75	162
23.	24,9	8	60	26,3	21	61	-	5	80
24.	8,7	92	274	0,6	91	212	2,9	63	124
25.	5,7	42	381	16,4	80	201	29,4	51	78
26.	10,5	18	91	15,8	19	57	18,3	13	42
27.	16,8	3	57	17,2	12	38	13,1	13	35
28.	-	-	138	-	-	61	-	-	-
29.	6,2	-	259	1,4	58	108	37,1	36	71
30.	4,4	86	350	10,7	122	201	1,2	122	108
31.	87,8	-	317	94,7	116	352	147,6	106	266

TABLE X

RaB in air; units  $10^{-12} \mu\text{C}/\text{cm}^3$ 

Station Designations: Z Zugspitze 2964 m a.s.l.  
 W Wank 1780 m a.s.l.  
 G Garmisch-Partenkirchen 730 m a.s.l.

Measurement periods : a = 2150 - 0920, b = 0950 - 1220,  
 c = 1250 - 1620. (Central European Time)

Month: April 1971 ("No measurement" is denoted by: - )

	a			b			c		
	Z	W	G	Z	W	G	Z	W	G
1.	13,4	75	324	3,2	87	210	64,6	85	189
2.	39,0	132	388	44,2	134	259	73,5	152	242
3.	82,1	122	382	108,0	141	229	115,3	98	179
4.	-	-	-	-	-	61	-	-	-
5.	35,5	74	316	38,7	98	139	73,0	67	104
6.	26,2	67	330	29,5	68	103	51,3	47	92
7.	56,2	109	276	75,1	99	147	105,4	111	157
8.	37,3	109	265	15,4	42	149	62,2	95	129
9.	-	-	311	-	-	156	-	-	-
10.	61,4	97	507	35,7	153	263	70,6	174	255
11.	-	-	203	-	-	132	-	-	-
12.	-	-	228	-	-	90	-	-	-
13.	8,5	44	261	1,6	47	94	30,3	56	75
14.	5,8	56	304	1,0	63	130	23,5	22	53
15.	8,5	63	242	1,8	76	162	34,7	105	130
16.	53,9	76	332	54,6	81	101	47,6	76	102
17.	-	145	381	52,6	24	88	16,0	19	91
18.	-	-	178	-	-	102	-	-	-
19.	8,1	122	256	32,4	145	203	92,2	139	166
20.	77,1	129	372	109,3	140	145	75,0	85	101
21.	-	122	289	48,4	117	187	61,9	110	138
22.	67,2	142	286	70,1	118	152	77,0	123	113
23.	54,4	92	254	62,2	72	104	45,4	63	90
24.	-	-	176	22,8	-	60	11,5	-	80
25.	-	-	49	-	-	58	-	-	-
26.	32,1	-	102	16,7	15	51	18,5	19	42
27.	52,5	87	295	50,4	79	169	39,8	54	73
28.	32,8	18	52	35,0	13	56	28,1	16	89
29.	28,8	71	245	41,0	76	185	49,7	88	114
30.	31,9	124	402	24,6	109	250	18,5	120	138

TABLE XI

RaB in air; units  $10^{-12} \mu\text{C}/\text{cm}^3$ 

Station Designations: Z Zugspitze 2964 m a.s.l.  
 W Wank 1780 m a.s.l.  
 G Garmisch-Partenkirchen 730 m a.s.l.

Measurement periods : a = 2150 - 0920, b = 0950 - 1220,  
 c = 1250 - 1620. (Central European Time)

Month: May 1971 ("No measurement" is denoted by: -)

	a			b			c		
	Z	W	G	Z	W	G	Z	W	G
1.	-	-	282	-	-	193	-	-	-
2.	-	-	203	-	-	190	-	-	-
3.	51,5	-	220	49,6	118	207	53,9	100	155
4.	67,6	91	220	70,0	98	195	92,6	95	194
5.	75,8	90	329	64,8	68	207	45,7	76	198
6.	39,3	64	299	53,1	49	140	61,4	79	110
7.	36,6	52	306	31,8	68	126	62,3	65	100
8.	30,3	-	429	37,3	-	317	26,4	-	223
9.	-	-	336	-	-	100	-	-	-
10.	49,2	-	395	65,6	130	247	32,7	47	144
11.	39,4	77	204	41,1	81	179	47,4	49	95
12.	28,5	56	185	49,0	53	68	53,0	80	103
13.	131,3	134	340	90,4	125	128	42,7	66	91
14.	35,9	29	260	13,6	8	128	28,0	61	139
15.	33,9	43	398	39,7	87	154	52,3	73	81
16.	-	-	228	-	-	75	-	-	-
17.	19,5	111	172	34,9	45	113	52,3	86	117
18.	29,0	129	277	40,2	39	103	45,4	45	111
19.	23,0	50	150	44,8	52	79	67,5	54	97
20.	-	-	251	-	-	158	-	-	-
21.	58,0	128	203	62,8	94	94	44,1	27	73
22.	19,5	33	174	35,5	46	69	45,8	39	78
23.	-	-	213	-	-	159	-	-	-
24.	85,2	110	289	84,7	97	118	72,2	53	114
25.	71,5	70	168	57,6	74	116	45,9	69	112
26.	31,1	42	128	48,8	41	102	35,8	25	58
27.	25,7	29	190	40,5	15	153	55,2	39	144
28.	24,6	44	147	25,0	56	89	14,3	21	69
29.	19,7	24	111	33,2	23	78	30,7	35	80
30.	-	-	148	-	-	121	-	-	-
31.	-	-	308	-	-	145	-	-	-

TABLE XIII

RaB in air; units  $10^{-12} \mu\text{G}/\text{cm}^2$

Station Designations: Z Zugspitze 2964 m a.s.l.  
 W Wank 1780 m a.s.l.  
 G Garmisch-Partenkirchen 730 m a.s.l.

Measurement periods : a = 2150 - 0920, b = 0950 - 1220,  
 c = 1250 - 1620. (Central European Time)

Month: June 1971 ("No measurement" is denoted by: -)

	a			b			c		
	Z	W	G	Z	W	G	Z	W	G
1.	25,7	101	450	25,7	89	165	21,0	75	104
2.	31,6	54	223	64,7	130	198	93,3	65	123
3.	54,8	102	368	87,3	98	158	97,6	78	142
4.	72,8	107	274	90,4	146	203	94,8	115	159
5.	42,4	83	201	47,4	68	96	72,2	49	97
6.	-	-	346	-	-	147	-	-	-
7.	26,9	62	251	22,7	40	150	21,6	70	113
8.	16,5	17	300	20,1	21	228	20,9	39	102
9.	30,1	47	299	32,4	47	193	47,6	65	96
10.	-	-	209	-	-	37	-	-	-
11.	34,4	32	121	10,0	12	54	30,2	10	55
12.	8,3	13	73	17,3	17	53	21,5	21	37
13.	-	-	169	-	-	39	-	-	-
14.	28,7	69	171	44,0	46	110	75,8	68	128
15.	60,6	80	99	12,4	4	29	2,0	5	27
16.	7,3	17	73	6,6	21	34	19,6	16	30
17.	-	-	150	-	-	67	-	-	-
18.	12,7	71	329	11,6	12	74	9,1	8	39
19.	-	26	206	5,9	7	91	1,3	13	89
20.	-	-	51	-	-	73	-	-	-
21.	-	39	110	-	14	43	-	12	48
22.	28,9	59	218	55,6	101	116	26,1	17	53
23.	44,4	58	111	42,5	37	81	43,5	32	76
24.	71,5	96	379	87,3	112	261	84,0	53	252
25.	40,3	40	391	48,1	93	187	71,8	71	96
26.	63,5	87	297	84,7	81	135	107,1	81	101
27.	-	-	61	-	-	55	-	-	-
28.	52,9	53	134	53,6	61	116	54,2	44	74
29.	5,1	9	26	7,2	11	25	6,9	8	33
30.	6,3	14	101	8,0	16	77	4,3	11	57

5. The Computer Program









PAGE 017

0024	00	PC1	TAB13-X
0035	0000	LDW	'FFAD'
0038	01FFAD	LDS	'00'
0039	1781	JAX	'01'
003D	00	RDA	'00'
003E	0000	LDW	'01'
0040	018A95	LDW	'A'68'
0043	001733	RTW	'00'
0044	001733	LDW	'A'68'
0045	001733	RTW	'00'
0046	0000	LDW	'01'
0047	7684	RTW	'00'
0048	0000	LDW	'01'
0050	018A95	LDW	'A'68'
0053	001733	RTW	'00'
0055	0000	LDW	'A'68'
0056	001733	RTW	'00'
0057	0000	LDW	'01'
0058	0000	RTW	'00'
0059	0000	LDW	'01'
0061	018A95	RTW	'00'
0070	011733	LDW	'A'68'
0077	010004	LDW	'A'68'
007D	0017D1	RTW	'00'
007D	0017D1	LDW	'A'68'
0080	017AAC	RTW	'00'
0081	0000	LDW	'01'
0085	018A95	RTW	'00'
0089	0017D1	LDW	'00'
009C	03AB	RTW	'00'
SC1			
0098	0000	LDW	'01'
00A1	018A95	LDW	'A'68'
00A4	001733	RTW	'00'
00A7	018A95	LDW	'A'68'
00AA	001678	RTW	'00'
00AB	0000	LDW	'01'
00B1	018A95	RTW	'00'
00B7	0000	LDW	'01'
00B8	0000	RTW	'00'
00B9	0000	LDW	'01'
00C1	018A95	RTW	'00'
00D7	011733	LDW	'A'68'
00E4	0017D1	RTW	'00'
00E5	0017D1	LDW	'A'68'
00F0	0000	RTW	'00'
00F4	0000	LDW	'01'
00F5	018A95	RTW	'00'
00F9	0017D1	LDW	'00'
SC2			
00F8	0000	LDW	'01'
00F9	018A95	RTW	'00'
00FA	0017D1	LDW	'A'68'
00FB	0000	RTW	'00'
00FC	0000	LDW	'01'
00FD	018A95	RTW	'00'
00FF	0017D1	LDW	'00'
0100	0000	RTW	'00'
0101	0000	LDW	'01'
0102	018A95	RTW	'00'
0105	0017D1	LDW	'00'
0106	0000	RTW	'00'
0107	0000	LDW	'01'
0108	018A95	RTW	'00'
010B	0017D1	LDW	'00'
010C	0000	RTW	'00'
010D	0000	LDW	'01'
010E	018A95	RTW	'00'
0111	0017D1	LDW	'00'
0112	0000	RTW	'00'
0113	0000	LDW	'01'
0114	018A95	RTW	'00'
0117	0017D1	LDW	'00'
0118	0000	RTW	'00'
0119	0000	LDW	'01'
011A	018A95	RTW	'00'
011D	0017D1	LDW	'00'
011E	0000	RTW	'00'
011F	0000	LDW	'01'
0120	018A95	RTW	'00'
0123	0017D1	LDW	'00'
0124	0000	RTW	'00'
0125	0000	LDW	'01'
0126	018A95	RTW	'00'
0129	0017D1	LDW	'00'
012A	0000	RTW	'00'
012B	0000	LDW	'01'
012C	018A95	RTW	'00'
012D	0017D1	LDW	'00'
012E	0000	RTW	'00'
012F	0000	LDW	'01'
0130	018A95	RTW	'00'
0133	0017D1	LDW	'00'
0134	0000	RTW	'00'
0135	0000	LDW	'01'
0136	018A95	RTW	'00'
0139	0017D1	LDW	'00'
013A	0000	RTW	'00'
013B	0000	LDW	'01'
013C	018A95	RTW	'00'
013D	0017D1	LDW	'00'
013E	0000	RTW	'00'
013F	0000	LDW	'01'
0140	018A95	RTW	'00'
0143	0017D1	LDW	'00'
0144	0000	RTW	'00'
0145	0000	LDW	'01'
0146	018A95	RTW	'00'
0149	0017D1	LDW	'00'
014A	0000	RTW	'00'
014B	0000	LDW	'01'
014C	018A95	RTW	'00'
014D	0017D1	LDW	'00'
014E	0000	RTW	'00'
014F	0000	LDW	'01'
0150	018A95	RTW	'00'
0153	0017D1	LDW	'00'
0154	0000	RTW	'00'
0155	0000	LDW	'01'
0156	018A95	RTW	'00'
0159	0017D1	LDW	'00'
015A	0000	RTW	'00'
015B	0000	LDW	'01'
015C	018A95	RTW	'00'
015D	0017D1	LDW	'00'
015E	0000	RTW	'00'
015F	0000	LDW	'01'
0160	018A95	RTW	'00'
0163	0017D1	LDW	'00'
0164	0000	RTW	'00'
0165	0000	LDW	'01'
0166	018A95	RTW	'00'
0169	0017D1	LDW	'00'
016A	0000	RTW	'00'
016B	0000	LDW	'01'
016C	018A95	RTW	'00'
016D	0017D1	LDW	'00'
016E	0000	RTW	'00'
016F	0000	LDW	'01'
0170	018A95	RTW	'00'
0173	0017D1	LDW	'00'
0174	0000	RTW	'00'
0175	0000	LDW	'01'
0176	018A95	RTW	'00'
0179	0017D1	LDW	'00'
017A	0000	RTW	'00'
017B	0000	LDW	'01'
017C	018A95	RTW	'00'
017D	0017D1	LDW	'00'
017E	0000	RTW	'00'
017F	0000	LDW	'01'
0180	018A95	RTW	'00'
0183	0017D1	LDW	'00'
0184	0000	RTW	'00'
0185	0000	LDW	'01'
0186	018A95	RTW	'00'
0189	0017D1	LDW	'00'
018A	0000	RTW	'00'
018B	0000	LDW	'01'
018C	018A95	RTW	'00'
018D	0017D1	LDW	'00'
018E	0000	RTW	'00'
018F	0000	LDW	'01'
0190	018A95	RTW	'00'
0193	0017D1	LDW	'00'
0194	0000	RTW	'00'
0195	0000	LDW	'01'
0196	018A95	RTW	'00'
0199	0017D1	LDW	'00'
019A	0000	RTW	'00'
019B	0000	LDW	'01'
019C	018A95	RTW	'00'
019D	0017D1	LDW	'00'
019E	0000	RTW	'00'
019F	0000	LDW	'01'
01A0	018A95	RTW	'00'
01A3	0017D1	LDW	'00'
01A4	0000	RTW	'00'
01A5	0000	LDW	'01'
01A6	018A95	RTW	'00'
01A9	0017D1	LDW	'00'
01AA	0000	RTW	'00'
01AB	0000	LDW	'01'
01AC	018A95	RTW	'00'
01AD	0017D1	LDW	'00'
01AE	0000	RTW	'00'
01AF	0000	LDW	'01'
01B0	018A95	RTW	'00'
01B3	0017D1	LDW	'00'
01B4	0000	RTW	'00'
01B5	0000	LDW	'01'
01B6	018A95	RTW	'00'
01B9	0017D1	LDW	'00'
01BA	0000	RTW	'00'
01BB	0000	LDW	'01'
01BC	018A95	RTW	'00'
01BD	0017D1	LDW	'00'
01BE	0000	RTW	'00'
01BF	0000	LDW	'01'
01C0	018A95	RTW	'00'
01C3	0017D1	LDW	'00'
01C4	0000	RTW	'00'
01C5	0000	LDW	'01'
01C6	018A95	RTW	'00'
01C9	0017D1	LDW	'00'
01CA	0000	RTW	'00'
01CB	0000	LDW	'01'
01CC	018A95	RTW	'00'
01CD	0017D1	LDW	'00'
01CE	0000	RTW	'00'
01CF	0000	LDW	'01'
01D0	018A95	RTW	'00'
01D3	0017D1	LDW	'00'
01D4	0000	RTW	'00'
01D5	0000	LDW	'01'
01D6	018A95	RTW	'00'
01D9	0017D1	LDW	'00'
01DA	0000	RTW	'00'
01DB	0000	LDW	'01'
01DC	018A95	RTW	'00'
01DD	0017D1	LDW	'00'
01DE	0000	RTW	'00'
01DF	0000	LDW	'01'
01E0	018A95	RTW	'00'
01E3	0017D1	LDW	'00'
01E4	0000	RTW	'00'
01E5	0000	LDW	'01'
01E6	018A95	RTW	'00'
01E9	0017D1	LDW	'00'
01EA	0000	RTW	'00'
01EB	0000	LDW	'01'
01EC	018A95	RTW	'00'
01ED	0017D1	LDW	'00'
01EE	0000	RTW	'00'
01EF	0000	LDW	'01'
01F0	018A95	RTW	'00'
01F3	0017D1	LDW	'00'
01F4	0000	RTW	'00'
01F5	0000	LDW	'01'
01F6	018A95	RTW	'00'
01F9	0017D1	LDW	'00'
01FA	0000	RTW	'00'
01FB	0000	LDW	'01'
01FC	018A95	RTW	'00'
01FD	0017D1	LDW	'00'
01FE	0000	RTW	'00'
01FF	0000	LDW	'01'
0101	0000	RTW	'00'
0102	0000	LDW	'01'
0103	018A95	RTW	'00'
0106	0017D1	LDW	'00'
0107	0000	RTW	'00'
0108	0000	LDW	'01'
0109	018A95	RTW	'00'
010C	0017D1	LDW	'00'
010D	0000	RTW	'00'
010E	0000	LDW	'01'
010F	018A95	RTW	'00'
0112	0017D1	LDW	'00'
0113	0000	RTW	'00'
0114	0000	LDW	'01'
0115	018A95	RTW	'00'
0118	0017D1	LDW	'00'
0119	0000	RTW	'00'
011A	0000	LDW	'01'
011B	018A95	RTW	'00'
011E	0017D1	LDW	'00'
011F	0000	RTW	'00'
0120	0000	LDW	'01'
0121	018A95	RTW	'00'
0124	0017D1	LDW	'00'
0125	0000	RTW	'00'
0126	0000	LDW	'01'
0127	018A95	RTW	'00'
012A	0017D1	LDW	'00'
012B	0000	RTW	'00'
012C	0000	LDW	'01'
012D	018A95	RTW	'00'
012E	0017D1	LDW	'00'
012F	0000	RTW	'00'
0130	0000	LDW	'01'
0131	018A95	RTW	'00'
0134	0017D1	LDW	'00'
0135	0000	RTW	'00'
0136	0000	LDW	'01'
0137	018A95	RTW	'00'
013A	0017D1	LDW	'00'
013B	0000	RTW	'00'
013C	0000	LDW	'01'
013D	018A95	RTW	'00'
013E	0017D1	LDW	'00'
013F	0000	RTW	'00'
0140	0000	LDW	'01'
0141	018A95	RTW	'00'
0144	0017D1	LDW	'00'
0145	0000	RTW	'00'
0146	0000	LDW	'01'
0147	018A95	RTW	'00'
014A	0017D1	LDW	'00'
014B	0000	RTW	'00'
014C	0000	LDW	'01'
014D	018A95	RTW	'00'
014E	0017D1	LDW	'00'
014F	0000	RTW	'00'
0150	0000	LDW	'01'
0151	018A95	RTW	'00'
0154	0017D1	LDW	'00'
0155	0000	RTW	'00'
0156	0000	LDW	'01'
0157	018A95	RTW	'00'
015A	0017D1	LDW	'00'
015B	0000	RTW	'00'
015C	0000	LDW	'01'
015D	018A95	RTW	'00'
015E	0017D1	LDW	'00'
015F	0000	RTW	'00'
0160	0000	LDW	'01'
0161	018A95	RTW	'00'
0164	0017D1	LDW	'00'
0165	0000	RTW	'00'
0166	0000	LDW	'01'
0167	018A95	RTW	'00'
016A	0017D1	LDW	'00'
016B	0000	RTW	'00'
016C	0000	LDW	'01'
016D	018A95	RTW	'00'
016E	0017D1	LDW	'00'
016F	0000	RTW	'00'
017			

Page 01

```

0000 000000 LDR  A1EW11
0053 6E1725 RTJ/ MLO
0054 F840 STV PT
0056 632B JRP/ PBJ
*
* EPT = FORMEL *
*
P08 RTJ/ P03
LDR  PL
LDW  PL
LDR  A1EW11
RTJ/ ADF
STV  EPT
JRP/ SC3+3
*
* OB FEUCHTIGKEIT VORHANDEN *
*
0944 0000 DC  **
0946 6C7C LDR  ZTA
0948 6EAB0D LDA/ TAB+12x2
0971 6FAPAF LDW  X'AFAP'
0974 63FA JRP/ LBF
*
* L- EICHWERTE IN PL *
*
0974 0000 DC  **
0978 0A P03
0979 6E54 LDW  PL0
0979 6E057F RTJ/ UP1
097C 6E0693 RTJ/ UP3
0941 6E0884 RTJ/ DZ1
0942 6E0885 STC  ZW1
0944 0A P03
0987 6E58 LDW  MLO
0989 6E0A7F RTJ/ UP1
098C 6E0692 RTJ/ UP3
098F 6C3B86 RTJ/ DZ1
0992 FAD4 STV  EWT
0994 63>0 JRP/ BL1
*
* PEI = FORMEL <L>-L</> /PL / MP
*
0996 0000 DC  **
0996 6E0776 RTJ/ BL1
0998 6E44 LDV  PL
099D 6E09CF RTJ/ MID
09A0 6E070D LDR  A1EW11
09A3 6E17D1 RTJ/ DVF
0946 F840 STV  PL
0948 6EAE0 LDV  ML
09AA 6E09CF RTJ/ MID
09AD 6E0024 LDR  A1EW11
0930 6E17D1 RTJ/ DVF
0953 F840 STV  AL
0953 6E17D4 LDW  <PL>
0959 6A1578 RTJ/ AD9
0988 F850 STV  L
0980 6E64 LDV  PL

```

08C3	FB0C	STV	RF	
08C5	E80E	LDW		
08C6	817065	LDR	A'KA'	
08C7	817173	RTJ/	MFL	376
08C9	818480	LDR	A'KA'	
08D0	821701	RTJ/	OUT	1000
08D3	F8D3	RTV		
08D5	8232	LDW		
08D7	870008	LDR	A'KA'	
08D8	881481	RTJ/	DET	
08D9	7F00	RTV		
08D9	8200	LDW		
08E1	878A4D	LDR	A'KA'	
08E4	881703	RTJ/	DET	488
08E7	870006	LDR	A'KA'	
08E8	8217D1	RTJ/	DUF	
08ED	F810	STV		
08E7	871484	LDR	A'KA'	
08F3	821733	RTJ/	MFL	
08F5	870001	LDR	A'KA'	
08F7	821701	RTV		1000
08F9	878A4D	LDR	A'KA'	
08F8	821678	RTJ/	DET	
0901	8828C3	RTJ/	MUS	
0904	670888	JMP	PCG	
PDI : PT-POPNULE-MR 1E 9				
0907	0000	PDI	DC	"
0909	E8B480	LDW		
090C	870034	LDR	A'KA'	
0907	8217D1	RTJ/	DUF	
0918	881807	RTV		
0918	881803	LDR	A'KA'	
0918	821701	RTV		
0918	878A4D	LDR	A'KA'	
0918	8217D1	RTJ/	DUF	
0921	AE1484	RTV		
0924	F8D0	RTV		
0926	871000	LDR	A'KA'	
0925	881733	RTV		
0926	878A4D	LDW	A'KA'	
0927	821733	RTV		
0929	821701	LDR	A'KA'	
0932	7F00	RTV		
0934	823B	JMP	PD1	
PDI : PT-POPNULE-MR 1E 9				
093C	0000	PDI	DC	"
0934	881707	RTJ/	PDI	
0941	878A41	LDW	MFL	8730
0944	878A43	LDR	A'KA'	
0947	8217D1	RTJ/	DUF	10
0944	870032	LDR	A'KA'	
0948	821678	RTJ/	DET	

10

```

        000F 870000
        000C 8217D1
        000C 870000
        000C 8217D3
        000B 8240
        000C 8307
        00CF 0000
        00D1 87BA00
        00D4 8217D3
        00D7 87BA00
        00LA 8217D1
        00D9 83F0

        * HID DC .. 00
        LDX# A'1H3'
        RTJ# DUP
        LDX# A'1H8'
        RTJ# DUP
        LDX# A'1H9'
        RTJ# DUP
        JMP# PEI

        * PCS : ID E:SURF/TU:EDT:CR-LB-6-BF ***** TRANSFER
        00DF 0000
        00E1 87001J
        00B2 00
        00B3 00AF
        00B7 87B008
        00E2 45
        00ED 1DPA
        00ED 0B
        00E9 83EF

        * PCS DC .. 00
        LDW# 19
        RDW# 00
        SCA LDW# X'1AF'
        STW# EXH
        DCX#
        MNW# SCA
        P04
        JNP# PCS

        * PPI : FORMEL INR : MR. ***** IS =
        00F0 0000
        00F3 0B
        00F2 82DA
        00F3 87BADD
        00F8 8217D3
        00F8 87BADD
        00F8 87BADD
        00B1 8217A5
        00A6 87BA00
        0007 8217D3
        00A0 87BA09
        00AD 8217D1
        0010 8260
        0018 83DC

        * PPI DC .. 00
        P04
        LDW# 19T
        LDX# A'1H9'
        RTJ# MLP
        LDX# A'1H8'
        RTJ# EXH
        LDX# A'1H9'
        RTJ# EXH
        LDX# A'1H4'
        RTJ# MLP
        LDX# A'1H0'
        RTJ# DUP
        STW# IHS
        JMP# PPI

        * PPI : FORMEL INR : MR.16 =
        * PPI DC .. 00
        P04
        LMW# SWA
        LDX# A'1H3'
        RTJ# SWA
        SWV# SWA
        LDW# SWA
        RTJ# SWA
        LDX# A'1H1'
        RTJ# SWF
        LDX# A'1H6'
        RTJ# DUP
        SWV# SWA
        RTJ# DUP

```





PAGE 030					
0200 070008		LDE	A'81'		
0200 051701		RTJ	DIF		
0200 0506		STV	DIF		
0200 070019		JMP	FII		
0200 0000		DC	**		
0200 00		R04			
0200 00TC		LDR	STA		
0200 02A819		LDV	TAB+17,X		
0200 02048A		RTJ	DEI		
0200 0204		RD4			
0200 0202		LDU	W03+3		
0200 00TC		LDR	STA		
0200 02A811		STV	TAB+17,X		
0200 02048E		RTJ	PHI		
0200 0202		JMP	PHI		
0200 0000		DC	**		
0200 00		R04			
0200 00TC		LDR	STA		
0200 02A819		LDV	TAB+85,X		
0200 02C0D3		RTJ	P03		
0200 02A819		STV	TAB+85,X		
0200 02048C		RTJ	PHI		
0201 032D		JMP	PHI		
0201 0000		DC	**		
0201 00		R04			
0201 00TC		LDR	STA		
0201 02A819		LDV	TAB+85,X		
0201 02C0D3		RTJ	P03		
0201 02A819		STV	TAB+85,X		
0201 02048C		RTJ	PHI		
0201 032D		JMP	PHI		
0202 0000		DC	**		
0202 02048A		R04			
0202 00		LDR	STA		
0202 00TC		LDV	W03+4		
0202 02A819		RTJ	DEI		
0202 02048C		RD4			
0202 0204		LDU	W03+4		
0202 00TC		LDR	STA		
0202 02048F		STV	W03+2		
0202 02048C		RTJ	PHI		
0202 0202		JMP	PHI		

Page 021

• PORTSETSUME V. NR. 30 I NR. 31 •

0F83 0000	PIN	DC	ee
0F83 08	R04		
0F83 60TC	LDX	ZTA	
0F83 KKA839	LDW/	TAB+83,X	
0F8D 45008A	RTJ,W	DIZ	
0J 30 680741	RTJ,W	PO4	
0F33 FPEA35	RTW/	TAB+83,X	
0F83 0000	R02		
0F37 2500	LDX	W03+8	
0F39 F1A834	BTW/	TAB+84,X	
0F3C A8CC08	RTJ,W	TRI	
0F37 61E4	JMP	PIN	
0F81 0000	P04	DC	ee
0F43 08	R01		
0F44 E8CB	LDW	W03	
0F44 60TC	LDX	ZTA	

2005-028

		JMP	PO4
OP4A 000C	PTR	DC	++
OP4B 00		POA	
OP4C 00		POB	
OP4D 007C		LDT	STA
OP4F 004F57		LDV	TAB+87,X
OP5E 00368A		RTJ	DZ
OP5B 002F64		RTJ	PO5
OP5C 002E50		BTJ	TAB+83,X
OP5B 1000		LDV	W03+8
OP5D 00AE86		STV	TAB+88,X
OP60 00CEFC		RTJ	PHI
OP63 03E5		JP PO	PTR
OP65 0000	P05	DC	++
OP66 0003		PO5	
OP68 00CD		LDV	W03+8
OP6A 000C			

0F83 63F3                  JMP4 F07

```

OP4E 601C LDU STA
OP4C 607F JMP$ POS

OP4E 0000 PBM DC **

OP70 0B P04 TAB+1,X
OP71 807C LDU STA
OP73 3EABED LDU TAB+92,X
OP76 6E068A RTJ$ DEI
OP79 6E8336 RTJ$ GER
OP7C FEA89D STV$ TAB+1,X
OP7F 9CCT LDU V0>4
OP81 FAE88Z STV$ TAB+84,X
OP84 6E0CC0 RTJ$ PRI
OP87 63E5 JMP$ PBM

```

		UP TO P. PRINT	IN
DFE5 0000	PRB	DC	**
DFE7 62118A		RT/J	PFT
DFEA 62118A		RT/J	PFT
DFED 637F		JMP	PRB
DFEF 0000	PP3	DC	**
DFF1 62118A		RT/J	PFT
DFF4 620F17		RT/J	PHS
DFF7 637F		JMP	PRD
DFFF 0000	PP4	DC	**
DFFB 620F17		RT/J	PRD
DFFC 62118A		RT/J	PFT
DFG1 637F		JMP	PR4
D03 0000	CO1	DC	**
D05 0FAC		LDV	C**
D07 626B2F		RT/J	OUT
DA0 62118A		RT/J	PTE

• PWR 8 IN AUE +DIF VORNE STATT RD AC BRINGEN  
•  
DF89 0000 PWR DC ee  
DF8D 04 PWR POL  
DF8C 807C LDX STA

JULY 1974 CO 1





PAGE 041

PAGE 04

				C'	L	-1+	L+	L-	R
				DC	DC	DC	DC	DC	DC
S407	DACGCGAG			A84	DC	C'	L	-1+	L+
S408	ADACGCGC								
S409	GGADGAGG								
S410	ADAGAGAG								
S411	CCAGBAGG								
S412	AGCAGGAG								
S413	TTAGAGAG								
S414	TTAGATCTAG								
S415	AGGAGGAG								
S416	GGAGGAGG								
S417	GGAGGAGG								
S418	GA								
S419	AGAGAGAGC			A86	DC	C'	L	-1+	L+
S420	AGAGAGAGC								
S421	GGAGAGAGC								
S422	AGAGAGAGC								
S423	AGAGAGAGC								
S424	AGAGAGAGC								
S425	AGAGAGAGC								
S426	AGAGAGAGC								
S427	ADCTTGAG								
S428	DIAACTTAC								
S429	DAADAGAGA								
S430	ADCGAGAG								
S431	AGGAGAGAG								
S432	AGGAGAGAG								
S433	AGGAGAGAG								
S434	AGGAGAGAG								
S435	AGGAGAGAG								
S436	CEAGAG								
S437	DAADGCGA			A86	DC	C'	L	-1+	L+
S438	C1GCGCGG								
S439	CDCDADSD								
S440	DCGD								
S441	DDAGGAGTCG			A86	DC	C'	L	-1+	L+
S442	DTAGTCG								
S443	DTAGTCG								
S444	DTAGTCG								
S445	DTAGTCG								
S446	DTAGTCG								
S447	DTAGTCG								
S448	DTAGTCG								
S449	DTAGTCG								
S450	DTAGTCG								
S451	DTAGTCG								
S452	DTAGTCG								
S453	DTAGTCG								
S454	DTAGTCG								
S455	DTAGTCG								
S456	DTAGTCG								
S457	DTAGTCG								
S458	DTAGTCG								
S459	DTAGTCG								
S460	DTAGTCG								
S461	DTAGTCG								
S462	DTAGTCG								
S463	DTAGTCG								
S464	DTAGTCG								
S465	DTAGTCG								
S466	DTAGTCG								
S467	DTAGTCG								
S468	DTAGTCG								
S469	DTAGTCG								
S470	DTAGTCG								
S471	DTAGTCG								
S472	DTAGTCG								
S473	DTAGTCG								
S474	DTAGTCG								
S475	DTAGTCG								
S476	DTAGTCG								
S477	DTAGTCG								
S478	DTAGTCG								
S479	DTAGTCG								
S480	DTAGTCG								
S481	DTAGTCG								
S482	DTAGTCG								
S483	DTAGTCG								
S484	DTAGTCG								
S485	DTAGTCG								
S486	DTAGTCG								
S487	DTAGTCG								
S488	DTAGTCG								
S489	DTAGTCG								
S490	DTAGTCG								
S491	DTAGTCG								
S492	DTAGTCG								
S493	DTAGTCG								
S494	DTAGTCG								
S495	DTAGTCG								
S496	DTAGTCG								
S497	DTAGTCG								
S498	DTAGTCG								
S499	DTAGTCG								
S500	DTAGTCG								
S501	DTAGTCG								
S502	DTAGTCG								
S503	DTAGTCG								
S504	DTAGTCG								
S505	DTAGTCG								
S506	DTAGTCG								
S507	DTAGTCG								
S508	DTAGTCG								
S509	DTAGTCG								
S510	DTAGTCG								
S511	DTAGTCG								
S512	DTAGTCG								
S513	DTAGTCG								
S514	DTAGTCG								
S515	DTAGTCG								
S516	DTAGTCG								
S517	DTAGTCG								
S518	DTAGTCG								
S519	DTAGTCG								
S520	DTAGTCG								
S521	DTAGTCG								
S522	DTAGTCG								
S523	DTAGTCG								
S524	DTAGTCG								
S525	DTAGTCG								
S526	DTAGTCG								
S527	DTAGTCG								
S528	DTAGTCG								
S529	DTAGTCG								
S530	DTAGTCG								
S531	DTAGTCG								
S532	DTAGTCG								
S533	DTAGTCG								
S534	DTAGTCG								
S535	DTAGTCG								
S536	DTAGTCG								
S537	DTAGTCG								
S538	DTAGTCG								
S539	DTAGTCG								
S540	DTAGTCG								
S541	DTAGTCG								
S542	DTAGTCG								
S543	DTAGTCG								
S544	DTAGTCG								
S545	DTAGTCG								
S546	DTAGTCG								
S547	DTAGTCG								
S548	DTAGTCG								
S549	DTAGTCG								
S550	DTAGTCG								
S551	DTAGTCG								
S552	DTAGTCG								
S553	DTAGTCG								
S554	DTAGTCG								
S555	DTAGTCG								
S556	DTAGTCG								
S557	DTAGTCG								
S558	DTAGTCG								
S559	DTAGTCG								
S560	DTAGTCG								
S561	DTAGTCG								
S562	DTAGTCG								
S563	DTAGTCG								
S564	DTAGTCG								
S565	DTAGTCG								
S566	DTAGTCG								
S567	DTAGTCG								
S568	DTAGTCG								
S569	DTAGTCG								
S570	DTAGTCG								
S571	DTAGTCG								
S572	DTAGTCG								
S573	DTAGTCG								
S574	DTAGTCG								
S575	DTAGTCG								
S576	DTAGTCG								
S577	DTAGTCG								
S578	DTAGTCG								
S579	DTAGTCG								
S580	DTAGTCG								
S581	DTAGTCG								
S582	DTAGTCG								
S583	DTAGTCG								
S584	DTAGTCG								
S585	DTAGTCG								
S586	DTAGTCG								
S587	DTAGTCG								
S588	DTAGTCG								
S589	DTAGTCG								
S590	DTAGTCG								
S591	DTAGTCG								
S592	DTAGTCG								
S593	DTAGTCG								
S594	DTAGTCG								
S595	DTAGTCG								
S596	DTAGTCG								
S597	DTAGTCG								
S598	DTAGTCG								
S599	DTAGTCG								
S600	DTAGTCG								
S601	DTAGTCG								
S602	DTAGTCG								
S603	DTAGTCG								
S604	DTAGTCG								
S605	DTAGTCG								
S606	DTAGTCG								
S607	DTAGTCG								
S608	DTAGTCG								
S609	DTAGTCG								
S610	DTAGTCG								
S611	DTAGTCG								
S612	DTAGTCG								
S613	DTAGTCG								
S614	DTAGTCG								
S615	DTAGTCG								
S616	DTAGTCG								
S617	DTAGTCG								
S618	DTAGTCG								
S619	DTAGTCG								
S620	DTAGTCG								
S621	DTAGTCG								
S622	DTAGTCG								
S623	DTAGTCG								
S624	DTAGTCG								
S625	DTAGTCG								
S626	DTAGTCG								
S627	DTAGTCG								
S628	DTAGTCG								
S629	DTAGTCG								
S630	DTAGTCG								
S63									

PAGE 04

SAB1	64000006	HR6	DC	N16400006
SAB2	71C00009	HAT	DC	N171C00009
SAB3	75B30007	YH1	DC	N175B30007
SAB4	75B30008	YH2	DC	N175B30008
SAB5	81C00000	K1H	DC	N181C00000
SAB6	90400004	KAH	DC	N190400004
SAB7	775C8B08	K2H	DC	N1775C8B08
SAB8	74E00000	KAH	DC	N174E00000
SAB9	48900010	KHM	DC	N148900010
SAB9	4ED00006	KTH	DC	N14ED00006
			PCB	DC 00
SAB9	09		PCB	DC 00
SAB10	61B1070	RTW	L0W	
SAB11	61B1070	RTW	A0W	
SAB12	61T1D1	RTW	D0W	
SAB13	61A1A66	RTW	E0W	
SAB14	61E1F	JMP	ACB	
		*		
SAB15	0000	GB1	DC	00
SAB22	6598	LDV	H1	
SAB23	67RA06	LDV	A'KB'	
SAB25	681733	RTW	MLP	
SAB26	7392	ATV	ME	
SAB27	7482	LDV	ME	
SAB28	67RA09	LDV	A'KB'	
SAB29	681733	RTW	MLP	
SAB30	7598	ATV	ME	
SAB31	63E6	JMP	GB1	
		*		
SAB36	0000	GB2	DC	00
SAB37	65CC	LDV	003+1	
SAB38	60TC	LDV	ITA	
SAB39	6377	JMP	GB2	
		*		
SAB37	6300	GB3	DC	00
SAB41	6511A9	RTW	E1V	
SAB42	6511A9	RTW	Z1V	
SAB43	65C9F9	RTW	P1V	
SAB44	65F97	RTW	PIX	
SAB45	637D	JMP	GB3	
		*		
SAB47	6300	GB4	DC	00
SAB48	6511A9	RTW	E1V	
SAB49	6511A9	RTW	Z1V	
SAB50	65C9F9	RTW	P1V	
SAB51	65F97	RTW	PIX	
SAB52	637D	JMP	GB3	
		*		
SAB47	6300	GB4	DC	00
SAB48	6511A9	RTW	E1V	
SAB49	6511A9	RTW	Z1V	
SAB50	65C9F9	RTW	P1V	
SAB51	65F97	RTW	PIX	
SAB52	637D	JMP	GB3	
		*		
SAB54	6300	GB5	DC	00
SAB55	6511A9	RTW	E1V	
SAB56	6511A9	RTW	Z1V	
SAB57	65C9F9	RTW	P1V	
SAB58	65F97	RTW	PIX	
SAB59	637D	JMP	GB3	
		*		
SAB54	6310	GB5	DC	00
SAB55	6511A9	RTW	E1V	
SAB56	6511A9	RTW	Z1V	
SAB57	65C9F9	RTW	P1V	
SAB58	65F97	RTW	PIX	
SAB59	637D	JMP	GB3	

PAGE 0

SBBG 0000	CBA	DC	++
SBBG AC		TAX	
SBBG HBBAPF		LDV/	CAS+1
SBBG P004		STA	V01
SBBG AE		THA	
SBBG R008		LDX	W01
SBC1 6373		JMP*	CBA
SBC2 0000	HUB	DC	++
SBC2 F004		STV	LIV1
SBC2 HBBAPF		LDV/	KBS
SBC2 V87A95		LDX	A1X*
SBC2 621701		RTJ/	DVF
SBCD P00C		STV	LVB
SBD0 H70030		LDX	A1T
SBD9 B1979		RTJ/	ADP
SBD9 E70059		LDW	LIV1
SBD9 B1973		RTJ/	MET
SBD9 621701		LDX	A1X*
SBE1 621849		RTJ/	BSP
SBE2 F014		STV	TV
SBE3 6200		JMP*	HUB
SBE5 0000	HUB	DC	++
SBEA 621170		RTJ/	WIZ
SBE5 6200CE		RTJ/	WET
SBD0 621701		JMP*	HUB
B			
SBF5 0000	OUT	DC	++
SBF6 OR		RJ1	
SBF5 3800		OS1	O,O
SBF7 6239		JMP*	OUT
SBF9 00		ROI	
SBF9 380C		STV	BUF
SBF9 3113		LEA	1,3
SBF9 D704		APU*	X/A
SC00 11PA		JAZ	++4
SC00 E904		LDV	BUF
SC04 3903		OSA	O,3
SC06 631A		JMP*	OUT
SC06 0001	HUB	DB	I
B			
SC09 0000	P3H	DC	++
SC09 DD		RD4	
SC0C 807C		LDX	ETA
SC0E 62A819		LDA/	TAB=85,X
SC11 87APAF		LDX*	X'APAF'
SC14 1711		JAZ	++4
SC1C 11CC		LDV	ETA
SC1D 62DD08		RTJ/	POS
SC1D 62A819		LDA/	TAB=85,X
SC1E 87APAF		LDX*	X'APAF'
SC21 1704		JAZ	S31
SC23 807C		LDX	STA
SC25 63E8		JMP*	P3H
SC27 87APAFAPAF	31	LDV/	EPAPAFAPAF
SC2C 620088		F28	
B			
SCCF 0000	P4H	DC	++

PAGE 04

Page 84

S851	0000		POA	DC	00
S852	0232D			RTJ/	PAD
S853	0232D0			RTJ/	T81
S857	6376			JMP	POA
S861	0000		POB	DC	00
S862	0232D			RTJ/	PAB
S863	0232D9			RTJ/	K31
S864	637F			JMP	POB
S868	0000		POC	DC	00
S869	0232D			RTJ/	PAB
S870	0232D			RTJ/	K31
S873	6376			JMP	POC
S875	0000		POD	DC	00
S877	0232D			RTJ/	PAR
S878	0232D1F			RTJ/	T18
S879	6376			JMP	POD
S897	0000		T18	DC	00
S901	0A			RD3	
S903	0B			LDV	W03+8
S904	FCC			STV	W03+1
S905	0B			RO4	
S907	62C9			LDV	W03
S908	027C			LDR	ZTA
S909	637F			JMP	T18
S90D	0000		T81	DC	00
S90F	0A			RD3	
S910	EBCF			LDV	W03+6
S911	FCC			STV	W03+1
S914	0B			RO4	
S915	62C9			LDV	W03
S917	027C			LDR	ZTA
S919	637F			JMP	T81
S919	0000	X31	DC	00	
S920	0B			RD3	
S921	62C9			LDV	W03+3
S920	607C			LDR	ZTA
S921	637F			JMP	K31
S944	0000		K81	DC	00
S945	0A			RD3	
S947	EBCF			LDV	W03+6
S948	027C			LDR	ZTA
S949	607C			JMP	K31
S949	637F				
S9AD	BAC5D9D8		AMB	DC	C' = TRET
S9B1	C5D7A0A0				
S9B5	DAC5C0				
S9B6	0000		PAB	DC	00
S9B9	0B			RD4	

PAGE 044

PAGE 04

		LDV	DBZ
S002	EC	RTJ	PAB
S002	65068A	JNP	
S002	6377		
		POE	
S002	0000	DC	00
S002	80TC	STX	ITA
S002	8700D	LDX	X'0'
S002	80E8	STX	ITA
S002	870CE	RTJ	NET
S002	9388	MUL	ZNP
S002	4B	TBL	
S002	807C	STX	ITA
S002	83ED	JNP	POE
		POY	
S002	0000	DC	00
S002	80D8	STX	ZNP
S002	88DA	STX	B1+8
S002	8088	STX	FNP
S002	807C	STX	KPA
S002	6374	JNP	POE
		POU	
S002	0000	DC	00
S002	807C	PRY	ITA
S002	6507C4	RTJ	TBL
S002	88E8C3	RTJ	POI
S002	17F6	MUL	PFT
S002	6378	JNP	POE
		POH	
S002	0000	DC	00
S002	09	ROE	
S002	E8P8	LDU	ZNP
S002	6119D	RTJ	CEP
S002	08	ROE	
S002	80E4	RTV	EVA
S002	80DA	LDU	ZNP
S002	8700E4	LNU	A7784
S002	8111D1	RTJ	

		DC	EE
SE03 0000	P01	DC	EE
SE03 670006		LDRW	A7E61
SE04 481479		ATJ	4
SE09 F6DE		STV	TWI
SE0D 6805CE		RTJS	NET
SE10 70E9		IWM	ZWR
SE12 E5A600		LDA5	TARX
SE15 87A940		LDRS	KTACAO
SE19 6259		JMP	P01
SE1A 0000	POK	DC	EE
SE1C 670006		LDRS	6
SE1F 673C		STX	ZTA
SE21 607C	PRE	LOX	ETA
SE23 6E0B11		ATJ	LNF
SE26 6BB030		ATJ	P01
SE29 1F76		NAR	PRE
SEED 62ED		JMP	POK
WE00 0000	POT	DC	EE



~~SECURITY CLASSIFICATION~~

**DOCUMENT CONTROL DATA - R & D**

(Security classification of title, body of abstract and indexing annotation must be entered when the overall report is classified)

1. ORIGINATING ACTIVITY (Corporate author) Physikalisch-Bioklimatische Forschungsstelle der Fraunhofer-Gesellschaft, 81 Garmisch- Partenkirchen, Germany, Skistadion		2a. REPORT SECURITY CLASSIFICATION Unclassified
		2b. GROUP N/A

3. REPORT TITLE  
**A Study of the Effects of Atmospheric Fine Structure Characteristics on  
the Vertical Distribution of Aerosols.**

4. DESCRIPTIVE NOTES (Type of report and inclusive date)

**Final Technical Report, July 1971**

5. AUTHORITY (First name, middle initial, last name)

**Reinhold Reiter; Rudolf Sladkowic; and Walter Carnuth**

6. REPORT DATE <b>July 1971</b>	7a. TOTAL NO. OF PAGES <b>110</b>	7b. NO. OF REPS <b>3</b>
8a. CONTRACTOR GRANT NO. <b>DAJA-37-70C-2647</b>	8b. ORIGINATOR'S REPORT NUMBER(S)	
8c. PROJECT NO. <b>ITO61102B53A</b>	8d. OTHER REPORT NO(S) (Any other numbers that may be assigned this report)	
9.	10.	

10. DISTRIBUTION STATEMENT

This document has been approved for public release and sale; its distribution  
is unlimited.

11. SUPPLEMENTARY NOTES	12. SPONSORING MILITARY ACTIVITY <b>US Army Research &amp; Development Gp (EUR) Box 15, FPO New York 09510</b>
-------------------------	---

13. ABSTRACT

The investigations continued during the reporting period essentially as described in preceding reports. The objectives were:  
a. To shield the cable car telemetry systems against all effects of the weather and to obtain by them homogeneous series of recordings;  
b. to develop and apply the physical and mathematical bases for the complete numeric evaluation of the recording runs, up to and including computation of the incremental exchange coefficients;  
c. to continually record at the three stations the Aitken nuclei concentrations, natural radioactivity (RaB, RaC), and polar conductivities, and to utilize them in the evaluations; and  
d. to derive initial deductions from the results.

The entire evaluation technique was completely changed. A new computer (Intertechnique Multi 8) with 12 k words (1 word = 9 bit) affords us the possibility to perform the entirety of all computation processes in one single operation, and to print them out in tables. / )

Key words:

**Aerosol; gradient; troposphere; boundary layer; exchange coefficient.**